Memoir of the Fukui Prefectural Dinosaur Museum 12: 35–78 (2013)

ARTICLE

DETRITAL ZIRCON GEOCHRONOLOGY OF THE SILURIAN–LOWER CRETACEOUS CONTINUOUS SUCCESSION OF THE SOUTH KITAKAMI BELT, NORTHEAST JAPAN

Hiroyuki OKAWA [1], Masanori SHIMOJO [2], Yuji ORIHASHI [3], Koshi YAMAMOTO [4], Takafumi HIRATA [5], Shin-ichi SANO [6], Yasuo ISHIZAKI [1], Yoshikazu KOUCHI [1], Shuichi YANAI [7] and Shigeru OTOH [1]

[1] Graduate School of Science and Engineering, University of Toyama, 3190 Gofuku, Toyama 930-8555, Japan
[2] Graduate School of Arts and Sciences, University of Tokyo, 3-8-1 Komaba, Meguro-ku, Tokyo 153-8902, Japan
[3] Earthquake Research Institute, University of Tokyo, 1-1-1 Yayoi, Bunkyo-ku, Tokyo 113-0032, Japan
[4] Graduate School of Environmental Studies, Nagoya University, Furo-cho, Chikusa-ku, Nagoya 464-8601, Japan
[5] Graduate School of Science, Kyoto University, Kitashirakawaoiwake-cho, Sakyo-ku, Kyoto 606-8502, Japan
[6] Fukui Prefectural Dinosaur Museum, 51-11 Terao, Muroko, Katsuyama, Fukui 911-8601, Japan
[7] Japan Geocommunications Co., Ltd., 2-10 Yotsuya, Shinjuku-ku, Tokyo 160-0004, Japan

ABSTRACT

U-Pb analyses of more than 1,000 single detrital zircons from 16 formations of the Silurian–Lower Cretaceous continuous succession of the South Kitakami Belt (SKB), Northeast Japan, provide a detrital zircon reference for the complex continental-margin orogen of Japan. As a result, three tectonic phases were discriminated. Siluro–Devonian sandstone samples contain many syn-sedimentary zircons and 36.5–48.0% of Precambrian zircons scattering between 700 Ma and 3,000 Ma, suggesting that they were deposited along an active continental margin of East Gondwana. Permian–Early Jurassic sandstone samples contain virtually no Precambrian zircons, suggesting that they were deposited along the active margin of an oceanic island arc. Middle Jurassic–Early Cretaceous sandstone samples contain many 300–170 Ma zircons and up to 28% of Paleoproterozoic (around 1,850 Ma) zircons but no Neoproterozoic zircons. Moreover, the zircons during the magmatic hiatus in Korea (158–110 Ma) were detected only in one Lower Cretaceous sandstone sample. The age distribution suggests that the Paleoproterozoic zircons in the Middle Jurassic–Lower Cretaceous sandstone of the SKB were most likely supplied from a Paleoproterozoic orogen in the North China Block. Thus, the South Kitakami Paleoland, which accumulated the continuous succession of the SKB was born along a margin of Gondwana in the Silurian–Devonian, rifted from the continent and drifted in the Tethys ocean as an oceanic island arc in the Permian–Early Jurassic, and finally amalgamated along an active continental margin where detrital zircons of the North China Block were supplied in the Middle Jurassic.

Key words: U-Pb age, detrital zircon, LA-ICPMS, South Kitakami Belt, Northeast Japan, Gondwana

大川泰幸・下條将徳・折橋裕二・山本鋼志・平田岳史・佐野晋一・石﨑泰男・高地吉一・柳井修一・大藤　茂（2013）東北日本，南部北上帯のシルル～前期白亜紀連続層序における砕屑性ジルコン年代分布の推移．福井県立恐竜博物館紀要 12：35–78.

南部北上帯の浅海成シルル～下部白亜系連続層序から 16 層を選び，砕屑性ジルコンのウラン－鉛年代を測定した結果，日本列島の標準となる砕屑性ジルコン年代分布の推移が示された．①シルル～下部石炭系は 1500–750 Ma のジルコンを特徴的に含む多峰型年代分布をなし，新原生代ジルコンを産するゴンドワナ大陸北東縁からのジルコン供給を示唆する．②ペルム～下部ジュラ系は，いずれもほぼ堆積時ジルコンのみからなる単峰型年代分布をなす．③中部ジュラ～下部白亜系は，北中国地塊から供給されたと見られる古原生代（1850 Ma 付近）ジルコンを含む二峰型年代分布をなす．以上より，本連続層序を堆積した南部北上古陸は，①シルル～前期石炭紀に位置したゴンドワナ大陸北東部の大陸縁から，②ペルム～前期ジュラ紀には分離してテチス海中の海洋性島弧として挙動し，③中期ジュラ紀には，北中国地塊からジルコンが供給される大陸縁に癒合したと見られる．

Received August 2, 2013. Accepted November 4, 2013.
Corresponding author—Shigeru OTOH
E-mail: shige@sci.u-toyama.ac.jp

INTRODUCTION

This paper aims (1) to introduce temporal transition of the detrital zircon age distributions recorded in the Silurian–Lower Cretaceous continuous succession of the South Kitakami Belt (SKB), Northeast Japan, and (2) to discuss the evolutionary history of the South Kitakami Paleoland, which accumulated the continuous succession of the SKB.

Recent progress in analytical technique has enabled rapid and exact U-Pb isotopic age determination of zircons using sensitive high-resolution ion-microprobe (SHRIMP) or inductively coupled plasma-mass spectrometry with laser ablation sampling (LA-ICPMS) (e.g., Compston, 1996; Kosler and Sylvester, 2003). Detrital zircon age distribution reflects the changes of provenance, paleogeography, and tectonic setting, and can be a powerful tool for inferring the plate tectonic evolution of a complex orogen like the Japanese Islands (e.g., Gehrels et al., 1995; Darby and Gehrels, 2006). To make such an inference, we have to know the temporal change of detrital zircon age distribution of each crustal block (or terrane) that makes up the orogen, and compare the data with the reference age distribution for the major crustal blocks in the world (e.g., Soreghan and Gehrels, 2000; Darby and Gehrels, 2006 and references therein). Such comparison enables us to know the origin and tectonic history of each crustal block in the orogen. The study of detrital zircon geochronology in Japan (Tsutsumi et al., 2000, 2003, 2006, 2009, 2011, 2012; Aoki et al., 2007, 2012; Otoh et al., 2010), however, is still local and is not comprehensive.

The SKB is the best target for a comprehensive study of detrital zircon geochronology in Japan, because it retains a 350-Myr continuous succession of shallow-marine to terrestrial beds formed during the Silurian to the Early Cretaceous (Kawamura et al., 1990; Mori et al., 1992; Ehiro and Kanisawa, 1999). The continuous succession of the SKB has already been studied as a standard succession of lithostratigraphy and paleobiogeography. It helps to estimate the transition of tectonic setting and affinities with the other crustal blocks or terranes of the Japanese Islands and East Asia (e.g., Kato, 1990; Nakamura and Tazawa, 1990; Otoh and Yanai, 1996; Ehiro and Kanisawa, 1999). The detrital zircon geochronological data of the SKB presented in this study will be another set of reference data. They can be much more useful than the paleobiogeographical data because even fossil-free sandstones of an accretionary prism or a metamorphic belt contain zircons, enabling to compare the SKB with any other belts but ultra-high-temperature metamorphic belts.

GEOLOGIC SETTING

The SKB consists mainly of basement rocks and overlying Ordovician to Early Cretaceous strata (Figs. 1 and 2). The outline of the basement rocks and the continuous succession we studied is described below.

Basement rocks

The basement rocks of the SKB are the Hayachine Complex (Ehiro et al., 1988) and its equivalents and the Hikami Granite (Murata et al., 1974).

The Hayachine Complex and its equivalents fringe northeastern to western boundary of the SKB (Fig. 1). They consist mainly of ultramafic to mafic rocks with small amounts of tonalite–trondhjemite–granodiorite (TTG). According to the petrological studies of Ozawa (1983, 1984) and Mori et al. (1992), they are fragments of volcanic-arc lithosphere. K-Ar hornblende ages of 421−484 Ma and a U-Pb zircon age of 462 Ma were reported from gabbro and tonalite, respectively (Ozawa et al., 1988; Shibata and Ozawa, 1992; Shimojo et al., 2010).

The Hikami Granite mainly exposes in the mid-eastern part of the SKB (Fig. 1). The Hikami Granite consists of massive to schistose granite, granodiorite, and tonalite, partly including blocks of gneissose metamorphic rocks (Tsubonosawa Metamorphic Rocks). Petrochemical studies suggested that the Hikami Granite is calc-alkaline, volcanic-arc granitoid (Kobayashi et al., 2000).

The Hikami Granite is unconformably overlain by the Silurian Kawauchi Formation (Murata et al., 1974, 1982), mentioned below, and has a SHRIMP U-Pb zircon age of 442 Ma (corresponding to the Late Ordovician; Watanabe et al., 1995). Shimojo et al. (2010), on the other hand, reported LA-ICPMS, U-Pb zircon ages of 416−403 Ma from four samples, suggesting that the granite at least partly forms Devonian intrusive bodies.

Silurian–Devonian strata

The Silurian to Devonian strata of the SKB crop out with the basement rocks (Fig. 1). They consist mainly of siliciclastic to volcaniclastic rocks with intercalations of felsic to mafic tuff and limestone, suggesting that they are deposits of a shallow-marine environment along an active continental margin.

In the northeastern part of the SKB, the Yakushigawa Formation overlies the Hayachine Complex and consists of interbedded basaltic volcaniclastic rocks, quartz-feldspathic sandstones, and felsic tuffs in the lower part, and of shales in the upper part. The shales of the Odagoe Formation, which yield a Silurian brachiopod *Trimerella* sp., overlie the Yakushigawa Formation (Ehiro et al., 1986). In the northern marginal part of the SKB to the south of Morioka (Fig. 1), the Hayachine Complex is associated with the Nameirizawa and Orikabetoge formations. The Nameirizawa Formation is lithologically correlated with the Yakushigawa Formation, whereas the Orikabetoge Formation consists of clastic rocks with orthoquartzite clasts (Okami et al., 1984) and yields Silurian fossils such as *Halysites kuraokaensis* and *Encrinurus* sp. (Kawamura et al., 1984; Yamazaki et al., 1984). In the Nagasaka area, western part of the SKB (Fig. 1), the Upper Devonian Tobigamori Formation overlies the Ohachimori Amphibolite, an equivalent of the Hayachine Complex, having K-Ar hornblende ages of 479−424 Ma (Kanisawa et al., 1992;

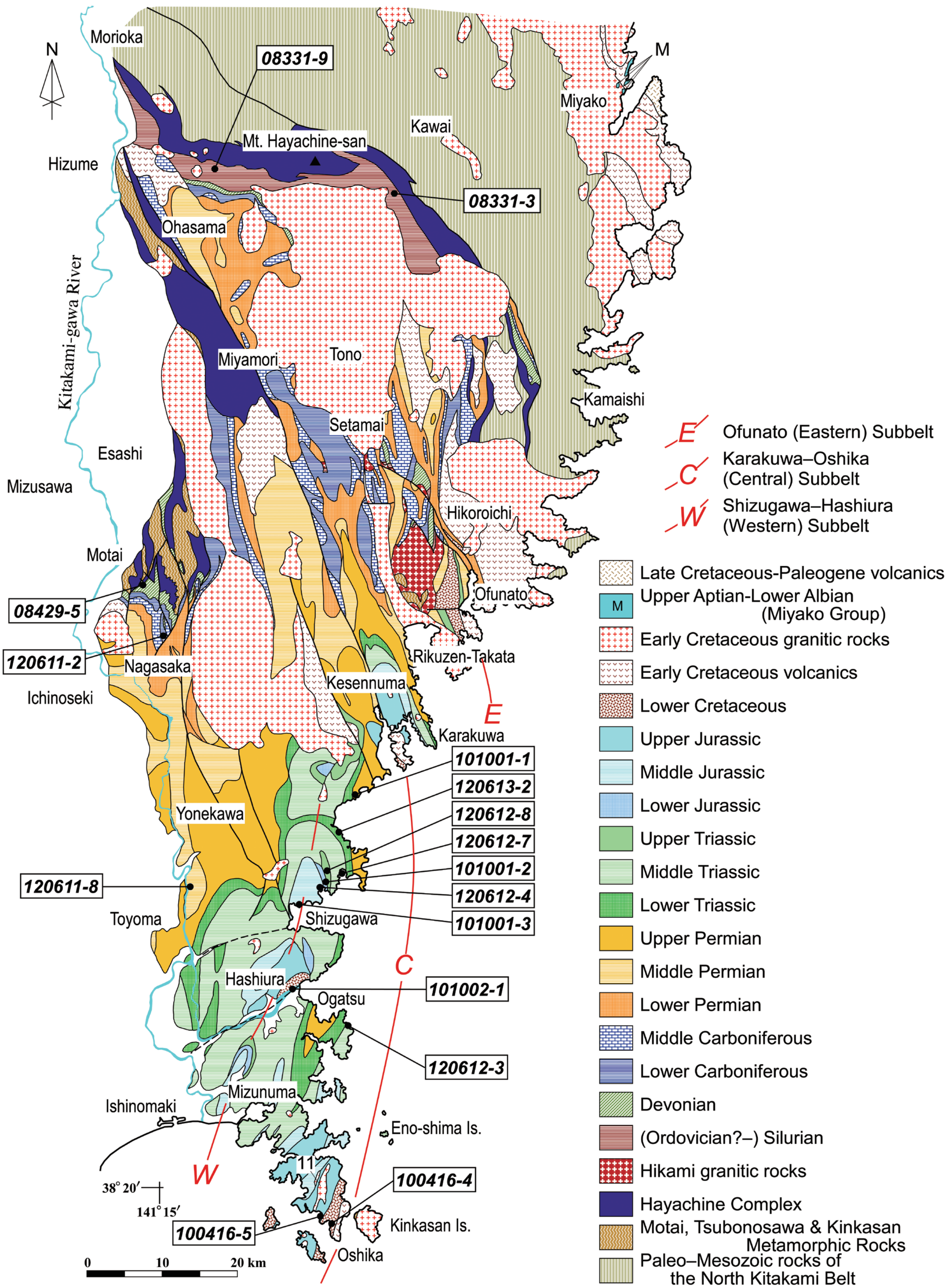

FIGURE 1. Geologic map of the South Kitakami Belt showing the sampling locations. Modified after Onuki (1981), Ehiro (1989), and Sasaki (2003). Abbreviations—Is.: Island, M: distribution of the Miyako Group.

Sasaki et al., 1997). The Tobigamori Formation consists of three members. The Lower Member consists of interbedded tuffaceous sandstone and shale yielding no fossils. The Middle Member consists of red conglomerate, sandstone, and shale, whereas the Upper Member consists mainly of sandy shale. The two members yield abundant brachiopod and plant fossils such as *Cyrtospirifer tobigamoriensis* and *Leptophloeum rhombicum*, and are correlated with the Famennian (Upper Devonian; Tachibana, 1950, 1952; Noda and Tachibana, 1959). Ehiro and Takaizumi (1992), on the other hand, found a Tournaisian ammonoid, *Protocanites* sp., from a float of the uppermost part of the Tobigamori Formation. In the Hikoroichi area, mid-eastern part of the SKB (Fig. 1), Siluro–Devonian Kawauchi, Ono, and Nakazato formations, in ascending order, lie on top of the Hikami Granite.

The Siluro–Devonian fauna and flora of the SKB have affinities with those of coeval northern East Gondwana: i.e., present-day Australia, South China, and the southern part of the Central Asian Orogenic Belt (CAOB). For example, tabulate corals from the Kawauchi Formation, such as *Schedohalysites* and *Falsicatenipora*, are abundant in the coeval strata of Australia and South China (e.g., Hamada, 1960; Kato, 1990), and the Eifelian brachiopod fauna from the Nakazato Formation has affinities with the coeval fauna from the CAOB in Inner Mongolia, China (Tazawa and Chen, 2001). Moreover, the Upper Devonian flora *Leptophloeum* of the Tobigamori Formation commonly occurs in the coeval strata of Australia, South China, CAOB, and the Imjingang Belt of North Korea (e.g., Kimura, 1987; Om et al., 1996; Tazawa et al., 2006).

Carboniferous strata

The distribution of the Carboniferous strata in the SKB is much wider than that of the Silurian to Devonian strata (Fig. 1). The Lower Carboniferous in the SKB is rich in felsic and mafic volcanic and pyroclastic rocks, whereas the Upper Carboniferous is rich in carbonate rocks (Kawamura and Kawamura, 1989a). Kawamura and Kawamura (1989b) and Kawamura et al. (1990) regarded that the Lower Carboniferous volcanic and pyroclastic rocks indicate the bimodal volcanism related to intra-arc rifting.

In the Nagasaka area, the Karaumedate Formation overlies the Tobigamori Formation, and is composed of interbedded sandstone and mudstone, felsic tuff, and calcareous sandstone (Kawamura and Kawamura, 1989a). The lower part of the Karaumedate Formation yields Tournaisian brachiopods, whereas the upper part yields Visean rugosa corals such as *Kueichouphyllum* sp. and *Dibunophyllum* sp., and brachiopods such as *Productus giganteus*. In the Hikoroichi area, the Lower Carboniferous Hikoroichi, Onimaru, and Lower to Upper Carboniferous Nagaiwa formations, in ascending order, overlies the Devonian Nakasato Formation. The Hikoroichi Formation, consisting mostly of felsic tuff and tuffaceous clastic rocks (Kawamura and Kawamura, 1989a), yields various rugosa corals such as *Amygdalophyllum etheridgei*, and brachiopods such as the *Rotaia-Marginatia-Syringothyris* assemblage and *Schizophoria resupinata*, whereas the Onimaru Formation yields Late Visean rugosa corals such as *Kueichouphyllum glacile, Yuanophyllum kansuense*, and *Diphyphyllum hochangpingense*.

Two Carboniferous faunal provinces have been discriminated in the Eurasian realm: the northern province characterized by the rugosa coral *Gangamophyllum* and the southern province characterized by *Kueichouphyllum*. The northern province includes present-day northern Siberia, whereas the southern province includes present-day South China, Indochina, and northern Australia (Liao, 1990). Moreover, the mixed fauna of the northern and southern provinces has been recognized in the CAOB. Lower Carboniferous fauna of the SKB still has affinities with that of coeval northern East Gondwana. For example, the rugosa coral *Amygdalophyllum* from the Hikoroichi Formation is abundant in Australia (southern province). Occurrence of *Kueichouphyllum* and absence of *Gangamophyllum* in the Onimaru Formation also suggest an affinity with the southern province. The *Rotaia-Marginatia-Syringothyris* brachiopod assemblage, on the other hand, indicates an affinity with the CAOB (Tazawa, 1996). Late Carboniferous fauna from the SKB has various boreal elements (e.g., Kato, 1990), probably indicating the influence of global cooling at that time.

Permian to Middle Triassic strata

Permian strata

Permian strata in the SKB were subdivided, in ascending order, into the Sakamotozawan, Kanokuran, and Toyoman series (Minato et al., 1978), although we do not follow this local chronostratigraphic division and will call these “series” as “groups”. The Permian strata consist mostly of shallow marine epiclastic rocks and limestone, with small amounts of felsic to intermediate tuff in the Sakamotozawan Group.

The Sakamotozawan Group includes the Sakamotozawa Formation in the Hikoroichi–Setamai area, the Notsuchi Formation in the Nagasaka area, and the Nishikori Formation in the Toyoma area to the south of Nagasaka (Fig. 1). They consist mostly of sandstone, mudstone, and interbedded sandstone and mudstone, with some limestone beds particularly in the middle horizon (Kanmera and Mikami, 1965; Saito, 1966; Ehiro, 1989). The Sakamotozawan Group yields fusulinids such as *Zellia, Monodiexodina*, and *Pseudofusulina* (Kanmera and Mikami, 1965). Among them, genus *Monodiexodina* characterizes the *Monodiexodina* territory (Ishii et al., 1985), which includes the CAOB in Tarim, northeastern China, and Primorye in southeastern Russia (Ozawa, 1987). Moreover, the Nishikori (or Rodai) Formation yields the Maiya Flora consisting of *Gigantopteris, Taeniopteris*, and *Sphenophyllum*, common with the coeval strata in the Cathaysian Floristic Province in China and Korea (Asama, 1985).

The Kanokuran Group includes the Kanokura Formation in the Setamai area, the upper part of the Notsuchi Formation and the Usuginu Conglomerates in the Nagasaka area, the Tenjinnoki Formation and the Yamazaki Conglomerates in the Toyoma area, and the Iwaizaki Limestones in the Motoyoshi

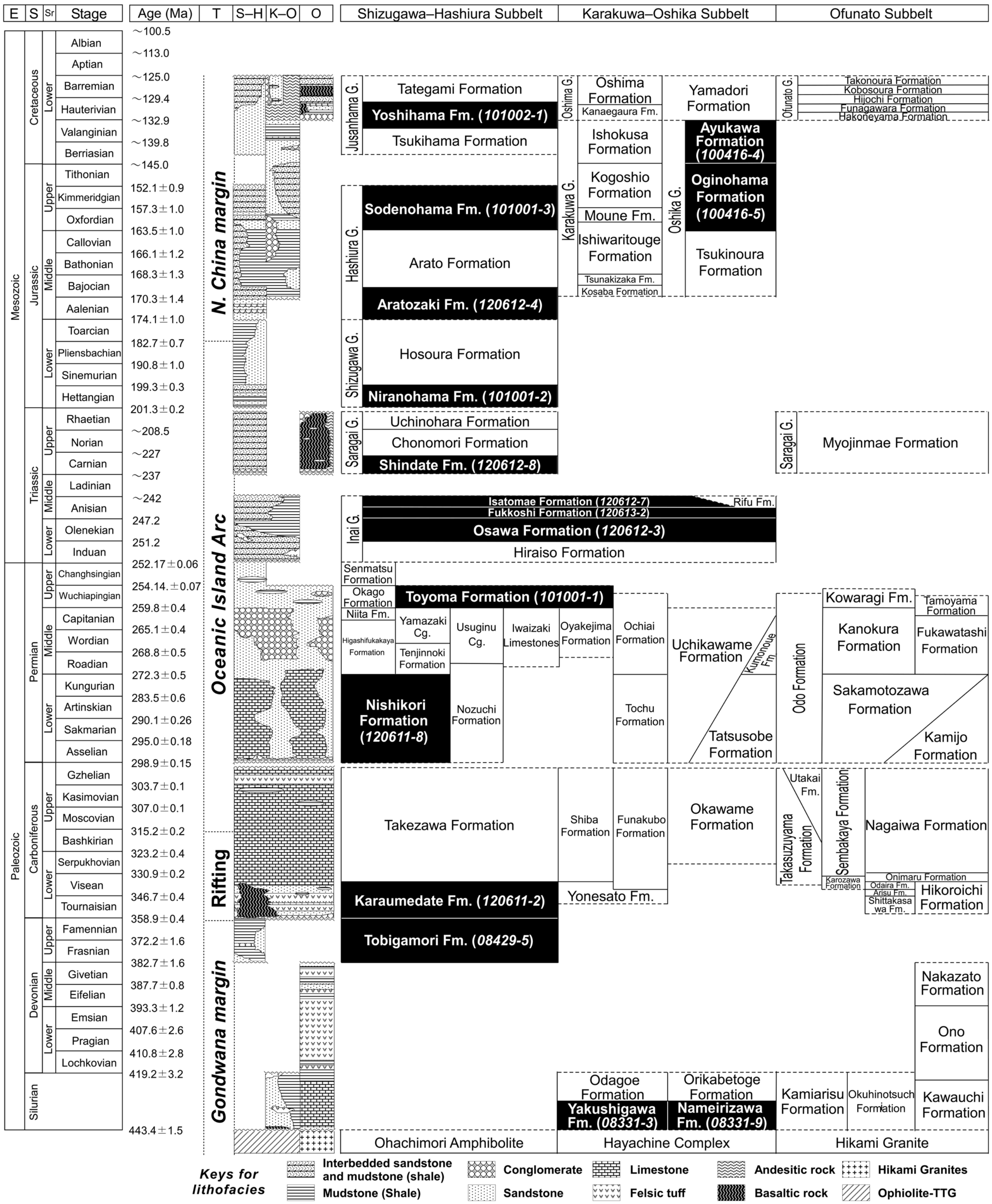

FIGURE 2. Stratigraphic division of the pre-Aptian sequences of the South Kitakami Belt showing the lithofacies and sampling horizons. Numerical ages for all systems are taken from International Commission on Stratigraphy (2013). Abbreviations—Cg.: Conglomerates, E: Erathem, Fm.: Formation, G: Group, K–O: Karakuwa–Oshika Subbelt, N. China: North China, O: Ofunato Subbelt, S: System, Sr: Series, S–H: Shizugawa–Hashiura Subbelt, T: Tectonic setting, TTG: Tonalite–trondhjemite–granodiorite.

area to the southeast of Nagasaka (Figs. 1 and 2). They consist generally of mudstone, sandstone, and conglomerate, with some interlayers of limestone. The conglomerate in the Kanokuran and overlying Toyoman groups is collectively called the Usuginu-type Conglomerate with granitic clasts of 300−280 Ma (LA-ICPMS U-Pb ages; Okawa, unpublished data). The Usuginu-type Conglomerate is particularly thick in the Kanokuran Group in the Nagasaka and Toyoma areas. The Kanokuran Group yields Roadian to Capitanian fusulinids of the *Monodiexodina matsubaishi, Colania kotsuboensis*, and *Lepidolina multiseptata* zones (Choi, 1973). The Kanokuran Group also yields such ammonoid genera as *Timorites, Paraceltites*, and *Cibolites*, and brachiopods such as *Leptodus nobilis* and *Spiriferellina cristata. Monodiexodina matsubaishi* and *Spiriferellina cristata* indicates a faunal affinity with Mongolia and the southern margin of Siberia, whereas the ammonoids and *Leptodus nobilis* show the similarity with the Tethyan realm such as the South China Block (Ehiro, 1998; Tazawa, 1991, 2001).

The Toyoman Group includes the Kowaragi Formation in the Setamai–Karakuwa area and the Toyoma Formation in the Nagasaka, Toyoma, and Motoyoshi areas (Figs. 1 and 2). They consist mostly of black mudstone with some interlayers of sandstone, limestone, and conglomerate. The black mudstone bears strong slaty cleavage, particularly along the western limb of synclines (Sasaki, 2001, 2003), and partly contains carbonate and phosphate nodules (Kanisawa and Ehiro, 1986). The Toyoman Group yields Wuchiapingian to Changhsingian ammonoids such as *Araxoceras* sp. and *Paratirolites compressus* (Murata and Bando, 1975; Ehiro, 1996). Among them *Araxoceras* is a typical genus of the Tethys Ocean (Bando et al., 1987).

Lower to Middle Triassic strata

Lower to Middle Triassic strata of the SKB are collectively called the Inai Group (Fig. 2). The Inai Group is distributed in the southeastern part of the SKB and consists of two sedimentary cycles: the Hiraiso and Osawa formations constitute the first cycle, whereas the Fukkoshi and Isatomae formations constitute the second cycle (Onuki and Bando, 1959). The Hiraiso Formation consists of an upward fining sequence, beginning with basal conglomerate and coarse calcareous sandstone, overlain by interbedded sandstone and mudstone. Rare felsic tuff layers are intercalated in the lower part of the formation. The Hiraiso Formation yields *Pleuromeia* flora, which commonly occurs from the North China Block and the southern part of the CAOB (Kimura, 1987). The Hiraiso Formation also yields bivalves such as *Eumorphotis nipponicus* and *"Pecten"* aff. *ussuricus*. The Olenekian Osawa Formation consists mainly of calcareous mudstone, with some intercalations of sandstone and submarine sliding deposits (Kamada, 1983). The formation yields *Utatsusaurus hataii*, one of the earliest ichthyosaur fossils in the world. The Osawa Formation also yields abundant ammonoids of the *Columbites-Subcolumbites* fauna (Bando and Shimoyama, 1974), which is concentrated in the coeval strata in the Tethyan region (Bando et al., 1987). The Fukkoshi Formation consists mainly of bedded sandstone, with subordinate amount of mudstone. The formation yields Anisian ammonoids such as *Bolatonites* cf. *kitakamicus, Hollandites* spp., and *Rikuzenites nobilis* (Shimizu, 1930; Yabe, 1949). The generic composition of the Anisian ammonoids from the SKB is the Pacific–Tethyan type (Ehiro, 1998) although they contain some common species with the coeval ammonoids from Primorye and Kolyma of eastern Russia (Nakazawa, 1991). The Fukkoshi Formation also yields brachiopods such as *Spiriferina* and *Terebratula* (Ichikawa, 1951). The Isatomae Formation consists of laminated muddy sandstone and mudstone, intercalated with some sandstone beds. The formation also yields Anisian Pacific–Tethyan ammonoids such as *Hollandites japonicus, "Danubites" naumanni,* and *Bolatonites kitakamicus* (Shimizu, 1930; Onuki and Bando, 1959; Bando, 1964; Ehiro, 1998).

Upper Triassic to Lower Cretaceous strata

Upper Triassic to Lower Cretaceous strata are distributed in the southeastern part of the SKB. They occur in three subbelts along the axes of three major synclines: the Shizugawa–Hashiura, Karakuwa–Oshika, and Ofunato subbelts from west to east (e.g., Yamashita, 1957; Takizawa, 1977, 1985; Fig. 1). The succession and thickness of the Mesozoic strata in the three subbelts substantially differ from each other. Sasaki (2003) reported that the regional strain is concentrated along the western limb of the major synclines and concluded that the major synclines are conical synclines with subvertical rotation axes and were formed through sinistral shearing along the high-strain zones (i.e., their western limbs at present).

Upper Triassic strata

Upper Triassic strata of the SKB are collectively called the Saragai Group (Fig. 2), which occurs in the Shizugawa–Hashiura and Ofunato subbelts but is absent in the Karakuwa–Oshika Subbelt (Fig. 1). The Saragai Group in the northern part of the Shizugawa–Hashiura Subbelt consists of the Shindate and Chonomori formations (Onuki and Bando, 1958), whereas the group in the Ofunato Subbelt is called the Myojinmae Formation (Kanagawa and Ando, 1983). The Shindate Formation consists mainly of massive feldspathic sandstone with subordinate amounts of mudstone, granule conglomerate, felsic tuff, and rare carbonaceous mudstone. The Carnian–Norian Chonomori Formation, overlying the Shindate Formation, consists of interbedded micaceous sandstone and mudstone. The Chonomori Formation is characterized by a rich *Monotis* fauna, which belongs to the Arcto-Pacific Realm (Kobayashi and Tamura, 1983; Tamura, 1987) and consists of *M. scutiformis, M. ochotica*, and *M. zabaikalica* (Nakazawa, 1964; Ando, 1987). The Myojinmae Formation in the Ofunato Subbelt consists mainly of tuff, with some andesite lava, tuffaceous sandstone, and volcanic conglomerate. A tuff clast in the conglomerate yields *Monotis ochotica* (Kanagawa and Ando, 1983).

Lower to lower Middle Jurassic strata

Lower to lower Middle Jurassic strata of the SKB is called the Shizugawa Group and occurs only in the Shizugawa–Hashiura Subbelt (Fig. 2). The Shizugawa Group in the type locality, northern part of the Shizugawa–Hashiura Subbelt, consists of the Niranohama and Hosoura formations, in ascending order (Inai, 1939). The Niranohama Formation consists of brackish-water black mudstone and trigoniid-bearing coarse sandstone. The former yields parallic bivalves such as *Bakevellia*, *Burmesia*, and *Geratrigonia*, whereas the latter is characterized by abundant occurrence of parallic bivalves (*Trigonia* and *Vaugonia*) and belemnites, together with middle to late Hettangian ammonoids such as *Alsatites* (or *Yebisites*) *onoderai* (Matsumoto, 1956; Hayami, 1961; Sato and Westermann, 1991; Iba et al., 2012). The Hosoura Formation consists mostly of laminated sandy mudstone and yields Sinemurian to Aalenian ammonoids (Sato, 1957, 1962; Takahashi, 1969; Sato and Westermann, 1991). Many ammonoid and bivalve species from the Shizugawa Group are endemic and have not been found in other regions of East Asia (Hayami, 1990).

Middle Jurassic to Lower Cretaceous strata in the Shizugawa–Hashiura Subbelt

The Middle Jurassic to Lower Cretaceous strata in the Shizugawa–Hashiura Subbelt consists of the Hashiura and Jusanhama groups, in ascending order (Fig. 2). The Hashiura Group in the northern part of the subbelt is subdivided into the Aratozaki, Arato, and Sodenohama formations (Mabuti, 1933; Matsumoto, 1953), whereas the strata correlative with the Aratozaki and Arato formations are called the Nakahara and Nagao formations, respectively, in the southern part of the subbelt (Mori, 1949; Kase, 1979). The Aratozaki Formation consists mainly of coarse quartz-feldspathic sandstone with some intercalations of conglomerate, and yields marine bivalves such as *Inoceramus morii* and *Vaugonia yokoyamai* (Hayami, 1961). The Arato Formation consists mainly of bedded black mudstone with interbedded mudstone and sandstone in its basal part. The Arato and Nagao formations yield abundant ammonoids such as Bajocian *Stephanoceras hashiuraense* and *Cadomites bandoi*, Callovian *Kepplerites mabutii*, and Oxfordian–Kimmeridgian *Kranaosphinctes* cf. *matsushimai* and *Taramelliceras* sp. (Sato, 1962; Takahashi, 1969; Kase, 1979). Among these, *Kepplerites* is a typical boreal genus, whereas *Kranaosphinctes* is a Tethys–Pacific genus (Bando et al., 1987). Kase (1979) also reported from the uppermost part of the Nagao Formation a poorly-preserved ammonoid belonging to Olcostephanidae or Berriasselidae, and suggested that the horizon may be of Tithonian or younger age. The Sodenohama Formation consists of massive sandstone and interbedded sandstone and mudstone, and yields Kimmeridgian (Takahashi, 1969) or Tithonian ammonoids (Matsumoto, 1953). The Jusanhama Group occurs only in the southern part of the subbelt and is subdivided into Yoshihama, Tategami, and Tsukihama formations, in ascending order (Mori, 1949; Kase, 1979). The Yoshihama and Tsukihama formations consist mostly of quartz-feldspathic sandstone, whereas the Tategami Formation consists of interbedded quartz-feldspathic sandstone and bituminous mudstone (Kase, 1979). Endemic species of such bivalve genus as *Filosina* and *Protocardia* occur in the Tategami Formation (Hayami, 1960), and Tashiro and Kozai (1989) pointed out that *Protocardia* characterizes the Nankai Fauna, a southern Tethyan fauna occurring restrictively in the Kurosegawa and Southern Chichibu belts of the Outer Zone of Southwest Japan. Considering the age of the underlying Hashiura Group, the Jusanhama Group is likely of Tithonian–Early Cretaceous age.

Middle Jurassic to Lower Cretaceous strata in the Karakuwa area, northern part of the Karakuwa–Oshika Subbelt

The Middle Jurassic to Lower Cretaceous strata in the Karakuwa area, northern part of the Karakuwa–Oshika Subbelt, are the Karakuwa and Oshima groups, in ascending order (Fig. 2). The Karakuwa Group is subdivided into the Kosaba, Tsunakizaka, Ishiwaritoge, Mone, Kogoshio, and Isokusa formations in ascending order (Shiida, 1940; Hayami, 1961), whereas the Oshima Group consists of the Kanaegaura and Yokonuma formations, in ascending order (Onuki, 1969).

Middle Jurassic to Lower Cretaceous strata in the Oshika area, southern part of the Karakuwa–Oshika Subbelt

The Middle Jurassic to Lower Cretaceous strata in the Oshika area, southern part of the Karakuwa–Oshika Subbelt, are the Oshika Group (Onuki, 1956) and Yamadori Formation (Inai and Takahashi, 1940), in ascending order (Fig. 2). The Oshika Group is subdivided into the Tsukinoura, Oginohama and Ayukawa formations, in ascending order (Takizawa et al., 1974; Takizawa, 1985). The Tsukinoura Formation consists of the lower sandstone and upper mudstone members. The upper part of the lower member yields ammonoids such as *Stephanoceras* cf. *plicatissimum* and *Normannites* (*Itinsaites*) sp. and is correlated with the *Otoites sauzei* and/or *Stephanoceras humphriesianum* zones of the European Middle Bajocian (Sato, 1972). The member also yields rich bivalves such as *Trigonia sumiyagura* and *Vaugonia kodaijimensis* (Hayami, 1961). The Oginohama Formation, consisting of sandstone and interbedded sandstone and mudstone with some layers of conglomerate, is subdivided into the Kitsunezaki Sandstone and Shale, Makinohama Sandstone, Kozumi Shale and Fukiura Shale and Sandstone members, in ascending order (Takizawa et al., 1974). The upper part of the Kozumi Shale Member yields late Oxfordian ammonoids such as *Perisphinctes* (*Perisphinctes*) *ozikaensis* and *Perisphinctes* (*Kranaosphinctes*). cf. *matsushimai* and early Kimmeridgian ammonoids such as *Discosphinctes* cf. *kiritaniensis*, *Lithacoceras onukii*, and *Aulacostephanus* (*Pararasenia*) sp. (Fukada, 1950; Sato, 1962; Takahashi, 1969). The Fukiura Shale and Sandstone Member yields Tithonian ammonoids such as *Virgatosphinctes* aff. *communis* and *Aulacosphinctoides*? sp. (Takahashi, 1969; Takizawa et al., 1974). Further, abundant plant fossils belonging to the Ryoseki Flora occur from the upper part of each member (Kimura and Ohana, 1989). The Ayukawa Formation, consisting of quartz-feldspathic sandstone and mudstone, is subdivided into the Kiyosaki Sandstone, Kobitawatashi Sandstone and Shale, Futawatashi Shale, and Domeki Sandstone members, in ascending order (Takizawa et al., 1974). The lower part of the Kobitawatashi Sandstone Member yields Berriasian ammonoids such as *Berriasella* sp. (Takizawa, 1970), whereas the upper part of the member and the upper part of the Futawatashi Shale Member yield Valanginian ammonoids such as *Thurmanniceras* cf. *isokusense, Kilianella* sp., and *Lyticoceras* sp. (Takizawa, 1970; Obata, 1988). The Yamadori Formation consists of andesitic to dacitic pyroclastic rocks and overlying basaltic lava and pyroclastic rocks (Takizawa et al., 1974).

Lower Cretaceous strata of the Ofunato Subbelt

The Ofunato Subbelt is mostly occupied by the Lower Cretaceous Ofunato Group, which is subdivided into the Hakoneyama, Funagawara, Hijochi, Kobosoura, and Takonoura formations, in ascending order (Onuki and Mori, 1961; Fig. 2). Among them, the Hakoneyama Formation, consisting mostly of volcanic conglomerate, has been interpreted to be a southern extension of the Upper Triassic Myojinmae Formation (Kanagawa and Ando, 1983).

SAMPLE DESCRIPTIONS

We studied the following 16 sandstone samples and examined their provenances from the age-distribution of detrital zircons. Here follow the descriptions of studied samples summarized in Fig. 3.

Silurian Nameirizawa Formation (Sample 08331-9; N39°32’55.8”, E141°20’20.2”)

Sample 08331-9 of the Silurian Nameirizawa Formation was collected from the middle part of the formation along the Nameirizawa River, Hanamaki City, Iwate Prefecture (Fig. 1). The sandstone sample was of medium to fine feldspathic wacke, with the matrix volume of a little more than 15%. The sandstone was angular and ill-sorted. The zircon grains were mostly abraded and anhedral, having columnar shapes with the longer dimension of 90−180 μm and the shorter dimension of 50−100 μm. Most of the zircons showed oscillatory zoning in cathodoluminescence (CL) images, a common feature of igneous zircons (Corfu et al., 2003), although few zircons were homogeneous or had metamorphic rim.

Silurian Yakushigawa Formation (Sample 08331-3; N39°32’06.8”, E141°37’30.5”)

Sample 08331-3 of the Silurian Yakushigawa Formation was collected from the lower part of the formation along the upper stream of the Yakushigawa River, Miyako City, Iwate Prefecture (Fig. 1). The sandstone sample was of angular and ill-sorted, fine feldspathic wake. Although quartz veins with the width of 1 mm or less sparsely cut the sample, no zircons have been microscopically detected in it. More than half of the zircon grains we collected were abraded and the others were euhedral. The zircon grains generally had columnar shapes with the longer dimension of 50−200 μm and shorter dimension of 50−90 μm. Most of the zircons showed oscillatory zoning in CL images although few zircons were homogeneous or had a detritus core.

Devonian Tobigamori Formation (Sample 08429-5; N39°04’02.0”, E141°14’37.0”)

Sample 08429-5 of the Tobigamori Formation was collected from the Lower Member of the formation along the Natsuyama Logging Road, Ichinoseki City, Iwate Prefecture (Fig. 1). The sandstone sample was of very ill-sorted, angular, medium lithic wacke. Two thirds of the zircon grains we collected were euhedral and the others were abraded. Most of the zircon grains had columnar shape with the longer dimension of 70−220 μm and the shorter dimension of 50−100 μm. Most of the zircons showed oscillatory zoning in CL images although few zircons had metamorphic rim and few abraded zircons were homogeneous.

Lower Carboniferous Karaumedate Formation (Sample 120611-2; N39°0’25.10”, E141°15’57.06”)

Sample 120611-2 of the Lower Carboniferous Karaumedate Formation was collected approximately 50 m above the base of the formation, 1 km to the east of Mt. Karaumedateyama, Ichinoseki City, Iwate Prefecture (Fig. 1). The sandstone sample was of angular and ill-sorted, fine to medium lithic wacke. Nearly half of the zircon grains we collected were colorless and the others were brown. 80% of the zircon grains were euhedral and had columnar shapes with the longer dimension of 70−200 μm, the shorter dimension of 40−100 μm, and aspect ratio of 1.5−2.5. The other zircon grains, all brown colored, were abraded and had anhedral shapes. Larger zircon grains tended to have inclusions and microcracks. Most of the zircons showed oscillatory zoning in CL images.

Lower Permian Nishikori Formation (Sample 120611-8; N38°41’14.17”, E141°17’24.39”)

Sample 120611-8 of the Lower Permian Nishikori Formation was collected 20 m below the top of the formation along the lower stream of the Kitakamigawa River, Tome City, Miyagi Prefecture (Fig. 1). The sandstone sample was of ill-sorted, rounded to sub-rounded, medium- to coarse-grained lithic sandstone. The lithic fragments were mostly of volcanic rocks having plagioclase phenocrysts, with few polycrystalline quartz grains. Most of the zircon grains we collected were euhedral and colorless, having columnar shapes with the longer dimension of 70−400 μm, the shorter dimension of 40−200 μm, and the aspect ratio of 1.5−2. Most of them showed oscillatory zoning in CL images, and larger zircon grains tended to contain many inclusions.

Upper Permian Toyoma Formation (Sample 101001-1; N38°48’02.3”, E141°33’04.0”)

Sample 101001-1 of the Upper Permian Toyoma Formation was collected from the uppermost part of the formation along the Maehama Coast, Kesennuma City, Miyagi Prefecture (Fig. 1).

Sample No.	Sampling Location	Formation	Modal Composition	Abraded Zircon (%)	Colorless Zircon (%)	Dimension Longer	Dimension Shorter	Aspect ratio
08331-9	N39°32'55.8", E141°20'20.2"	Nameirizawa	(No numerical data)	(No numerical data)		90–180 μm	50–100 μm	1.8–2.5
08331-3	N39°32'06.8", E141°37'30.5"	Yakushigawa				50–200 μm	50–90 μm	1.2–2.0
08429-5	N39°04'02.0", E141°14'37.0"	Tobigamori				70–220 μm	50–100 μm	1.4-2.2
120611-2	N39°0'25.10", E141°15'57.06"	Karaumedate		60	84	70–200 μm	40–100 μm	1.5–2.5
120611-8	N38°41'14.17", E141°17'24.39"	Nishikori		17	75	70–400 μm	40–200 μm	1.5–2.0
101001-1	N38°48'02.3", E141°33'04.0"	Toyoma		63	89	50–180 μm	20–80 μm	1.5–2.5
120612-3	N38°31'56.7", E141°32'2.43"	Osawa		36	87	70–180 μm	40–110 μm	1.7–2.5
120613-2	N38°45'28.5", E141°31'39.19"	Fukkoshi		17	75	150–300 μm	70–200 μm	1.2–2.0
120612-7	N38°42'48.27", E141°31'25.91"	Isatomae		16	52	120–220 μm	70–150 μm	1.5–2.5
120612-8	N38°42'33.27", E141°30'36.32"	Shindate		31	78	60–200 μm	30–120 μm	1.5–2.5
101001-2	N38°41'35.3", E141°30'05.0"	Niranohama		78	91	100–600 μm	30–150 μm	1.5–5.0
120612-4	N38°41'46.3", E141°29'54.7"	Aratozaki		9	69	50–180 μm	20–80 μm	1.5–3.0
101001-3	N38°40'22.9", E141°28'05.2"	Sodenohama		38	96	180–700 μm	100–200 μm	1.5–3.0
100416-5	N38°18'16.3", E141°29'50.2"	Oginohama		20	89	120–600 μm	120–200 μm	1.5–2.5
101002-1	N38°34'25.4", E141°26'52.9"	Yoshihama		51	91	100–500 μm	80–200 μm	1.0–2.5
100416-4	N38°17'29.8", E141°30'36.8"	Ayukawa		50	87	60–180 μm	30–100 μm	1.0–2.5

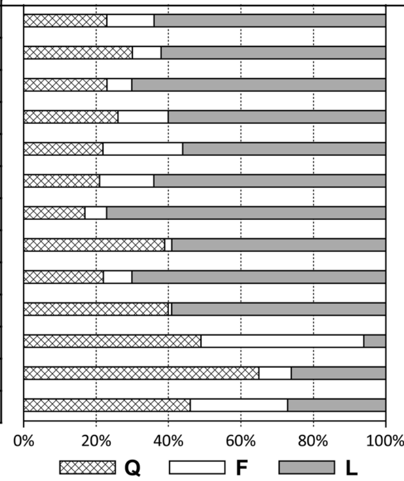

FIGURE 3. Diagram summarizing the sample description. Abbreviations—F: feldspars, L: lithic fragments, Q: single quartz.

The sandstone sample was of ill-sorted, sub-angular, and fine- to medium-grained lithic arenite. The zircon grains we collected were mostly euhedral and not abraded, among which 80% were colorless and the others were brown. The zircon grains had columnar shapes with the longer dimension of 50−180 μm, the shorter dimension of 20−80 μm, and the aspect ratio of 1.5−2.5. Most of them showed oscillatory zoning in CL images, and larger zircon grains tended to contain many inclusions and microcracks.

Lower Triassic Osawa Formation (Sample 120612-3; N38°31'56.7", E141°32'2.43")

Sample 120612-3 of the Lower Triassic Osawa Formation of the Inai Group was collected from the middle part of the formation on the east side of the Arahama Beach, Ishinomaki City, Miyagi Prefecture (Fig. 1). The sandstone sample was of well-sorted, sub-angular to sub-rounded, and fine- to medium-grained lithic arenite. The zircon grains we collected were mostly euhedral to subhedral and colorless, having columnar shapes with the longer dimension of 70−180 μm, the shorter dimension of 40−110 μm, and the aspect ratio of 1.7−2.5. All of them showed oscillatory zoning in CL images, and larger zircon grains tended to contain many inclusions and microcracks.

Middle Triassic Fukkoshi Formation (Sample 120613-2; N38°45'28.5", E141°31'39.19")

Sample 120613-2 of the Lower Triassic Fukkoshi Formation was collected from the middle part of the formation along the Kesaiso Coast, Kesennuma City, Miyagi Prefecture (Fig. 1). The sampling horizon was 120 m below the top of the formation. The sandstone sample was of moderately-sorted, angular to sub-angular, and medium- to coarse-grained lithic arenite. The collected zircon grains were euhedral to subhedral and colorless, having columnar shapes with the longer dimension of 150−300 μm, the shorter dimension of 70−200 μm, and the aspect ratio of 1.2−2.0. Most of them showed oscillatory zoning in CL images, and few zircon grains contained inclusions and/or microcracks.

Middle Triassic Isatomae Formation (Sample 120612-7; N38°42'48.27", E141°31'25.91")

Sample 120612-7 of the Middle Triassic Isatomae Formation of the Inai Group was collected from the middle part of the formation along the coast on the northeast of Cape Bentenzaki, Minamisanriku Town, Miyagi Prefecture (Fig. 1). The sampling horizon was a little more than 500 m below the base of the Upper Triassic Saragai Group. The sandstone sample was of poorly- to moderately-sorted, angular to sub-angular, and medium-grained lithic arenite. The Isatomae sandstone is characterized by the lower content of volcanic-rock fragments and inclusion of K-feldspar grains. The zircon grains we collected were euhedral to subhedral and virtually not abraded, among which 70% were colorless and the others were brown. The zircon grains had columnar shapes with the longer dimension of 120−220 μm, the shorter dimension of 70−150 μm, and the aspect ratio of 1.5−2.5. Most of them showed oscillatory zoning in CL images, and larger zircon grains tended to contain many inclusions and microcracks.

Upper Triassic Shindate Formation (Sample 120612-8; N38°42'33.27", E141°30'36.32")

Sample 120612-8 of the Upper Triassic Shindate Formation of the Saragai Group was collected from the horizon several meters below the top of the formation near the bottom of the Saragaizaka Slope, Minamisanriku Town, Miyagi Prefecture (Fig. 1). The Shindate Formation at this location, conformably lying beneath the Carnian–Norian Chonomori Formation, is probably of Carnian age. The sandstone sample was of moderately- to well-sorted, angular, and fine lithic arenite. The zircon grains we collected were mostly euhedral to subhedral and virtually not abraded, among which 90% were colorless and the others were brown. The zircon grains had columnar shapes with the longer dimension of 60−200 μm, the shorter dimension of 30−120 μm, and the aspect ratio of 1.5−2.5. Most of them showed oscillatory zoning in CL images, and larger zircon grains tended to contain many inclusions and microcracks.

Lower Jurassic Niranohama Formation (Sample 101001-2; N38°41'35.3", E141°30'05.0")

Sample 101001-2 of the Lower Jurassic Niranohama Formation of the Shizugawa Group was collected from the upper part of the formation (Fig. 1), the Niranohama or Hoinyashiki sandstone of Kobayashi and Mori (1955) and Takahashi (1969). The Niranohama Sandstone at this location is probably of Middle Hettangian age, because an ammonoid of this age, *Alsatites* (*Yebisites*) *onoderai*, was reported from the same sandstone close to this location (Matsumoto, 1956). The sandstone sample was of well-sorted, sub-angular, and very fine- to fine-grained feldspathic arenite. Most of the zircon grains we collected were euhedral and colorless, having columnar shapes with the longer dimension of 100−600 μm, the shorter dimension of 30−150 μm, and the aspect ratio of 1.5−5.0. Most of them showed oscillatory zoning in CL images, and larger zircon grains tended to contain many inclusions and microcracks.

Middle Jurassic Aratozaki Formation (Sample 120612-4; N38°41'46.3", E141°29'54.7")

Sample 120612-4 of the Middle Jurassic Aratozaki Formation of the Hashiura Group was collected from the horizon approximately 10 m above the base of the formation (Fig. 1) and is probably of Aalenian–Bajocian age. The sandstone sample was of ill-sorted, sub-angular, and fine- to medium-grained lithic arenite. The zircon grains we collected were mostly euhedral, among which 80% were colorless and the others were brown. The zircon grains had columnar shapes with the longer dimension of 50−180 μm, the shorter dimension of 20−80 μm, and the aspect ratio of 1.5−3.0. Most of them showed oscillatory zoning in CL images, and many zircon grains contained inclusions and microcracks.

Upper Jurassic Sodenohama Formation (Sample 101001-3; N38°40'22.9", E141°28'05.2")

Sample 101001-3 of the Upper Jurassic Sodenohama Formation of the Hashiura Group was collected from the middle part of the formation on the coast near the Sodenohama Beach, 2 km to ESE from the center of the Minamisanriku Town, Miyagi Prefecture (Fig. 1). The Sodenohama Formation at this location is probably of Kimmeridgian age (Takahashi, 1969). The sandstone sample was of moderately-sorted, sub-angular to sub-rounded, and fine-grained lithic arenite. The zircon grains we collected were mostly euhedral to anhedral and colorless, having columnar shapes with the longer dimension of 180−700 μm, the shorter dimension of 100−200 μm, and the aspect ratio of 1.5−3.0. Most of them showed oscillatory zoning in CL images, and many zircon grains contained inclusions and microcracks.

Upper Jurassic Oginohama Formation (Sample 100416-5; N38°18'16.3", E141°29'50.2")

Sample 100416-5 of the Upper Jurassic Oginohama Formation of the Oshika Group was collected from the Fukiura Shale and Sandstone Member at the eastern end of the Kukunarihama Beach, Ishinomaki City, Miyagi Prefecture (Fig. 1), and is probably of Tithonian age. The sandstone sample was of ill-sorted, sub-angular, and fine- to medium-grained lithic arenite. The lithic fragments were mostly volcanic-rock fragments with minor polycrystalline quartz grains. The zircon grains we collected were euhedral or subhedral and virtually not abraded, among which 80% were colorless and the others were brown. The zircon grains had columnar shapes with the longer dimension of 120−600 μm, the shorter dimension of 120−200 μm, and the aspect ratio of 1.5−2.5. All of them showed oscillatory zoning in CL images and contained inclusions and microcracks.

Lower Cretaceous Yoshihama Formation (Sample 101002-1; N38°34'25.4", E141°26'52.9")

Sample 101002-1 of the Lower Cretaceous Yoshihama Formation of the Jusanhama Group was collected from the upper part of the formation at Jusanhama-Tsukihama, Ishinomaki City, Miyagi Prefecture (Fig. 1). The sandstone sample was of well-sorted, sub-angular, and fine-grained feldspathic arenite. The zircon grains we collected were mostly euhedral, among which 90% were colorless and the others were brown. The zircon grains had columnar shapes with the longer dimension of 100−500 μm, the shorter dimension of 80−200 μm, and the aspect ratio of 1.0−2.5. Most of them showed oscillatory zoning in CL images, and approximately 20% of these zircon grains, larger ones in particular, contained inclusions and microcracks.

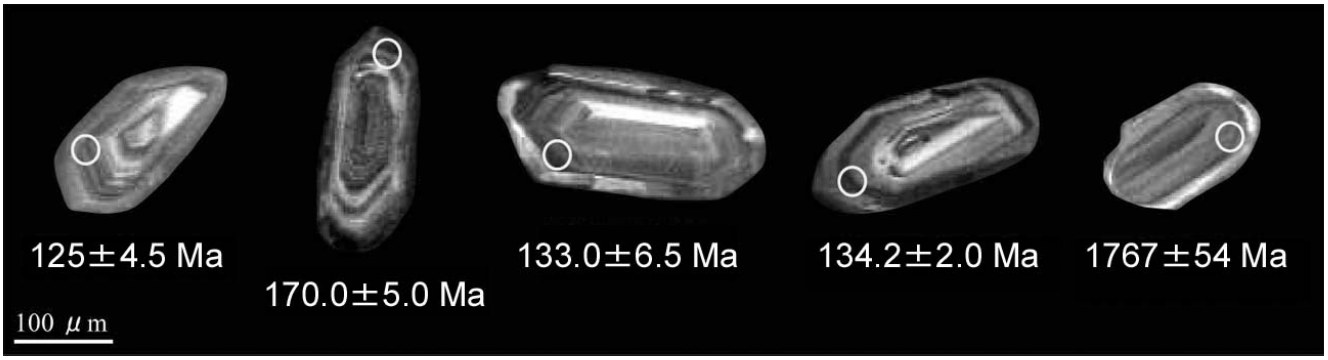

FIGURE 4. Cathodoluminescence images of some zircons from the Domeki Sandstone Member of the Ayukawa Formation, Oshika Group (sample 100416-4) .

Lower Cretaceous Ayukawa Formation (Sample 100416-4; N38°17'29.8", E141°30'36.8")

Sample 100416-4 of the Lower Cretaceous Ayukawa Formation of the Oshika Group was collected from the Domeki Sandstone Member at the southeastern end of Ayukawa Port (Fig. 1), and must be of Valanginian or younger age. The sandstone sample was of ill-sorted, angular, and very coarse- to coarse-grained lithic wacke. The lithic fragments were mainly polycrystalline quartz grains with some volcanic-rock fragments. The zircon grains we collected were mostly euhedral, among which 90% were colorless and the others were brown. The zircon grains had columnar shapes with the longer dimension of 60−180 μm, the shorter dimension of 30−100 μm, and the aspect ratio of 1.0−2.5. Most of them showed oscillatory zoning in CL images (Fig. 3), and approximately 20% of these zircon grains, larger ones in particular, contained inclusions and microcracks.

ANALYTICAL METHOD

The zircon samples for analyses were prepared in accordance with the procedures described in Kawagoe et al. (2012). The measurement was carried out on laser ablation inductively coupled plasma mass spectrometers (LA-ICPMS) equipped in the (1) Department of Earth and Planetary Sciences, Graduate School of Science and Engineering, Tokyo Institute of Technology (TITech; former Hirata Laboratory), (2) Earthquake Research Institute of the University of Tokyo (ERI), and (3) Graduate School of Environmental Studies, Nagoya University (NU).

The ICPMS instrument equipped in TITech was a Thermo Electron VG Plasma Quad 2 quadropole-based ICPMS applied with a chicane-type ion lens system and connected with a MicroLas GeoLas 200CQ laser ablation system, which utilizes 193 nm wave-length ArF excimer laser (Iizuka and Hirata, 2004). The measurement conditions were as follows: the ablation pit size of 16−32 μm, energy density of 7−8 J/cm^{-2}, and pulse repetition rate of 5−10 Hz. The analyses were carried out in a peak-jumping mode and the peaks of ^{202}Hg, ^{206}Pb, ^{207}Pb, ^{208}Pb,^{232}Th, and ^{238}U were monitored. Data were acquired in sequences of 30 analyses, consisting of an analysis of gas blank, 4 NIST (National Institute of Standards and Technology, U.S.A.) SRM 610 glass standard, 4 standard zircon (91500 zircon with the ^{206}Pb/^{238}U age of 1062.4 ± 0.4 Ma; Wiedenbeck et al., 1995), 1 gas blank, 10 unknown, 4 SRM 610 standard, 4 91500 zircon, and 1 gas blank.

The ICPMS instrument equipped in ERI was a Thermo Elemental Plasma Quad 3 quadropole-based ICPMS connected with a New Wave UP-213 LA system, which used the frequency quintupled Nd-YAG 213-nm wavelength (Orihashi et al., 2008). The measurement conditions were as follows: the ablation pit size of 30 μm, energy density of 11−13 J/cm^{-2}, and pulse repetition rate of 10 Hz. The analyses were carried out in a peak-jumping mode and the peaks of ^{202}Hg, ^{206}Pb, ^{207}Pb, ^{208}Pb, ^{232}Th, and ^{238}U were monitored. Data were acquired in sequences of 28 analyses, consisting of 5 analyses of gas blank, 4 SRM 610 glass standard, 1 standard zircon (91500 zircon), 9 unknown, 4 SRM 610 standard, and 5 gas blank.

The ICPMS instrument equipped in NU was an Agilent 7700x quadropole-based ICPMS connected with a New Wave Research NWR-213-type LA system, which used the frequency quintupled Nd-YAG 213-nm wavelength. The measurement conditions, optimized to reduce matrix effects, were as follows: energy density of 11.7 J/cm^{-2}, pulse repetition rate of 10 Hz, pre-ablation time of 8 s, ablation time of 10 s, and the ablation pit size of 25 μm (Kouchi et al., 2012). The analyses were carried out in a peak-jumping mode and the peaks of ^{202}Hg, ^{206}Pb, ^{207}Pb, ^{208}Pb, ^{232}Th, and ^{238}U were monitored. Data were acquired in the same sequences with the ERI system.

Analytical bias among three laboratories was tested by using OD-3 zircon standard. The bias was within the range of their analytical errors (Iwano et al., 2013) and is neglected in the following discussion.

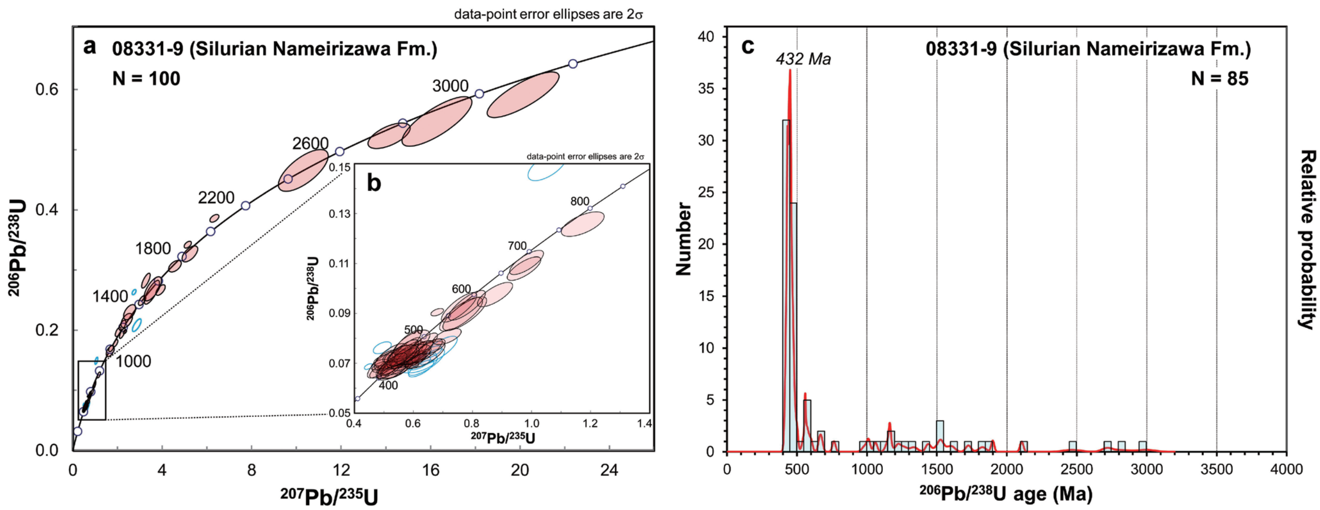

FIGURE 5. Analytical data of detrital zircons from sandstone of the Silurian Nameirizawa Formation (sample 08331-9). **a,** Concordia diagram for all data; **b,** Concordia diagram for 850−350 Ma data set; **c,** Probability density plot and histogram. Open (blue) circles in the concordia diagrams from Fig. 5 to Fig. 20 show the analytical data for discordant grains. Abbreviations (Figs. 5–20)—Fm.: Formation, N: total number of analyses.

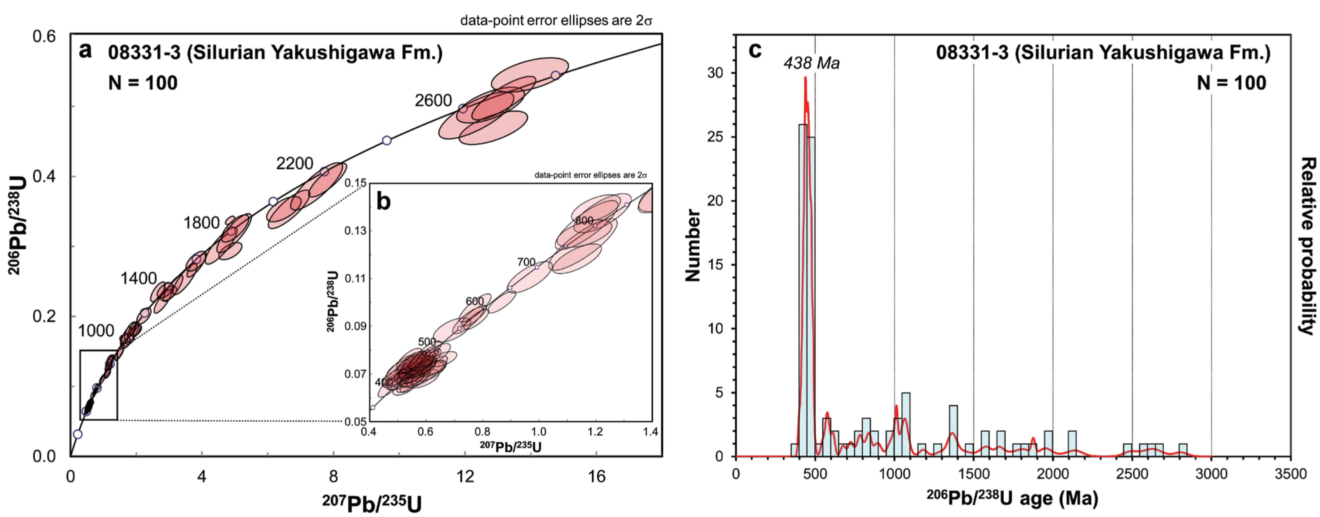

FIGURE 6. Analytical data of detrital zircons from sandstone of the Silurian Yakushigawa Formation (sample 08331-3). **a,** Concordia diagram for all data; **b,** Concordia diagram for 850−350 Ma data set; **c**, Probability density plot and histogram.

RESULTS

We sampled an outer part (rim or mantle) of collected zircon grains with the laser ablation technique, and analyzed with an ICPMS. After the analyses we first distinguished age clusters on a concordia diagram. Then we chose grains with the % conc value (100•(^{206}Pb/^{238}U age)/(^{207}Pb/^{235}U age)) between 90 and 110 and drew a probability density plot and a histogram with the data interval of 50 Myr (^{206}Pb/^{238}U age). The data processing was carried out using the Isoplot 3.70 software (Ludwig, 2008). Here follow the results of our analyses.

Silurian Nameirizawa Formation (Sample 08331-9)

We obtained 100 analyses from 97 zircon grains collected from sample 08331-9 of the Silurian Nameirizawa Formation in TITech; we sampled the outer and inner parts of 3 zircon grains. Detrital zircons were divided into 5 age groups on the concordia

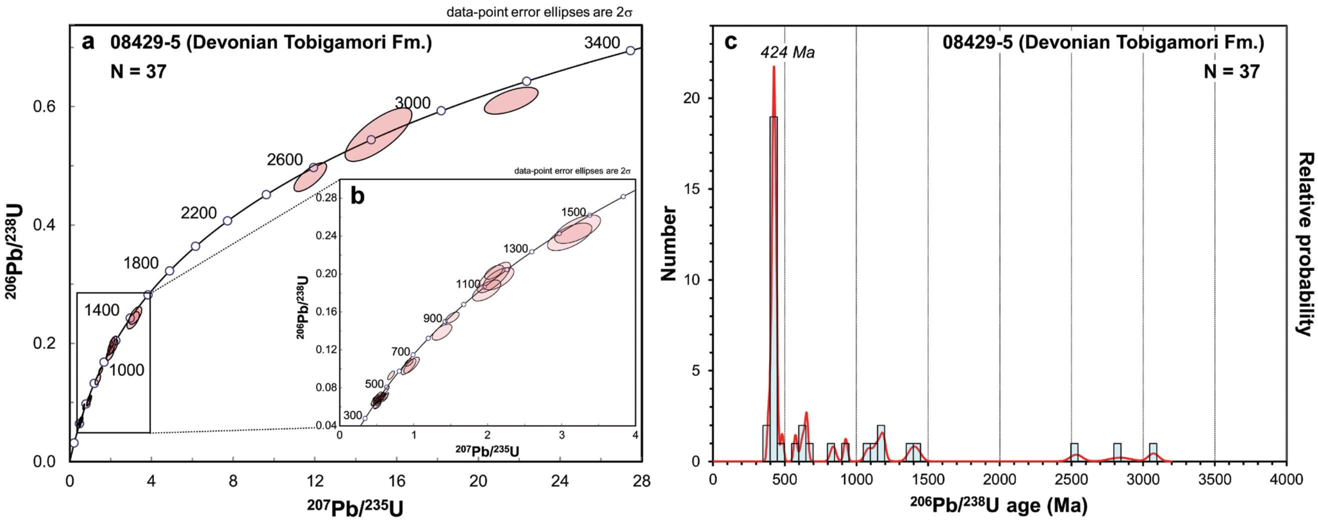

FIGURE 7. Analytical data of detrital zircons from sandstone of the Upper Devonian Tobigamori Formation (sample 08429-5). **a,** Concordia diagram for all data; **b,** Concordia diagram for 1600−300 Ma data set; **c,** Probability density plot and histogram.

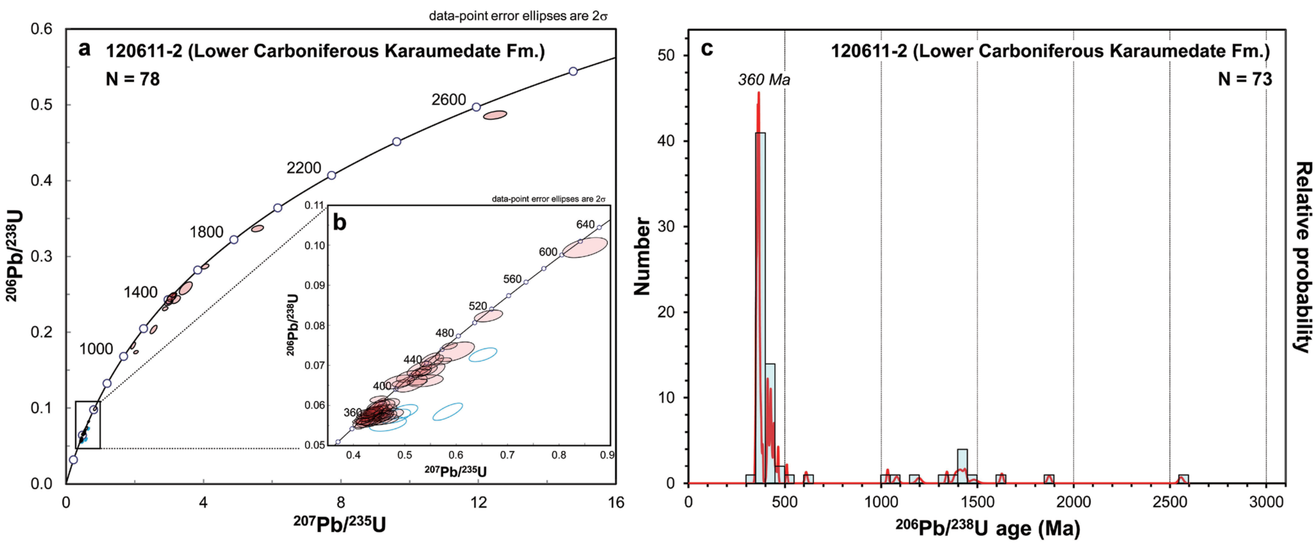

FIGURE 8. Analytical data of detrital zircons from sandstone of the Lower Carboniferous Karaumedate Formation (sample 120611-2). **a,** Concordia diagram for all data; **b,** Concordia diagram for 640−320 Ma data set; **c,** Probability density plot and histogram.

diagram (Fig. 5a, b): 698−403 Ma (73%), 1087−945 Ma (4%), 1390−1111 Ma (7%), 1620−1402 Ma (5%), and 2955−2642 Ma (2%). We further chose 85 concordant grains with the % conc value between 90 and 110 and drew a probability density plot and a histogram with the data interval of 50 Myr ($^{206}Pb/^{238}U$ age; Fig. 5c). The histogram showed a multimodal pattern with the youngest concordant age of 416 ± 13 Ma (2σ) and %Pc of 36.5. The youngest peak on the probability density plot was 432 Ma. The Th/U ratio of each analysis was 0.22−2.22 and fell in the range of igneous zircon, Th/U>0.1 (Rubatto and Hermann, 2003).

Silurian Yakushigawa Formation (Sample 08331-3)

We obtained 100 analyses from 100 zircon grains collected from sample 08331-3 of the Silurian Yakushigawa Formation in TITech. Detrital zircons were divided into 5 age groups on the concordia diagram (Fig. 6a, b): 868−385 Ma (65%), 1232−845

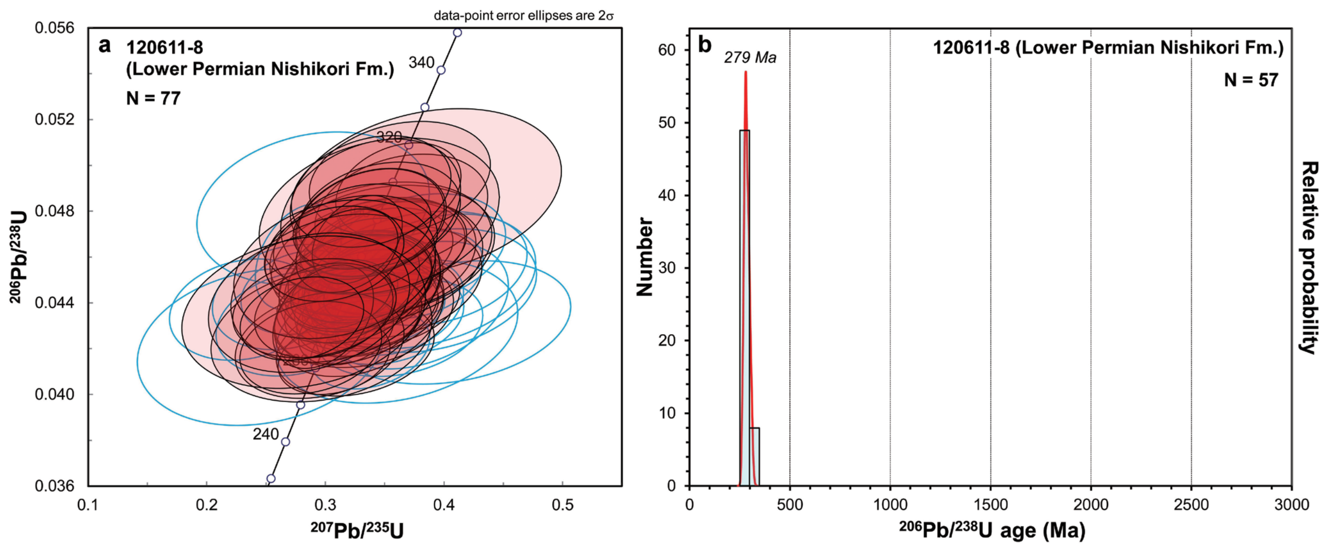

FIGURE 9. Analytical data of detrital zircons from sandstone of the Lower Permian Nishikori Formation (sample 120611-8). **a,** Concordia diagram for all data; **b,** Probability density plot and histogram.

Ma (13%), 1899−1220 Ma (13%), 2238−1845 Ma (4%), and 2891−2398 Ma (5%). All of the 100 grains had the % conc value between 90 and 110. The histogram of the $^{206}Pb/^{238}U$ ages of 100 concordant grains showed a multimodal pattern with the youngest concordant age of 398 ± 13 Ma and %Pc of 48.0. The youngest peak on the probability density plot was 438 Ma (Fig. 6c). The Th/U ratio of each analysis was 0.11−1.77 and fell in the range of igneous zircon.

Devonian Tobigamori Formation (Sample 08429-5)

We obtained 37 analyses from 37 zircon grains collected from sample 08429-5 of the Upper Devonian Tobigamori Formation in TITech. Detrital zircons were divided into 4 age groups on the concordia diagram (Fig. 7a, b): 503−367 Ma (59%), 673−589 Ma (8%), 1220−1033 Ma (11%), and 1449−1322 Ma (5%). The histogram of the $^{206}Pb/^{238}U$ ages of 37 concordant grains showed a multimodal pattern with the youngest concordant age of 386 ± 19 Ma and %Pc of 40.5. The youngest peak on the probability density plot was 424 Ma (Fig. 7c). The Th/U ratio of each analysis was 0.20−2.15 and fell in the range of igneous zircon.

Lower Carboniferous Karaumedate Formation (Sample 120611-2)

We obtained, in ERI, 78 analyses from 78 zircon grains collected from sample 120611-2 of the Lower Carboniferous Karaumedate Formation. Detrital zircons were divided into 3 age groups on the concordia diagram (Fig. 8a, b): 389−341 Ma (58%), 470−405 Ma (22%), and 1451−1365 Ma (7%). The histogram of the $^{206}Pb/^{238}U$ ages of 73 concordant grains showed a multimodal pattern with the youngest concordant age of 348.9 ± 7.8 Ma and %Pc of 19.2. The youngest peak on the probability density plot was 360 Ma (Fig. 8c). The Th/U ratio of each analysis was 0.23−1.20 and fell in the range of igneous zircon.

Lower Permian Nishikori Formation (Sample 120611-8)

We obtained 77 analyses from 77 zircon grains collected from sample 120611-8 of the Lower Permian Nishikori Formation in NU. Detrital zircons formed a single cluster on the concordia diagram at 324−255 Ma (100%; Fig. 9a). The histogram of the $^{206}Pb/^{238}U$ ages of 57 concordant grains showed a unimodal pattern with the youngest concordant age of 263.0 ± 8.4 Ma and %Pc of 0. The peak on the probability density plot was 279 Ma (Fig. 9b). The Th/U ratio of each analysis was 0.31−1.16 and fell in the range of igneous zircon.

Upper Permian Toyoma Formation (Sample 101001-1)

We obtained 70 analyses from 70 zircon grains collected from sample 101001-1 of the Upper Permian Toyoma Formation in ERI (24 grains) and NU (46 grains). Detrital zircons are divided into 3 age groups on the concordia diagram (Fig. 10a, b): 374−224 Ma (78%), 468−445 Ma (3%), and 530−497 Ma (5%). The histogram of the $^{206}Pb/^{238}U$ ages of 59 concordant grains showed a quasi-unimodal pattern with the youngest concordant age of 227.8 ± 4.3 Ma and %Pc of 8.5. The youngest peak on the probability density plot was 249 Ma (Fig. 10c). The Th/U ratio of each analysis was 0.19−1.79 and fell in the range of igneous zircon.

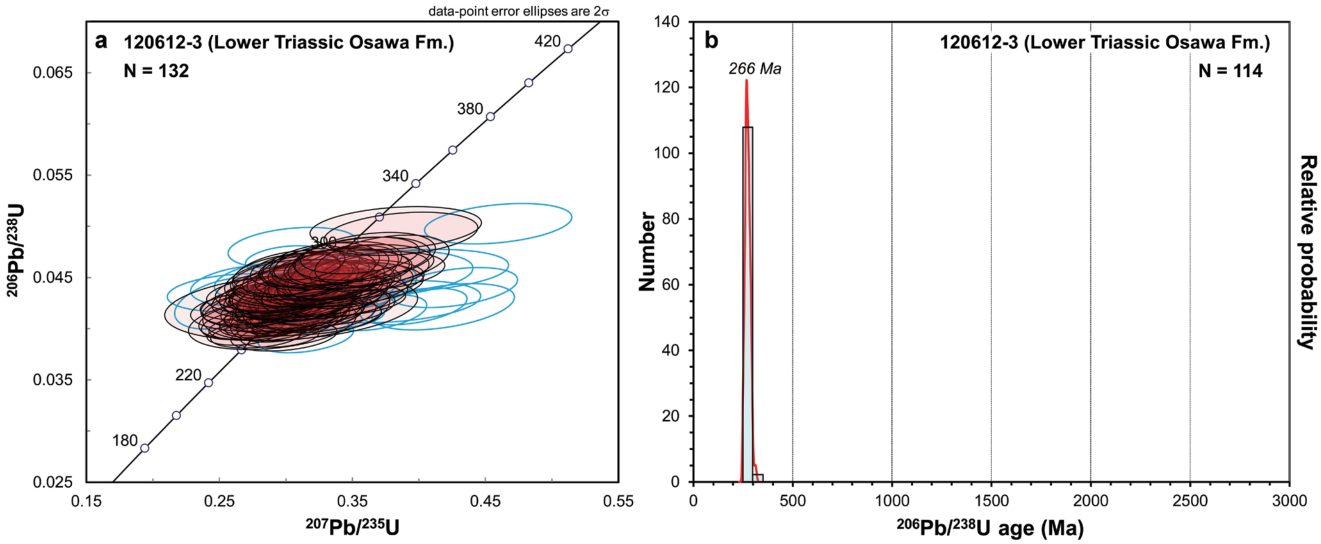

FIGURE 11. Analytical data of detrital zircons from sandstone of the Lower Triassic Osawa Formation of the Inai Group (sample 120612-3). **a,** Concordia diagram for all data; **b,** Probability density plot and histogram.

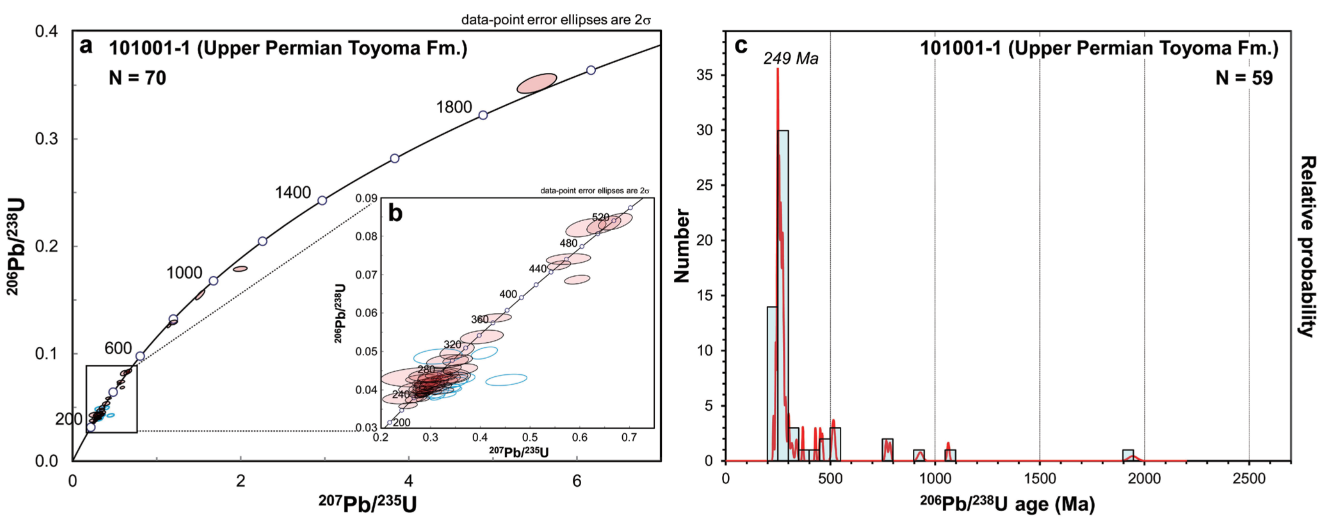

FIGURE 10. Analytical data of detrital zircons from sandstone of the Upper Permian Toyoma Formation (sample 101001-1). **a,** Concordia diagram for all data; **b,** Concordia diagram for 560–200 Ma data set; **c,** Probability density plot and histogram.

Lower Triassic Osawa Formation (Sample 120612-3)

We obtained 132 analyses from 132 zircon grains collected from sample 120612-3 of the Lower Triassic Osawa Formation of the Inai Group in NU. Detrital zircons formed a single cluster on the concordia diagram at 324–243 Ma (100%; Fig. 11a). The histogram of the $^{206}Pb/^{238}U$ ages of 114 concordant grains showed a unimodal pattern with the youngest concordant age of 248.6 ± 5.7 Ma and %Pc of 0. The youngest peak on the probability density plot was 266 Ma (Fig. 11b). The Th/U ratio of each analysis was 0.42–1.09 and fell in the range of igneous zircon.

Middle Triassic Fukkoshi Formation (Sample 120613-2)

We obtained 107 analyses from 107 zircon grains collected from sample 120613-2 of the Middle Triassic Fukkoshi Formation of the Inai Group in NU. Detrital zircons formed a single cluster on the concordia diagram at 336–230 Ma (100%; Fig. 12a). The histogram of the $^{206}Pb/^{238}U$ ages of 90 concordant grains showed a unimodal pattern with the youngest concordant

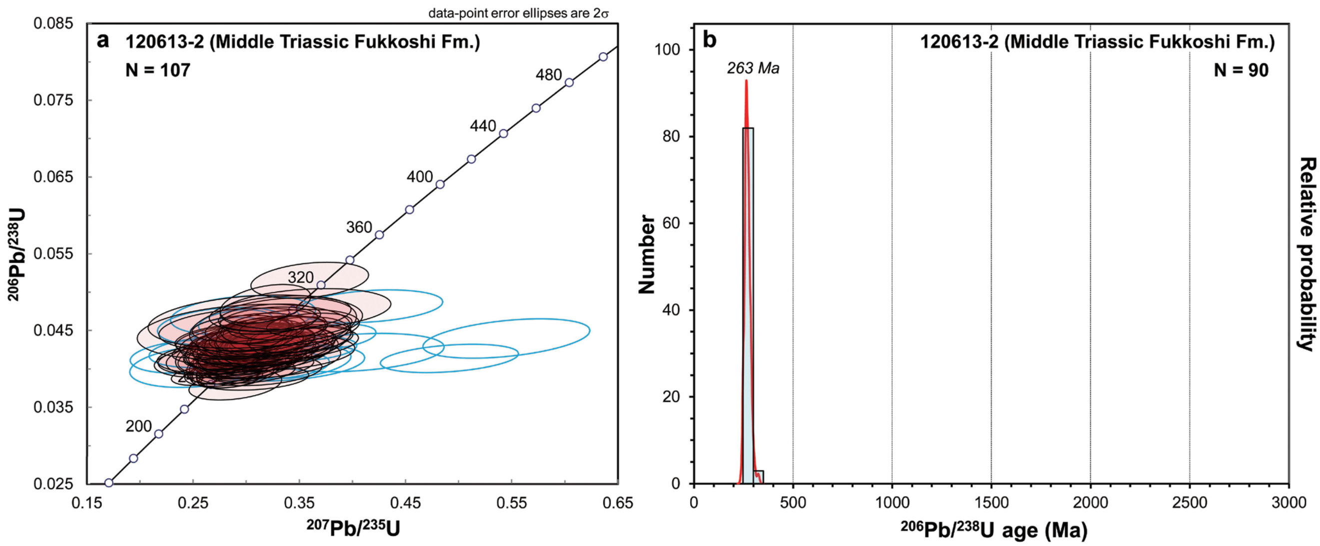

FIGURE 12. Analytical data of detrital zircons from sandstone of the Middle Triassic Fukkoshi Formation of the Inai Group (sample 120613-2). **a,** Concordia diagram for all data; **b,** Probability density plot and histogram.

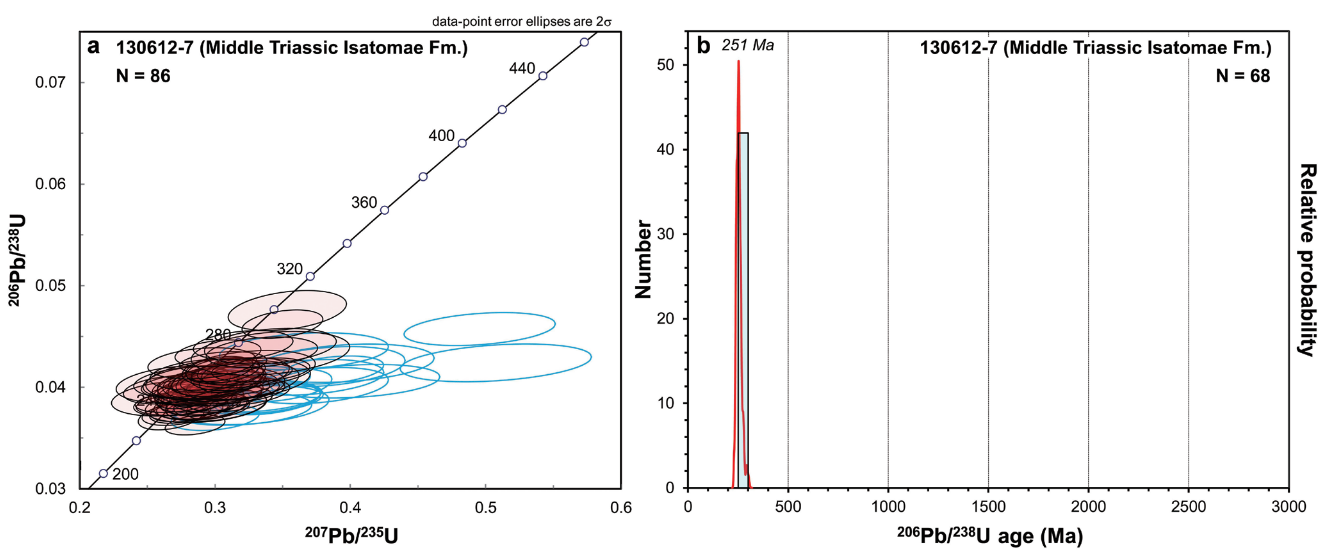

FIGURE 13. Analytical data of detrital zircons from sandstone of the Middle Triassic Isatomae Formation of the Inai Group (sample 130612-7). **a,** Concordia diagram for all data; **b,** Probability density plot and histogram.

age of 240 ± 10 Ma and %Pc of 0. The youngest peak on the probability density plot was 263 Ma (Fig. 12b). The Th/U ratio of each analysis was 0.3−0.9 and fell in the range of igneous zircon.

Middle Triassic Isatomae Formation (Sample 120612-7)

We obtained 86 analyses from 86 zircon grains collected from sample 1230612-7 of the Middle Triassic Isatomae Formation of the Inai Group in NU. Detrital zircons formed a single cluster on the concordia diagram at 310−223 Ma (100%; Fig. 13a). The histogram of the $^{206}Pb/^{238}U$ ages of 68 concordant grains showed a unimodal pattern with the youngest concordant age of 230.0 ± 5.1 Ma and %Pc of 0. The youngest peak on the probability density plot was 251 Ma (Fig. 13b). The Th/U ratio of each analysis was 0.37−1.16 and fell in the range of igneous zircon.

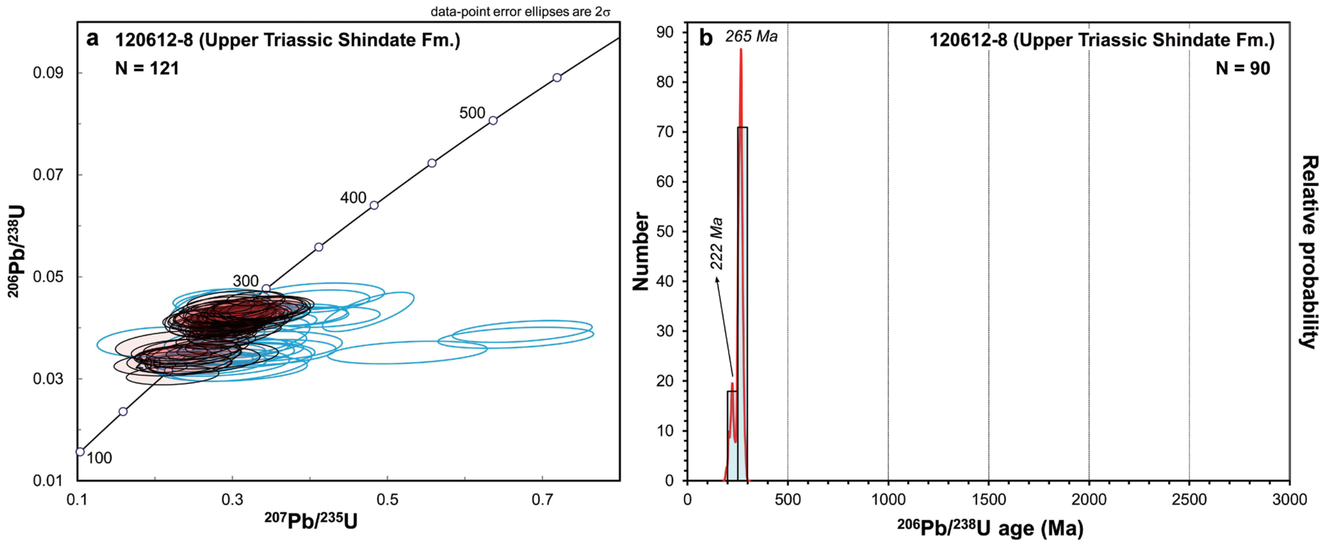

FIGURE 14. Analytical data of detrital zircons from sandstone of the Upper Triassic Shindate Formation of the Saragai Group (sample 120612-8). **a,** Concordia diagram for all data; **b,** Probability density plot and histogram.

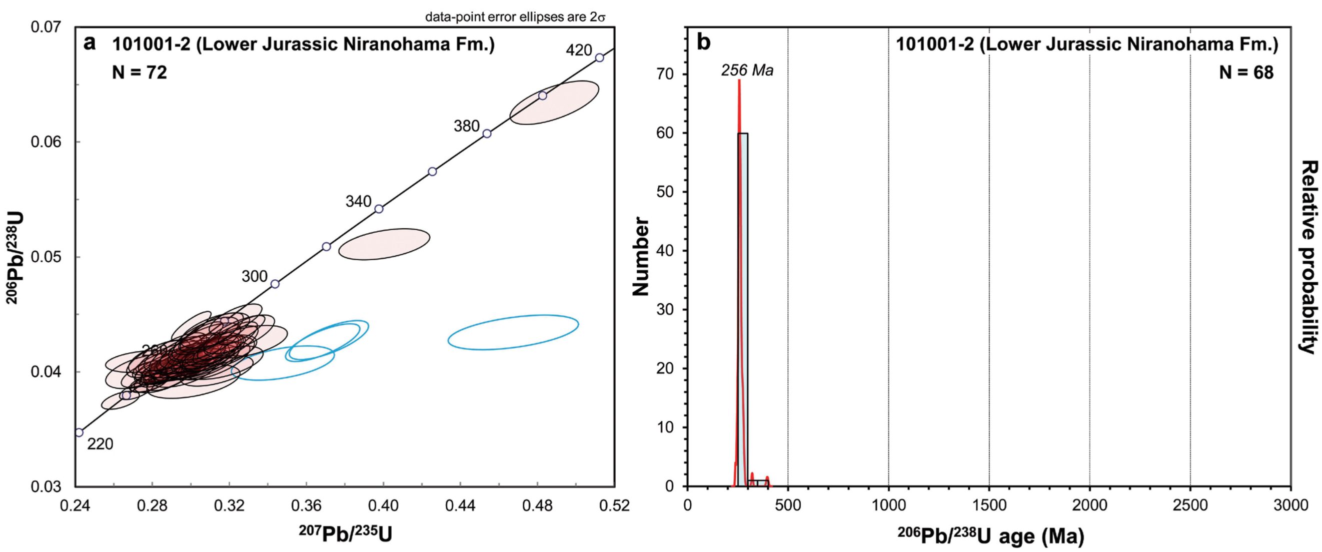

FIGURE 15. Analytical data of detrital zircons from sandstone of the Lower Jurassic Niranohama Formation of the Shizugawa Group (sample 101001-2). **a,** Concordia diagram for all data; **b,** Probability density plot and histogram.

Upper Triassic Shindate Formation (Sample 120612-8)

We obtained 121 analyses from 121 zircon grains collected from sample 120612-8 of the Upper Triassic Shindate Formation of the Saragai Group in NU. Detrital zircons formed a single cluster on the concordia diagram at 296–186 Ma (100%; Fig. 14a). The histogram of the $^{206}Pb/^{238}U$ ages of 90 concordant grains showed a unimodal pattern with the youngest concordant age of 195.1 ± 9.6 Ma and %Pc of 0. The youngest peak on the probability density plot was 222 Ma (Fig. 14b). The Th/U ratio of each analysis was 0.39–1.33 and fell in the range of igneous zircon.

Lower–Middle Jurassic Niranohama Formation (Sample 101001-2)

We obtained 72 analyses from 72 zircon grains collected from sample 101001-2 of the Lower Jurassic Niranohama Formation

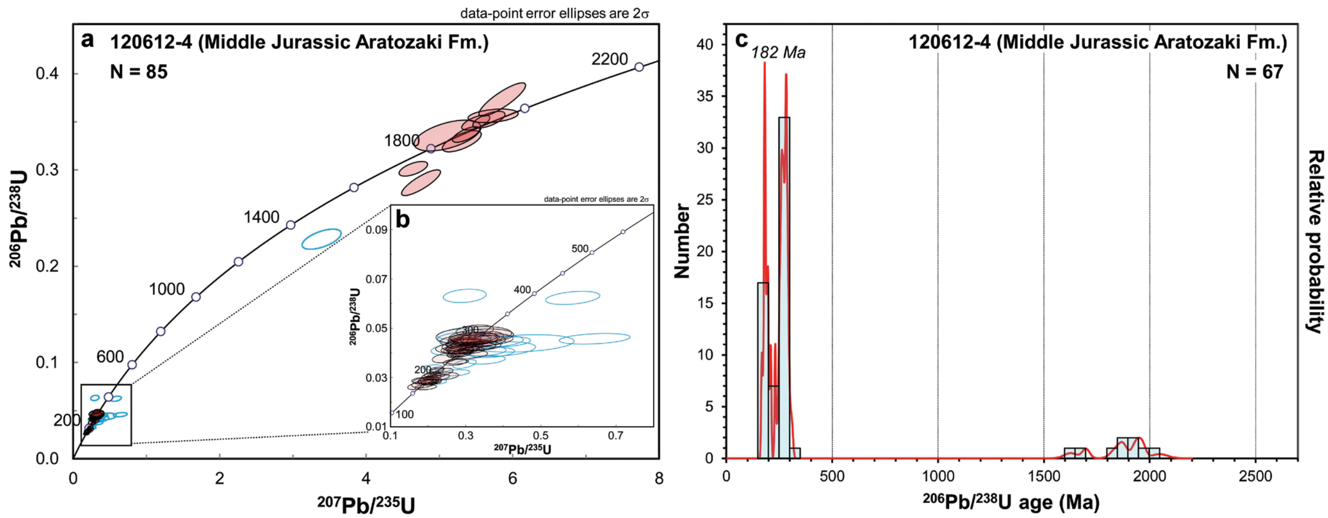

FIGURE 16. Analytical data of detrital zircons from sandstone of the Middle Jurassic Aratozaki Formation of the Hashiura Group (sample 120612-4). **a,** Concordia diagram for all data; **b,** Concordia diagram for 550−150 Ma data set; **c,** Probability density plot and histogram.

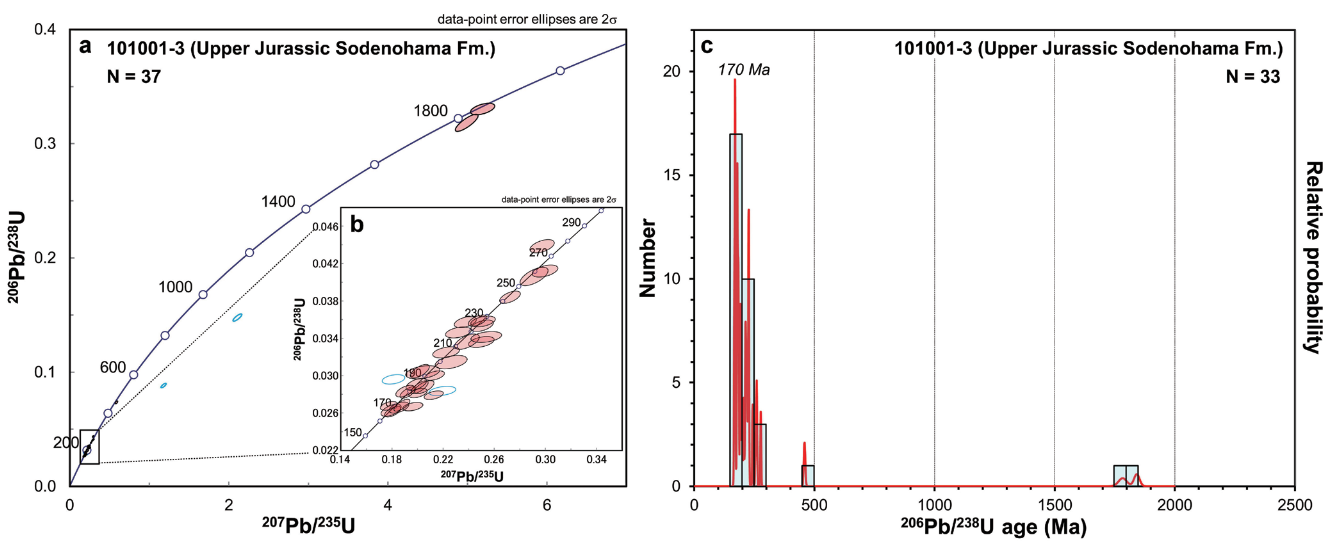

FIGURE 17. Analytical data of detrital zircons from sandstone of the Upper Jurassic Sodenohama Formation of the Hashiura Group (sample 101001-3). **a,** Concordia diagram for all data; **b,** Concordia diagram for 300−150 Ma data set; **c,** Probability density plot and histogram.

of the Shizugawa Group in ERI. Detrital zircons formed a single cluster on the concordia diagram at 288−234 Ma (100%; Fig. 15a). The histogram of the ^{206}Pb/^{238}U ages of 68 concordant grains showed a unimodal pattern with the youngest concordant age of 237.6 ± 4.0 Ma and %Pc of 0. The youngest peak on the probability density plot was 256 Ma (Fig. 15b). The Th/U ratio of each analysis was 0.26−1.28 and fell in the range of igneous zircon.

Middle Jurassic Aratozaki Formation (Sample 120612-4)

We obtained 85 analyses from 85 grains collected from sample 120612-4 of the lower Middle Jurassic Aratozaki Formation of the Hashiura Group in NU. Detrital zircons are divided into 3 age groups on the concordia diagram (Fig. 16a, b): 216−161 Ma (30%, 321−223 Ma (57%), and 2124−1789 Ma (10%). The histogram of the ^{206}Pb/^{238}U ages of 67 concordant grains showed a bimodal pattern with the youngest concordant age of 166.4 ±

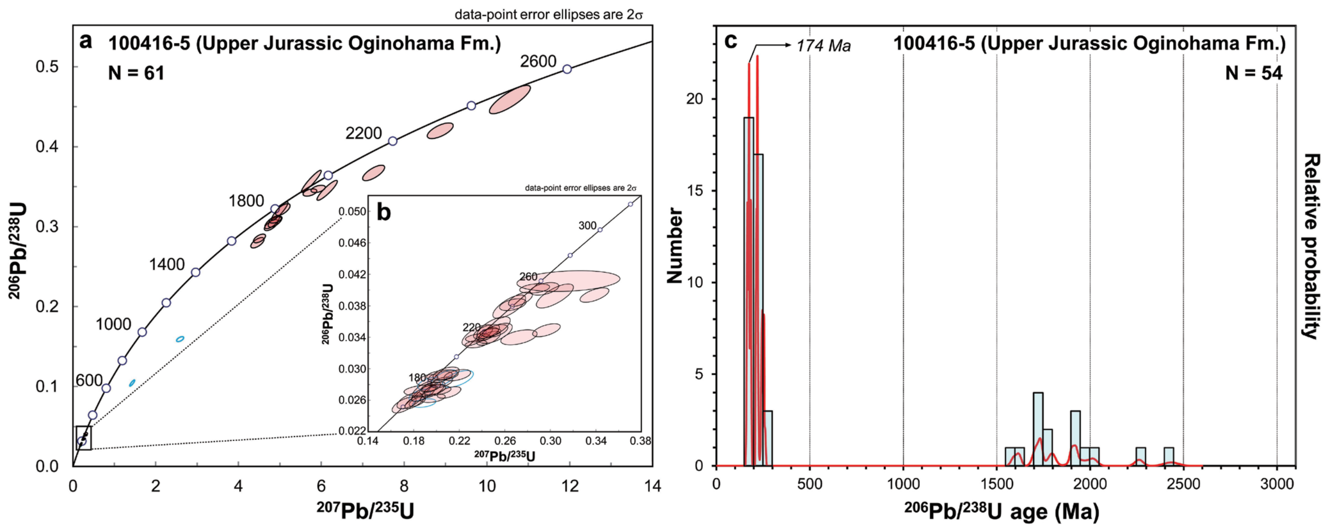

FIGURE 18. Analytical data of detrital zircons from sandstone of the Upper Jurassic Fukiura Shale and Sandstone Member of the Oginohama Formation, Oshika Group (sample 100416-5). **a,** Concordia diagram for all data; **b,** Concordia diagram for 340−150 Ma data set; **c,** Probability density plot and histogram.

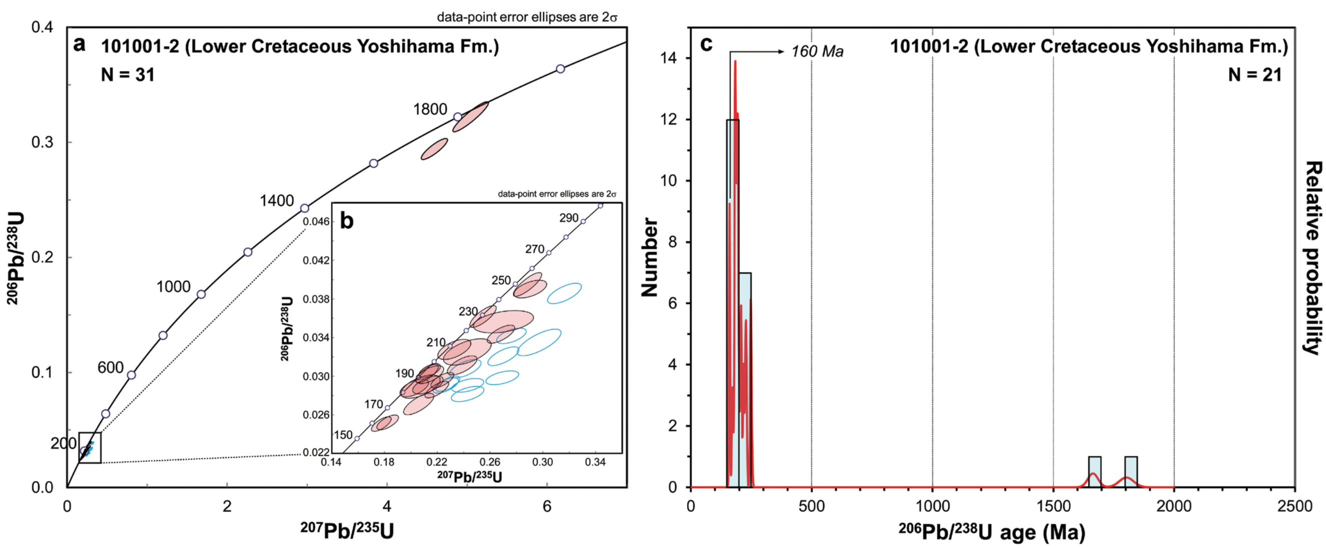

FIGURE 19. Analytical data of detrital zircons from sandstone of the Lower Cretaceous Yoshihama Formation of the Jusanhama Group (sample 101001-2). **a,** Concordia diagram for all data; **b,** Concordia diagram for 310−150 Ma data set; **c,** Probability density plot and histogram.

5.4 Ma and %Pc of 13.4. The youngest peak on the probability density plot was 182 Ma (Fig. 16c). The Th/U ratio of each analysis was 0.10−1.03 and fell in the range of igneous zircon.

Upper Jurassic Sodenohama Formation (Sample 101001-3)

We obtained 37 analyses from 37 zircon grains collected from sample 101001-3 of the Upper Jurassic (Kimmeridgian) Sodenohama Formation of the Hashiura Group in ERI. Detrital zircons are divided into 3 age groups on the concordia diagram (Fig. 17a, b): 231−164 Ma (70%), 264−252 Ma (5%), and 1865−1749 Ma (5%). The histogram of the ^{206}Pb/^{238}U ages of 33 concordant grains showed a bimodal pattern with the youngest concordant age of 166.5 ± 3.0 Ma and %Pc of 7.7. The youngest peak on the probability density plot was 170 Ma (Fig. 17c). The Th/U ratio of each analysis was 0.18−1.49 and fell in the range of igneous zircon.

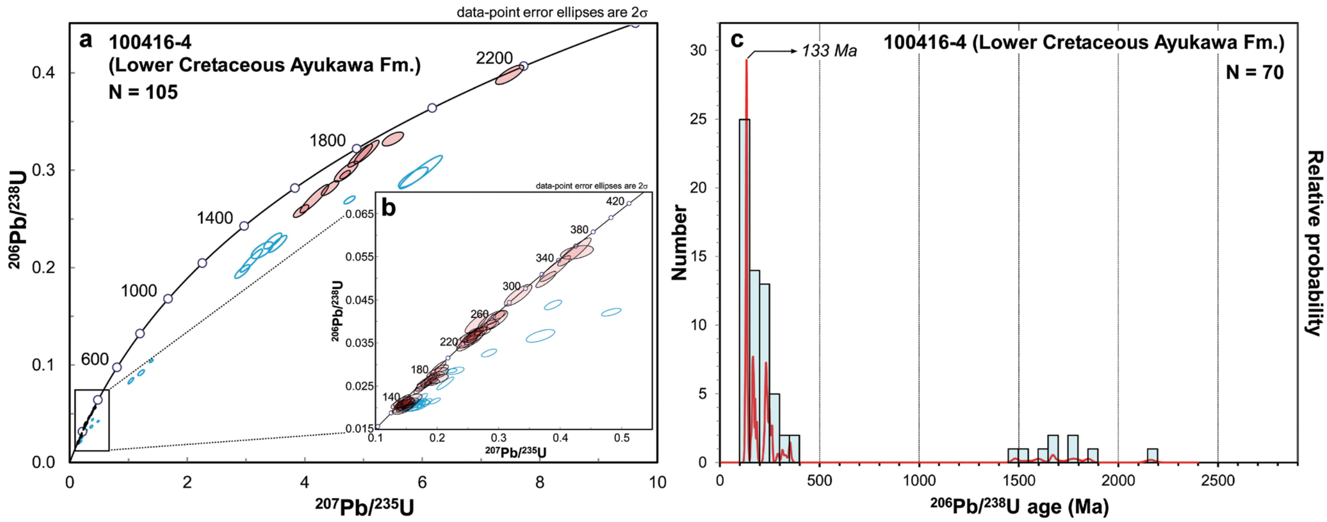

FIGURE 20. Analytical data of detrital zircons from sandstone of the Lower Cretaceous Domeki Sandstone Member of the Ayukawa Formation, Oshika Group (sample 100416-4). **a,** Concordia diagram for all data; **b,** Concordia diagram for 420–120 Ma data set; **c,** Probability density plot and histogram.

Upper Jurassic Oginohama Formation (Sample 100416-5)

We obtained, in ERI, 61 analyses from 61 zircon grains collected from sample 120416-5 of the Tithonian Fukiura Shale and Sandstone Member of the Oginohama Formation, Karakuwa Group. Detrital zircons are divided into 5 age groups on the concordia diagram (Fig. 18a, b): 191–157 Ma (35%), 267–208 Ma (37%), 1645–1562 Ma (4%), 1831–1671 Ma (11%), and 2030–1881 Ma (7%). The histogram of the $^{206}Pb/^{238}U$ ages of 54 concordant grains showed a bimodal pattern with the youngest concordant age of 161.7 ± 5.2 Ma and %Pc of 27.8. The youngest peak on the probability density plot was 174 Ma (Fig. 18c). The Th/U ratio of each analysis was 0.15–1.14 and fell in the range of igneous zircon.

Lower Cretaceous Yoshihama Formation (Sample 101002-1)

We obtained 31 analyses from 31 zircon grains collected from sample 101002-1 of the Lower Cretaceous Yoshihama Formation of the Jusanhama Group in ERI. Detrital zircons are divided into 3 age groups on the concordia diagram (Fig. 19a, b): 165–156 Ma (10%), 235–167 Ma (74%), and 256–242 Ma (10%). The histogram of the $^{206}Pb/^{238}U$ ages of 21 concordant grains showed a bimodal pattern with the youngest concordant age of 159.6 ± 3.9 Ma and %Pc of 9.5. The youngest peak on the probability density plot was 160 Ma (Fig. 19c). The Th/U ratio of each analysis was 0.15–1.43 and fell in the range of igneous zircon.

Lower Cretaceous Ayukawa Formation (Sample 100416-4)

We obtained, in ERI, 105 analyses from 105 zircon grains collected from sample 100416-4 of the Valanginian or younger Domeki Sandstone Member of the Ayukawa Formation, Oshika Group. Detrital zircons are divided into 4 age groups on the concordia diagram (Fig. 20a, b): 147–120 Ma (36%), 268–149 Ma (44%), 369–303 Ma (6%), and 1840–1451 Ma (10%). The histogram of the $^{206}Pb/^{238}U$ ages of 70 concordant grains showed a bimodal pattern with the youngest concordant age of 125.9 ± 6.3 Ma and %Pc of 15.3. The youngest peak on the probability density plot was 133 Ma. The Th/U ratio of each analysis was 0.12–1.99 and fell in the range of igneous zircon (Fig. 20c).

DISCUSSION

Comparison of the new U-Pb ages and the age of deposition of the studied samples

The accuracy of the U-Pb isotopic ratios obtained with the ICPMS instruments is guaranteed by comparing the weighted mean of several tens of measurements of a standard zircon and the published ID-TIMS (isotope dilution-thermal ionization mass spectrometry) or SHRIMP data for the same zircon. The weighted mean shows good agreement with the published isotopic ratio within ± 2% (e.g., Orihashi et al., 2008). Hence the weighted mean of the youngest age cluster, which is usually close to the youngest peak age in the probability density plot, is a good measure of the depositional age, provided that syn-sedimentary volcanism in the hinterland supplied certain amount of igneous zircons to the measured sample. Figure 21 compares, for each sample, the youngest peak age in the probability density plot and the biostratigraphical age-range, i.e., the age-range previously inferred from stratigraphy and index fossils. For all samples except sample 101001-1 (Upper Permian Toyoma Formation), the youngest peak age falls in the biostratigraphical

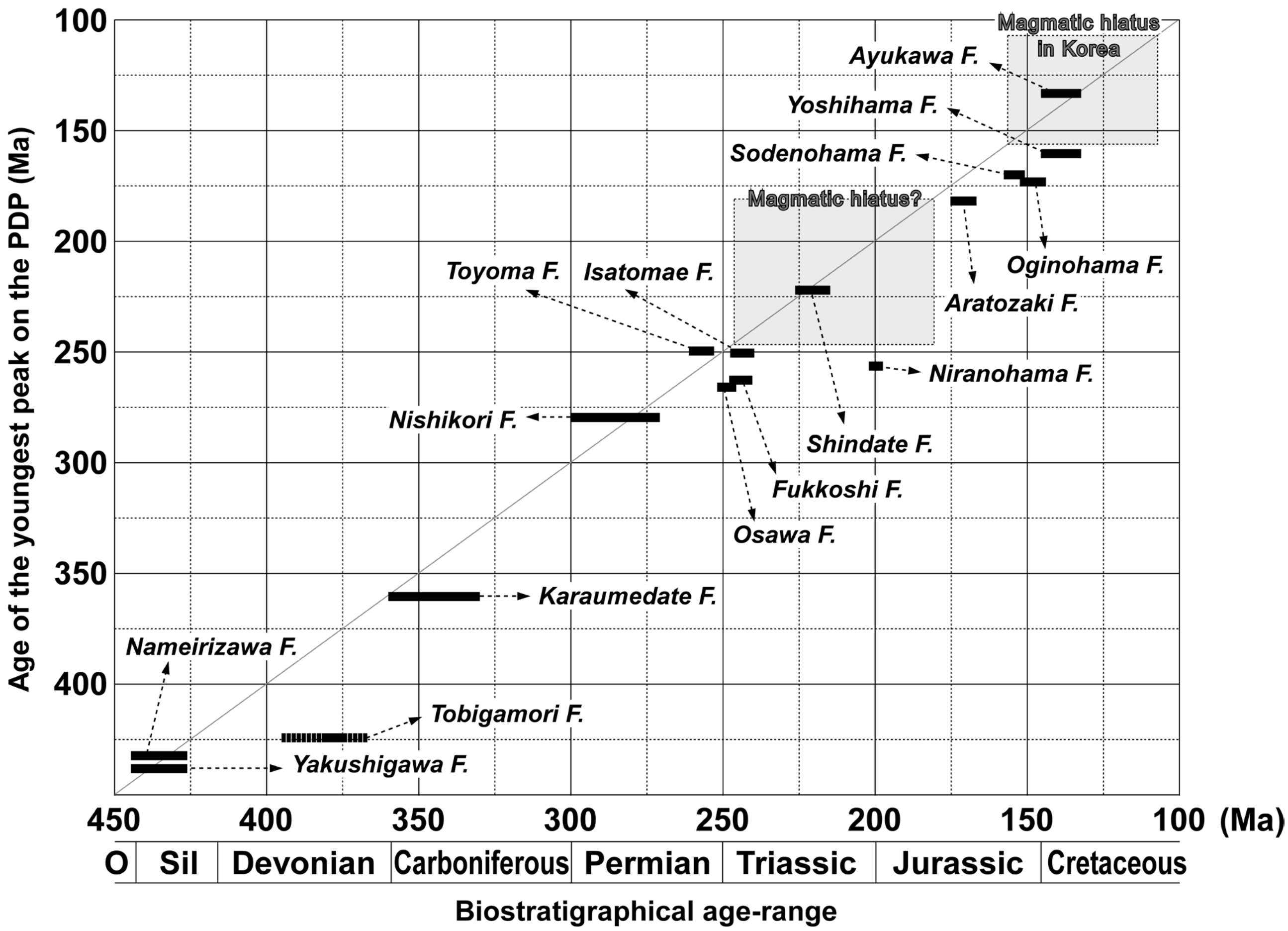

FIGURE 21. Diagram comparing the youngest peak age in the probability density plot (PDP; ordinate) and biostratigraphical age-range (abscissa). The age-range of the magmatic hiatus in Korea (158−110 Ma) and a possible magmatic hiatus during the Triassic and the Early Jurassic are also shown. Abbreviations—F.: Formation, O: Ordovician, Sil: Silurian.

age-range or older than it. Thus we are convinced that the results of our measurement are mostly concordant with the litho- and biostratigraphy of the SKB.

The youngest peak ages of the following formations are significantly older than the biostratigraphical ages: Middle Triassic to Lower Jurassic formations (Osawa, Fukkoshi, and Niranohama formations) and Middle Jurassic to Lower Cretaceous formations (Aratozaki, Sodenohama, Oginohama, and Yoshihama formations; Fig. 21). The fact suggests that there were no significant syn-sedimentary volcanism in Middle Triassic–Early Jurassic times and Middle Jurassic–Early Cretaceous times. The latter interval falls within the magmatic hiatus in Korea, 158−110 Ma (Sagong et al., 2005), and likely indicates its influence to the South Kitakami Paleoland.

Three tectonic stages of the South Kitakami Paleoland

Provenance analysis based on detrital zircon ages has been carried out in various parts of the world including eastern Asia (e.g., Darby and Gehrels, 2006; Rojas-Agramonte et al., 2011; Yao et al., 2011, 2012; Diwu et al., 2012). According to these studies, the sand and sandstones of the North China Block are characterized by the abundance of 2.5 Ga and 1.85 Ga zircons and absence or very rare occurrence of Neoproterozoic zircons (Darby and Gehrels, 2006; Diwu et al., 2012; Choi et al., 2013). 2.5 Ga was the age of a major tectonothermal event associated with the crustal growth of the North China Block (Diwu et al., 2012). 1.85 Ga was the age of crustal assembly in the North China Block associated with the formation of the supercontinent Columbia (e.g., Rogers and Santosh, 2002; Zhao et al., 2004). Grenvillian tectonothermal event (1250−980 Ma) related to the formation of the supercontinent Rodinia was not recorded in the North China Block, which was isolated following the breakup of Rodinia (Yin and Nie, 1996). Zircons formed during the Grenvillian tectonothermal event are well preserved in the sand and sandstones of the South China Block (Yangtze and Cathaysia blocks), Australia, and some blocks in the CAOB including the Tarim Block (e.g., Rino et al., 2008; Iizuka et al.,

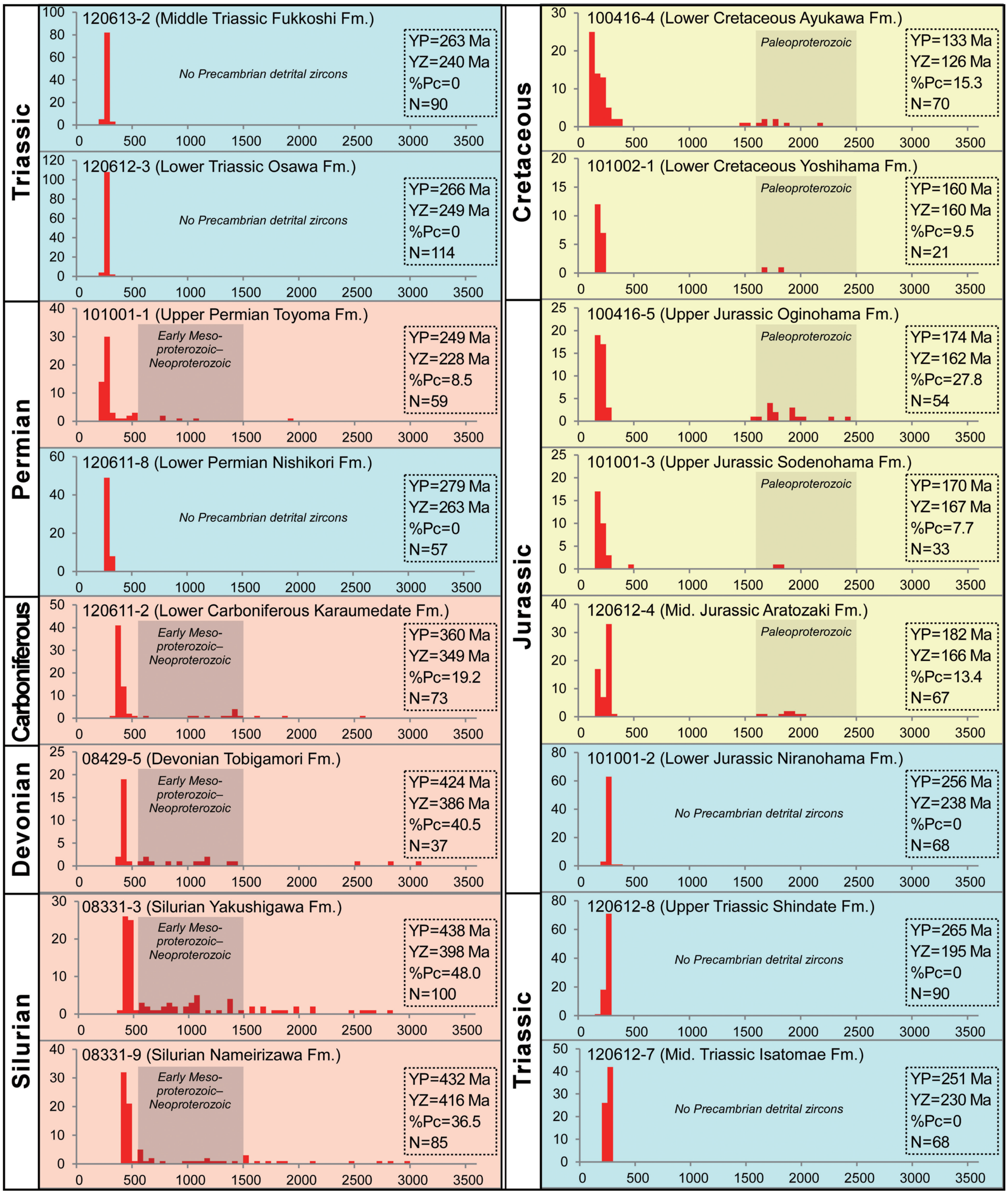

FIGURE 22. Histograms showing the age distributions of detrital zircon grains of all sandstone samples described in this study. The horizontal axes are for the age of zircon grains (best estimate in Ma) and the vertical axes are for the number of grains. Abbreviations—Fm.: Formation, N: total number of analyses, YP: age of the youngest peak in the probability density plot, YZ: age of the youngest zircon.

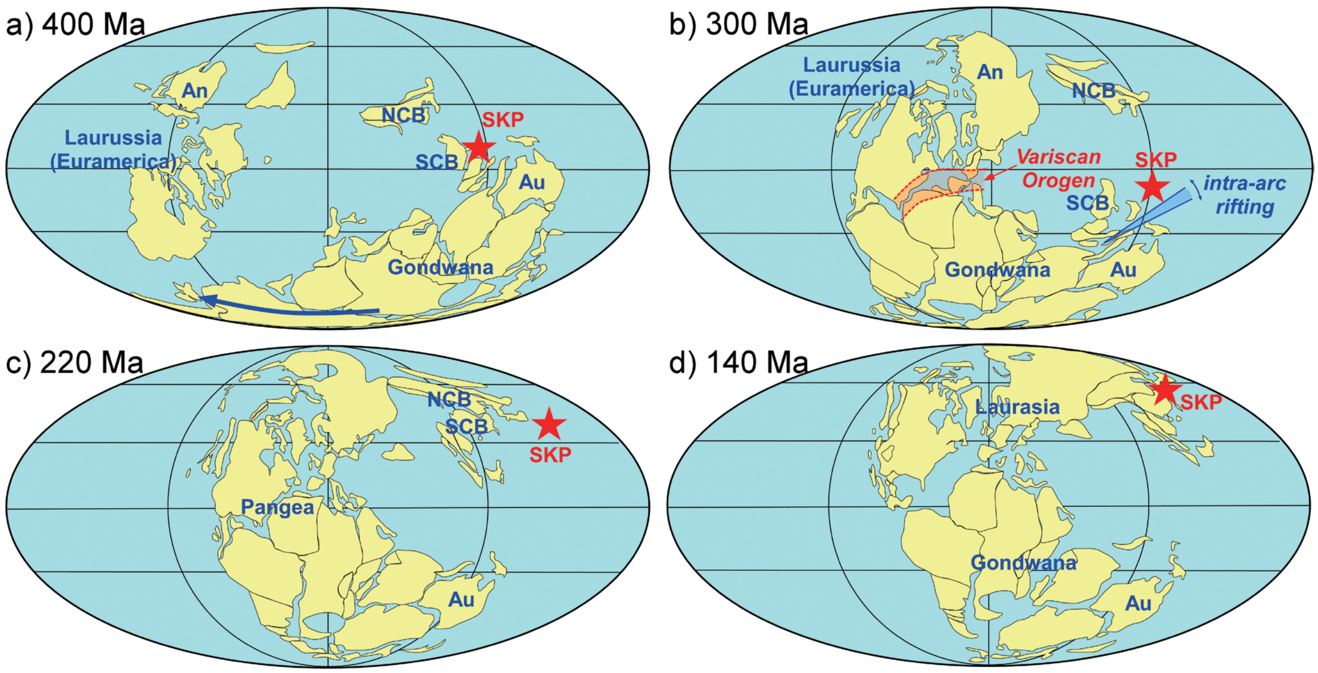

FIGURE 23 Plate reconstruction maps showing the position of the South Kitakami Paleoland at each period. The base reconstruction maps are taken from Lawver et al. (2009). **a,** 400 Ma (Early Devonian); **b,** 300 Ma (end Carboniferous); **c,** 220 Ma (Late Triassic); **d,** 140 Ma (end Jurassic). Abbreviations—An: Angara Craton, Au: Australia, NCB: North China Block, SCB: South China Block, SKP: South Kitakami Paleoland.

2010; Rojas-Agramonte et al., 2011; Yao et al., 2011, 2012; Diwu et al., 2012; Choi et al., 2013). All of these blocks were assembled in the northern part of East Gondwana during Early to Middle Paleozoic times (e.g., Scotese and McKerrow, 1990; Turner, 2010; Metcalfe, 2011).

By comparing the age distribution of detrital zircons of the SKB (Fig. 22) with that of Australia and continental blocks in eastern Asia, three stages of tectonic development have been discriminated of the SKB. From the following paragraph, we combine our new data with previous geological studies and present our model for the tectonic development.

Silurian–Early Carboniferous: Magmatic arc in the northern margin of East Gondwana

The age distribution of detrital zircons from the Siluro–Devonian sandstone of the SKB is characterized by more than 50% of syn-sedimentary zircons, i.e., zircons of ca. 500 Ma to the age of sedimentation, and relatively high proportion of Precambrian zircons (%Pc = 36.5−48.0). The abundance of syn-sedimentary detrital zircons, along with the abundant pyroclastic and volcaniclastic rocks in the Siluro–Devonian strata in the SKB, indicates an igneous activity in the provenance. Moreover the relatively high %Pc value suggests that the Siluro–Devonian sandstone was deposited in front of a continental magmatic arc with Precambrian basement rocks. The Precambrian detrital zircons on the concordia diagram shows several small clusters ranging in age from Neoarchean to Neoproterozoic. The presence of Neoarchean to Neoproterozoic zircons including those of Grenvillian times excludes the North China Block from the candidates of the provenance. Considering the facts that the Siluro–Devonian corals, brachiopods, and plants of the SKB have affinities with those of Australia, South China, and the southern part of the CAOB (e.g., Hamada, 1960; Kato, 1990; Tazawa and Chen, 2001; Kimura, 1987; Tazawa et al., 2006), and that these blocks constituted northern East Gondwana in the Middle Paleozoic, the Siluro–Devonian sandstone must have been deposited along the northern margin of East Gondwana (Fig. 23a). Although Tazawa and Chen (2001) and Tazawa et al. (2006) demonstrated that the SKB was located in the eastern extension of the southern part of the CAOB (or the Tienshan–Xinganling Belt) along the northern margin of the North China Block in the Devonian, the absence of 1.85 Ga zircons in the Devonian Tobigamori Formation denies their idea. Isozaki et al. (2010), on the other hand, stated that the Japanese Islands grew along the margin of an oceanic island arc originated from the ophiolite obduction within an oceanic plate (Paleo-Pacific plate). The Hayachine complex may have been a part of the obducted ophiolite that forms an oceanic island arc. However, the oceanic island arc, if existed, must have collided with the northern East Gondwana by the Silurian. The inclusion of some 40% of Precambrian zircons in the Siluro–Devonian sandstone of the SKB cannot be explained with the oceanic-island-arc setting, because Precambrian zircons are generally concentrated in the continental crust.

The Early Carboniferous sandstone of the Karaumedate

Formation shows similar pattern of detrital zircon age distribution with the Siluro–Devonian sandstone although the %Pc value is significantly lower (19.2). The lower %Pc value likely indicate the commencement of the intra-arc rifting, mentioned in the next paragraph, and the decrease of the area of the hinterland with Precambrian rocks.

Permian–Early Jurassic: Oceanic island arc in the Tethys Ocean

Bimodal volcanic activity is recorded in the Lower Carboniferous sequence of the SKB and has been assumed to indicate intra-arc rifting (Kawamura et al., 1990). The Permian–Lower Jurassic sandstones that overlie the Carboniferous bimodal volcanic and pyroclastic rocks contain virtually no Precambrian zircons. The result is in contrast with the detrital zircon age distribution of coeval supracontinental strata of Korea (Pyeongan Supergroup on the Yeongnam Massif) that contain more than 80% of Paleoproterozoic zircons and show a strong affinity with the North China Block (Lee et al., 2012a). The absence of Precambrian zircons in the Permian–Lower Jurassic sandstones indicates that they were deposited along the margin of an oceanic island or microcontinent apart from a large continental block. The inclusion of syn-sedimentary igneous zircons in the Lower Permian Nishikori Formation (Fig. 21) suggests that the oceanic island or microcontinent had evolved to an active oceanic island arc by the Early Permian. Thus we interpret that the South Kitakami Paleoland was rifted from an active margin of East Gondwana in the Early Carboniferous and drifted as an oceanic island arc in the Tethys Ocean from the Early Permian (Fig. 23b). The unimodal age distribution of detrital zircons (centered at 280−250 Ma) in the Permian–Lower Jurassic sandstones indicates that the land surface of the oceanic island arc was mostly occupied by Permian igneous rocks. However, the detection of some Precambrian zircons from the Toyoma Formation (sample 101001-1; %Pc = 8.5) indicates that a certain amount of Precambrian basement rocks were exposed in the South Kitakami Paleoland.

The Siluro–Devonian faunal and floral affinity between the South Kitakami Paleoland and Australia disappeared in the Carboniferous; i.e., the South Kitakami Paleoland was in the tropical to subtropical Cathaysia floristic province, whereas Australia moved southward as a part of Gondwana to the Gondwana floristic province of the south polar region and partly covered with the continental ice sheet. The paleobiogeographical contrast between the SKB and Australia is concordant with the rifting model (Ehiro and Kanisawa, 1999). We suggest that the rifting was related to the clockwise rotation of Gondwana in Carboniferous–Permian times, which finally collided with the Laurussia or Euramerica continent to form a collision zone of the Variscan orogen in Europe, northwestern Africa, and eastern North America (Fig. 23b).

The South Kitakami Paleoland during the Carboniferous–Permian was paleobiogeographically allied to the South China or Indochina block (corals, fusulinids, and ammonoids; e.g., Minato and Kato, 1965; Nakazawa, 1991; Ozawa, 1987; Ehiro, 1998), the North China Block (plants; e.g., Asama, 1985), or the CAOB along the northern and eastern margins of the North China Block at present (brachiopods; Tazawa, 1991, 2001). These studies indicated that the South Kitakami Paleoland was in the Tethyan realm (e.g., Ehiro, 1998), with some brachiopod genera indicating the mixture of boreal elements (e.g., Tazawa, 1991). Although we have a tentative idea that the South Kitakami Paleoland lay in the northern part of the Tethyan realm, between the continental blocks of CAOB and South China, and in the same climate zone with the North China Block, our detrital zircon data cannot indicate the exact position of the South Kitakami Paleoland in the Carboniferous–Permian. Our new data can only indicate that the South Kitakami Paleoland was not along the margin of a large continental block (Fig. 23c, d).

The boreal or arctic elements gradually increased in the Triassic strata. For example, the Anisian ammonoids contain some common species with the coeval ammonoids from Primorye and Kolyma (Nakazawa, 1991), and the Late Triassic *Monotis* fauna belongs to the Arcto-Pacific Realm (Kobayashi and Tamura, 1983; Tamura, 1987). Faunal connection between the SKB and the Angara Craton seems to have been strengthened through the Triassic. The Lower Jurassic Shizugawa Group is characterized by endemic species of ammonoids and bivalves (Hayami, 1990). The fact is concordant with our oceanic-island-arc model, but we have to evaluate the influence of mass extinction across the Triassic–Jurassic boundary.

Middle Jurassic–Early Cretaceous: Amalgamation with the North China Block

The age distribution of detrital zircons from the Middle Jurassic–Early Cretaceous sandstone of the SKB is characterized by more than 70% of syn-sedimentary zircons along with small amounts of Paleoproterozoic zircons (%Pc = 7.7−27.8), and absence of Neoproterozoic zircons. Although syn-sedimentary zircons are abundant, both the youngest zircon age and the youngest peak age in the probability density plot of the Upper Jurassic Sodenohama and Oginohama formations and of the Lower Cretaceous Yoshihama Formation are significantly younger than the age of sedimentation. Zircons younger than 160 Ma were not detected from the three formations. We interpret that the magmatic hiatus in South Korea (Sagong et al., 2005) gave an influence to the age composition of the detrital zircons in these formations. The absence of zircons youger than 160 Ma together with the absence of Neoproterozoic zircons strongly indicate that the South Kitakami Paleoland was along the margin of the North China Block during the sedimentation of the Aratozaki, Sodenohama, Oginohama, and Yoshihama formations (Fig. 23d). However the proportion of Paleoproterozoic zircons in these formations is significantly lower than that of the sandstone on the North China Block (e.g., the Jangsan Formation and Pyeongan Supergroup in South Korea; Lee et al., 2012a, b). Moreover the Ryoseki-type flora that flourished on South China, Indochina, and the Malay Peninsula in Late Jurassic to Early Cretaceous times occur from the Oginohama Formation. Hence we interpret that the South Kitakami Paleoland was a little far away from the Paleoproterozoic orogens in the North China

Block, e.g., the Jiao–Liao–Ji Belt in the eastern part of the North China Block (Zhao et al., 2005), in the Middle Jurassic–Early Cretaceous. The Lower Cretaceous Ayukawa Formation (sample 100416-4) contains many zircons in the period of the magmatic hiatus in South Korea, i.e., from 158 Ma to 110 Ma (Sagong et al., 2005). Considering the occurrence of the Ryoseki-type flora from the underlying Oginohama Formation (Kimura and Ohana, 1989), we interpret that the 150−130 Ma zircons in the Ayukawa sandstone came from the Jurassic–Cretaceous wide magmatic province in the Cathaysia Block (Li and Li, 2007), although their possible origin from the coeval metamorphic core complexes in the North China Block and CAOB (Davis et al., 1996, 2001; Wang et al., 2004) cannot be ruled out.

CONCLUSIONS

We carried out U-Pb analyses of more than 1,000 single detrital zircons from 16 formations of the Silurian–Early Cretaceous continuous succession of the South Kitakami Belt, Northeast Japan. The data set provides a detrital zircon reference for the complex continental-margin orogen of Japan for the first time. The results and interpretations can be summarized as follows.

1. Siluro–Devonian sandstone samples contain many syn-sedimentary zircons and 36.5−48.0% of Precambrian zircons, scattering in age between 700 Ma and 3000 Ma, suggesting that they were deposited along an active continental margin of northern East Gondwana.
2. Permian–Lower Jurassic sandstone samples contain virtually no Precambrian zircons, suggesting that they were deposited along the active margin of an oceanic island arc. From biostratigraphical evidence, the South Kitakami Paleoland seems to have drifted northward in the Tethyan realm between the continental blocks of CAOB (north) and South China (south) where boreal brachiopods and bivalves sometimes reached.
3. Middle Jurassic–Lower Cretaceous sandstone samples contain many 300−170 Ma zircons and up to 28% of Paleoproterozoic (around 1,850 Ma) zircons but no Neoproterozoic zircons. Moreover the zircons during the magmatic hiatus in Korea (158−110 Ma) were detected only in one Early Cretaceous sandstone sample. The age distribution suggests that the Paleoproterozoic zircons in the Middle Jurassic–Lower Cretaceous sandstone of the SKB were most likely supplied from a Paleoproterozoic orogen in the North China Block.
4. The South Kitakami Paleoland, which accumulated the continuous succession of the South Kitakami Belt, was thus born along a margin of Gondwana in the Silurian–Devonian, rifted from the continent and drifted in the Tethys ocean as an oceanic island arc in the Permian–Early Jurassic, and finally amalgamated along an active continental margin where detrital zircons of the North China Block were supplied in the Middle Jurassic.

ACKNOWLEDGMENTS

We would like to express our sincere gratitude to Emeritus Professor Kenji Konishi of Kanazawa University for his encouragement to submit our work to this issue; and to Professor Masaaki Shimizu and Associate Professor Kenji Kashiwagi of the University of Toyama for various discussions and instructions during the course of this study. Critical reviews of the submitted manuscript by Professor Yasufumi Iryu of Tohoku University, Professor Keitaro Kunugiza of the University of Toyama, Emeritus Professor Kenji Konishi, and Dr. Hiroto Ichishima of the Fukui Prefectural Dinosaur Museum are greatly appreciated. This study was supported by the Earthquake Research Institute (University of Tokyo) cooperative research program 2013-G-04, JSPS KAKENHI Grant Number 25400484, and the discretionary budget of the President of the University of Toyama.

REFERENCES

Ando, H. 1987. Paleobiological study of the Late Triassic bivalve *Monotis* from Japan. The University Museum, the University of Tokyo Bulletin 30, Tokyo,109 pp.

Aoki, K., T. Iizuka, T. Hirata, S. Maruyama and M. Terabayashi. 2007. Tectonic boundary between the Sanbagawa belt and Shimanto belt in central Shikoku, Japan. Journal of the Geological Society of Japan 113: 171−183.

Aoki, K., Y. Isozaki, S. Yamamoto, K. Maki, T. Yokoyama and T. Hirata. 2012. Tectonic erosion in a Pacific-type orogeny: Detrital zircon response to Cretaceous tectonics in Japan. Geology 40: 1087−1090.

Asama, K. 1985. Permian to Triassic floral changes and some problems of the paleobiogeography, parallelism, mixed floras and origin of the angiosperms; pp. 199−218 *in* K. Nakazawa and J. M. Dickins (eds.), The Tethys. Tokai University Press, Tokyo.

Bando, Y. 1964. The Triassic stratigraphy and ammonite fauna of Japan. Science Reports of the Tohoku University, Second Series, 36: 1−137.

Bando, Y., T. Sato and T. Matsumoto. 1987. Chapter 3: Palaeobiogeography of the Mesozoic Ammonoidea, with special reference to Asia and the Pacific; pp. 65−95 *in* A. Taira and M. Tashiro (eds.), Historical Biogeography and Plate Tectonic Evolution of Japan and Eastern Asia. TERRAPUB, Tokyo.

Bando, Y., and S. Shimoyama. 1974. Late Schythian ammonoids from the Kitakami Massif. Transactions and Proceeedings of the Palaeontological Society of Japan, New Series, 94: 293−312.

Choi, D. R. 1973. Permian fusulinids from the Setamai–Yahagi district, Southern Kitakami Mountains, N. E. Japan. Journal of the Faculty of Sciences, Hokkaido University, Series 4, 16: 1−132.

Choi, T., Y. I. Lee, Y. Orihashi and H. I. Yi. 2013. The provenance of the southeastern Yellow Sea sediments constrained by detrital zircon U–Pb age. Marine Geology 337: 182−194.

Compston, W. 1996. SHRIMP: Origins, impact and continuing evolution. Journal of the Royal Society of Western Australia 79: 109–117.

Corfu, F., J. M. Hanchar, P. W. O. Hosikin and P. Kinny. 2003. Atlas of zircon textures; pp. 469–500 *in* J. M. Hanchar and P. W. O. Hoskin (eds.), Zircon, Reviews in Mineralogy and Geochemistry 53. Mineralogical Society of America, Washington, DC.

Darby, B. J., and G. Gehrels. 2006. Detrital zircon reference for the North China block. Journal of Asian Earth Sciences 26: 637–648.

Davis, G. A., X. Qian, Y. Zheng, H.-M. Tong, H. Yu, C. Wang, G. E. Gehrels, M. Shafiquallah and J. E. Fryxell. 1996. Mesozoic deformation and plutonism in the Yunmeng Shan: A metamorphic core complex north of Beijing, China; pp. 253–280 *in* A. Yin and T. M. Harrison (eds.), The Tectonic Evolution of Asia. Cambridge University Press, Cambridge.

Davis, G. A., Y. Zheng, C. Wang, B. J. Darby, C. Zhang and G. E. Gehrels. 2001. Mesozoic tectonic evolution of the Yanshan fold and thrust belt, with emphasis on Hebei and Liaoning provinces, northern China; pp. 171–197 *in* M. S. Hendrix and G. A. Davis (eds.), Paleozoic and Mesozoic Tectonic Evolution of Central Asia: From Continental Assembly to Intracontinental Deformation, Geological Society of America Memoir 194. Geological Society of America, Boulder.

Diwu, C. R., Y. Sun, H. Zhang, Q. Wang, A. Quo and L. Fan. 2012. Episodic tectonothermal events of the western North China Craton and North Qinling Orogenic Belt in central China: Constraints from detrital zircon U-Pb ages. Journal of Asian Earth Sciences 47: 107–122.

Ehiro, M. 1989. Figure 2.1; p. 9 *in* Editorial Committee of “Geology of Japan 2 Tohoku District” (ed.), Geology of Japan 2 Tohoku District. Kyoritsu Shuppan, Tokyo.*

Ehiro, M. 1996. Latest Permian ammonoid *Paratirolites* from the Ofunato district, Southern Kitakami Massif, Northeast Japan. Transactions and Proceedings of the Palaeontological Society of Japan, New Series, 184: 592–596.

Ehiro, M. 1998. Permian ammonoid fauna of the Kitakami Massif, Northeast Japan—Biostratigraphy and paleobiogeography. Palaeoworld 9: 113–122.

Ehiro, M., and S. Kanisawa. 1999. Origin and evolution of the South Kitakami Microcontinent during the Early Middle Palaeozoic; pp. 283–295 *in* I. Metcalfe (ed.), Gondwana Dispersion and Asian Accretion: IGCP 321 Final Results Volume. A.A. Balkema, Rotterdam.

Ehiro, M., K. Okami and S. Kanisawa. 1988. Recent progress and further subject in studies on the “Hayachine Tectonic Belt” in the Kitakami Massif, Northeast Japan. Earth Science (Chikyu Kagaku) 42: 317–335.**

Ehiro, M., and Y. Takaizumi. 1992. Late Devonian and Early Carboniferous ammonoids from the Tobigamori Formation in the Southern Kitakami Massif, Northeast Japan and their stratigraphic significance. Journal of the Geological Society of Japan 98: 197–204.

Ehiro, M., J. Tazawa, M. Oishi and K. Okami. 1986. Discovery of *Trimerella* (Silurian Brachiopoda) from the Odagoe Formation, south of Mt. Hayachine in the Kitakami Massif, Northeast Japan and its significance. Journal of the Geological Society of Japan 92: 753–756.*

Fukada, A. 1950. On the occurrence of *Perisphinctes* (s. s.) from the Ozika Peninsula in the southern Kitakami mountainland. Journal of the Faculty of Science, Hokkaido University, Series 4, 7: 211–216.

Gehrels, G. E., W. R. Dickinson, G. M. Ross, J. H. Stewart and D. G. Howell. 1995. Detrital zircon reference for Cambrian to Triassic miogeoclinal strata of western North America. Geology 23: 831–834.

Hamada, T. 1960. The Middle Palaeozoic formations in China and Korea, II. Northwest and South China. Japanese Journal of Geology and Geography 31: 219–239.

Hayami, I. 1960. Pelecypods of the Jusanhama Group (Purbeckian or Wealden) in Hashiura area, northeast Japan. Japanese Journal of Geology and Geography 31: 13–21.

Hayami, I. 1961. Successions of the Kitakami Jurassic. Jurassic stratigraphy of South Kitakami, Japan, I. Japanese Journal of Geology and Geography 32: 159–177.

Hayami, I. 1990. Geographic distribution of Jurassic bivalve faunas in eastern Asia; pp. 361–369 *in* K. Ichikawa, S. Mizutani, I. Hara and A. Yao (eds.), Pre-Cretaceous Terranes of Japan. IGCP Project no. 224, Osaka.

Iba, Y., S. Sano., J. Mutterlose. and Y. Kondo. 2012. Belemnites originated in the Triassic—A new look at an old group. Geology 40: 911–914.

Ichikawa, K. 1951. Triassic formations in the southern part of the Kitakami Massif; pp. 7–26 *in* Geological Society of Japan (ed.), The Triassic Stratigraphy of Japan. Reports Special Number, Geological Survey of Japan.*

Iizuka, T., and T. Hirata. 2004. Simultaneous determinations of U-Pb age and REE abundances for zircons using ArF excimer laser ablation-ICPMS. Geochemical Journal 38: 229–241.

Iizuka, T., T. Komiya, S. Rino, S. Maruyama and T. Hirata. 2010. Detrital zircon evidence for Hf isotopic evolution of granitoid crust and continental growth. Geochimica et Cosmochimica Acta 74: 2450–2472.

Inai, Y. 1939. Geology of the Environs of Sizugawa-mati, Miyagi Prefecture (preliminary report). Journal of the Geological Society of Japan 46: 231–242.*

Inai, Y., and T. Takahashi. 1940. On the geology of the southernmost part of the Kitakami Massif. Contributions from the Institute of Geology and Paleontology, Tohoku University 34: 1–40.*

International Commission on Stratigraphy. 2013. International chronostratigraphic chart, v2013/01. http://www.stratigraphy.org/ICSchart/ChronostratChart2013-01.pdf.

Ishii, K., Y. Okimura and K. Ichikawa. 1985. Notes on Tethys biogeography with reference to Middle Permian fusulinaceans; pp. 131–155 *in* K. Nakazawa and J. M. Dickins (eds.), The Tethys. Tokai University Press, Tokyo.

Isozaki, Y., K. Aoki, T. Nakama and S. Yanai. 2010. New insight into a subduction-related orogeny: A reappraisal of the geotectonic framework and evolution of the Japanese Islands.

Gondwana Research 18: 82–105.

Iwano, H., Y. Orihashi, T. Hirata, M. Ogasawara, T. Danhara, K. Horie, N. Hasebe, S. Sueoka, A. Tamura, Y. Hayasaka, A. Katsube, H. Ito, K. Tani, J. Kimura, Q. Chang, Y. Kouchi, Y. Haruta and K. Yamamoto. 2013. An inter-laboratory evaluation of OD-3 zircon for use as a secondary U-Pb dating standard. Island Arc 22: 382−394.

Kamada, K. 1983. Triassic Inai Group in the Toyoma area in the southern Kitakami Mountains, Japan with special reference to the submarine sliding deosits in the Triassic Osawa Formation. Earth Science (Chikyu Kagaku) 37: 147−161.**

Kanagawa, K., and H. Ando. 1983. Discovery of *Monotis* in the Ofunato area, southern Kitakami Mountains and its significance. Journal of the Geological Society of Japan 89: 187−190.*

Kanisawa, S., and M. Ehiro. 1986. Occurrence and geochemical nature of phosphatic rocks and Mn-rich carbonate rocks in the Toyoman Series, Kitakami Mountains, Northeastern Japan. Journal of the Japanese Association of Mineralogists, Petrologists and Economic Geologists 81: 12−31.

Kanisawa, S., M. Ehiro and K. Okami. 1992. K-Ar ages of amphibolites from the Matsugadaira–Motai Metamorphics and their significance. Journal of Mineralogy, Petrology and Economic Geology 87: 412−419.**

Kanmera, K., and T. Mikami. 1965. Succession and sedimentary features of the Lower Permian Sakamotozawa Formation. Memoirs of the Faculty of Science, Kyushu University, Series D Geology, 16: 265−274.

Kase, T. 1979. Stratigraphy of the Mesozoic formations in the Hashiura area, Southern Kitakami Mountainland, northern Japan. Journal of the Geological Society of Japan 85: 111−122.**

Kato, M. 1990. Paleozoic corals; pp. 307−312 *in* K. Ichikawa, S. Mizutani, I. Hara and A. Yao (eds.), Pre-Cretaceous Terranes of Japan. IGCP Project no. 224, Osaka.

Kawagoe, Y., S. Sano, Y. Orihashi, H. Obara, Y. Kouchi and S. Otoh. 2012. New detrital zircon age data from the Tetori Group in the Mana and Itoshiro areas of Fukui Prefecture, central Japan. Memoir of the Fukui Prefectural Dinosaur Museum 11: 1−18.

Kawamura, M., M. Kato and Kitakami Paleozoic Research Group. 1990. Southern Kitakami Terrane; pp. 249−266 *in* K. Ichikawa, S. Mizutani, I. Hara and A. Yao (eds.), Pre-Cretaceous Terranes of Japan. IGCP Project no. 224, Osaka.

Kawamura, T., and M. Kawamura. 1989a. The Carboniferous System of the South Kitakami Terrane, northeast Japan (Part 1) —Summary of the stratigraphy—. Earth Science (Chikyu Kagaku) 43: 84−97.**

Kawamura, T., and M. Kawamura. 1989b. The Carboniferous System of the South Kitakami Terrane, northeast Japan (Part 2) —Sedimentary and tectonic environment—. Earth Science (Chikyu Kagaku) 43: 157−167.**

Kawamura, T., H. Nakai and M. Kawamura. 1984. A new occurrence of Silurian fossils in the northern marginal part of the South Kitakami Belt. Journal of the Geological Society of Japan 90: 61−64.*

Kimura, T. 1987. Chapter 6: Geographical distribution of Palaeozoic and Mesozoic plants in East and Southeast Asia; pp. 135−200 *in* A. Taira and M. Tashiro (eds.), Historical Biogeography and Plate Tectonic Evolution of Japan and Eastern Asia. TERRAPUB, Tokyo.

Kimura, T., and T. Ohana. 1989. Late Jurassic plants from the Oginohama Formation, Oshika Group in the Outer Zone of Northeast Japan (I). Bulletin of the National Science Museum, Series C Geology and Paleontology, 15: 1−24.

Kobayashi, T., and K. Mori. 1955. The Vaugoniinae from the Kitakami Mountains in north Japan. Japanese Journal of Geology and Geography 26: 73−88.

Kobayashi, Y., H. Takagi, K. Kato, K. Sango and K. Shibata. 2000. Petrochemistry and correlation of Paleozoic granitic rocks in Japan. Memoirs of the Geological Society of Japan 56: 65−88.**

Kobayashi, T., and M. Tamura. 1983. The Arcto-Pacific Realm and the Trigoniidae in the Triassic Period. Proceedings of the Japan Academy, Series B, 59: 207−210.

Kosler, J., and P. J. Sylvester. 2003. Present trends and the future of zircon in geochronology: Laser ablation ICPMS; pp. 243−275 *in* J. M. Hanchar and P. W. O. Hoskin (eds.), Zircon, Reviews in Mineralogy and Geochemistry 53. Mineralogical Society of America, Washington, DC.

Kouchi, Y., Y. Orihashi, H. Obara, T. Fujimoto, Y. Haruta, K. Tsukada and K. Yamamoto. 2012. U-Pb age dating for a zircon using 213 nm Nd-YAG laser ablation ICP mass spectrometry: An attempt on optimization of the analytical condition to reduce matrix effect. Abstracts for the 59th annual meeting of the Geochemical Society of Japan: 135.*

Lawver, L.A., Dalziel, I.W.D., Norton, I.O., and Gahagan, L.M., The PLATES 2009 Atlas of Plate Reconstructions (750 Ma to Present Day), PLATES Progress Report 325-0509, 157 pp. http://www.ig.utexas.edu/research/projects/plates/recons.htm

Lee, Y. I., T. Choi and Y. Orihashi. 2012a. Depositional ages of upper Pyeongan Supergroup strata in the Samcheok coalfield, eastern central Korea. Journal of the Geological Society of Korea 48: 93−99.***

Lee, Y. I., T. Choi, H. S. Lim and Y. Orihashi. 2012b. Detrital zircon U-Pb ages of the Jangsan Formation in the northeastern Okcheon belt, Korea and its implications for material source, provenance, and tectonic setting. Sedimentary Geology 282: 256−267.

Li, Z.-X., and X.-H. Li. 2007. Formation of the 1300-km-wide intracontinental orogeny and postorogenic magmatic province in Mesozoic South China: A flat-slab subduction model. Geology 35: 179−182.

Liao, W. H. 1990. The biogeographic affinities of East Asian corals; pp. 175−179 *in* W. S. McKerrow and C. R. Scotese (eds.), Palaeozoic Palaeogeography and Biogeography, Geological Society Memoir 12. Geological Society, London.

Ludwig, K. R. 2008. Isoplot 3.70: Geochronological Toolkit for Microsoft Excel. Berkeley Geochronology Center Special Publication 4, 77 p.

Mabuti, S. 1933. Jurassic stratigraphy of the southern part of the Kitakami Mountainland, North-east Japan. Proceedings of the Imperial Academy of Japan 9: 313–316.

Matsumoto, T. 1953. Chapter 17 Jurassic Period; pp. 325–377 *in* J. Makiyama (ed.), Historical Geology 2. Asakura Book Company, Tokyo.*

Matsumoto, T. 1956. *Yebisites*, a new Lower Jurassic ammonite from Japan. Transactions and Proceedings of the Palaeontological Society of Japan, New Series, 23: 205–212.

Metcalfe, I. 2011. Palaeozoic–Mesozoic history of SE Asia; pp. 7–35 *in* R. Hall, M. A. Cottam and M. E. J. Wilson (eds.), The SE Asian gateway: History and tectonics of the Australia–Asia collision, Geological Society of London, Special Publications 355. Geological Society, London.

Minato, M., and M. Kato. 1965. Waagenophyllidae. Journal of the Faculty of Science, Hokkaido University, Series 4, 12: 1–241.

Minato, M., M. Kato, K. Nakamura, Y. Hasegawa, D. R. Choi and J. Tazawa. 1978. Biostratigraphy and correlation of the Permian of Japan. Journal of the Faculty of Science, Hokkaido University, Series 4, 18: 11–47.

Mori, K. 1949. On the Jurassic formations in the Hashiura district, Province of Rikuzen. Japanese Journal of Geology and Geography 21: 315–322.

Mori, K., K. Okami and M. Ehiro. 1992. Paleozoic and Mesozoic sequences in the Kitakami Mountains (29th IGC Field Trip A05); pp. 81–114 *in* M. Adachi and K. Suzuki (eds.), 29th IGC Field Trip Guide Book Vol. 1, Paleozoic and Mesozoic Terranes: Basement of the Japanese Islands Arcs. Nagoya University, Japan.

Murata, M., and Y. Bando. 1975. Discovery of Late Permian *Araxoceras* from the Toyoma Formation in the Kitakami Massif, Northeast Japan. Transactions and Proceedings of the Palaeontological Society of Japan, New Series, 97: 22–31.

Murata, M., S. Kanisawa, Y. Ueda and N. Takeda. 1974. Base of the Silurian system and the pre-Silurian granites in the Kitakami Massif, Northeast Japan. Journal of the Geological Society of Japan 80: 475–486.**

Murata, M., K. Okami, S. Kanisawa and M. Ehiro. 1982. Additional evidence for the Pre-Silurian basement in the Kitakami massif, Northeast Honshu, Japan. Memoirs of the Geological Society of Japan 21: 245–259.

Nakamura, K., and J. Tazawa. 1990. Faunal provinciality of the Permian brachiopods in Japan; pp. 313–320 *in* K. Ichikawa, S. Mizutani, I. Hara and A. Yao (eds.), Pre-Cretaceous Terranes of Japan. IGCP Project no. 224, Osaka.

Nakazawa, K. 1964. On the Upper Triassic *Monotis* beds, especially, on the *Monotis typica* zone. Journal of the Geological Society of Japan 70: 523–535.**

Nakazawa, K. 1991. The Permian and Triassic systems in the Tethys—their paleogeography; pp. 93–111 *in* K. Nakazawa and J. M. Dickins (eds.), The Tethys. Tokai University Press, Tokyo.

Noda, M., and K. Tachibana. 1959. Some Upper Devonian cyrtospiriferids from the Nagasaka district, Kitakami Mountainland. Science Bulletin of the Faculty of Liberal Arts and Education, Nagasaki University 10: 15–21.

Obata, I. 1988. Cretaceous formations in Northeast Japan. Earth Science (Chikyu Kagaku) 42: 385–395.*

Okami, M., M. Ehiro, M. Yamazaki and M. Oishi. 1984. Orthoquartzite clasts from the Silurian Orikabetoge Formation, southern Kitakami Mountains, Northeast Japan. Journal of the Geological Society of Japan 90: 911–913.*

Om, H. Y., C. C. Ryang, Y. H. Kim and D. S. Rim. 1996. Chapter 2 Section 4 Paleozoic Era; pp. 80–154 *in* Institute of Geology, State Academy of Sciences, DPR of Korea (ed.), Geology of Korea, Foreign Languages Books Publishing House, Pyongyang.

Onuki, Y. 1956. Geology of the Kitakami Mountains. Explanatory text of the Geologic map of Iwate Prefecture (1:100,000) II. Iwate Prefecture, Morioka, 189 pp.

Onuki, Y. 1969. Geology of the Kitakami Massif, Northeast Japan. Contributions from the Institute of Geology and Paleontology, Tohoku University 69: 1–239.**

Onuki, Y. 1981. The Kitakami Massif; pp. 3–223 *in* Y. Onuki, N. Kitamura and H. Nakagawa (eds.), Explanatory text of the geological map around the Kitakami River in the scale 1:200,000. Hase Geological Survey Inc., Sendai.*

Onuki, Y., and Y. Bando. 1958. On the Saragai Group of the Upper Triassic System. Journal of the Geological Society of Japan 64: 481–493.**

Onuki, Y., and Y. Bando. 1959. On the Inai Group of the Lower and Middle Triassic System. Contributions from the Institute of Geology and Paleontology, Tohoku University 50: 1–69.**

Onuki, Y., and K. Mori. 1961. Geology of the Ofunato district, Iwate Prefecture, southern part of the Kitakami Massif, Japan. Journal of the Geological Society of Japan 67: 641–654.**

Orihashi, Y., S. Nakai and T. Hirata. 2008. U-Pb age determination for seven standard zircons using inductively coupled plasma-mass spectrometry coupled with frequency quintupled Nd-YAG (λ = 213 nm) laser ablation system: Comparison with LA-ICP-MS zircon analyses with a NIST glass reference material. Resource Geology 58: 101–123.

Otoh, S., M. Shimojo, K. Aoki, T. Nakama, S. Maruyama and S. Yanai. 2010. Age distribution of detrital zircons in the psammitic schist of the Sanbagawa Belt, Southwest Japan. Journal of Geography 119: 333–346.**

Otoh, S., and S. Yanai. 1996. Mesozoic inversive wrench tectonics in far east Asia: examples from Korea and Japan; pp. 401–419 *in* A. Yin and M. Harrison (eds.), The Tectonic Evolution of Asia. Cambridge University Press, Stanford.

Ozawa, K. 1983. Relationships between tectonite and cumulate in ophiolites: The Miyamori ultramafic complex, Kitakami Mountains, northeast Japan. Lithos 16: 1–16.

Ozawa, K. 1984 Geology of the Miyamori ultramafic complex in the Kitakami Moutains, northeast Japan. Journal of the Geological Society of Japan 90: 697–716.

Ozawa, K., K. Shibata and S. Uchiumi. 1988. K-Ar ages of hornblende in gabbroic rocks from the Miyamori ultramafic complex of the Kitakami Mountains. Journal of Mineralogy, Petrology and Economic Geology 83: 150−159.**

Ozawa, T. 1987. Chapter 2: Permian fusulinacean biogeographic provinces in Asia and their tectonic implications; pp. 45−63 *in* Taira, A. and M. Tashiro, (eds), Historical Biogeography and Plate Tectonic Evolution of Japan and Eastern Asia. TERRAPUB, Tokyo.

Rino, S., Y. Kon, W. Sato, S. Maruyama, M. Santosh and D. Zhao. 2008. The Grenvillian and Pan-African orogens: World's largest orogenies through geologic time, and their implications on the origin of superplume. Gondwana Research 14: 51−72.

Rogers, J. J. W., and M. Santosh. 2002. Configuration of Columbia, a Mesoproterozoic supercontinent. Gondwana Research 5: 5−22.

Rojas-Agramonte, Y., A. Kröner. A. Demoux. X. Xia. W. Wang. T. Donskaya. D. Liu and M. Sun. 2011. Detrital and xenocrystic zircon ages from Neoproterozoic to Palaeozoic arc terranes of Mongolia: Significance for the origin of crustal fragments in the Central Asian Orogenic Belt. Gondwana Research 19: 751−763.

Rubatto, D., and J. Hermann. 2003. Zircon formation during fluid circulation in eclogites (Monviso, Western Alps): Implications for Zr and Hf budget in subduction zones. Geochimica et Cosmochimica Acta 67: 2173−2187.

Sagong, H., S. T. Kwon and J. H. Ree. 2005. Mesozoic episodic magmatism in South Korea and its tectonic implication. Tectonics 24: TC5002.

Saito, Y. 1966. Geology of the Setamai district, Southern Kitakami Massif, Northeast Japan. Contributions from the Institute of Geology and Paleontology, Tohoku University 62: 56–67.**

Sasaki, M. 2001. Restoration of Early Cretaceous sinistral displacement and deformation in the South Kitakami Belt, NE Japan: An example of the Motai–Nagasaka area. Earth Science (Chikyu Kagaku) 55: 83−101.

Sasaki, M. 2003. Early Cretaceous sinistral shearing and associated folding in the South Kitakami Belt, northeast Japan. Island Arc 12: 92−109.

Sasaki, M., K. Tsukada and S. Otoh. 1997. An outcrop of unconformity at the base of the Upper Devonian Tobigamori Formtion, Southern Kitakami Mountains. Journal of the Geological Society of Japan 103: 647−655.**

Sato, T. 1957. Biostratigraphie de la série de Shizukawa (Jurassique inférieur), au Japon septentrional. Journal of the Faculty of Science of the University of Tokyo, Section 2, 10: 313−350.

Sato, T. 1962. Études Biostratigraphiques des ammonites du Jurassique du Japon. Mémoires de la Société géologique de France, Nouvelle série, 41: 1−122.

Sato, T. 1972. Some Bajocian ammonites from Kitakami, Northeast Japan. Transactions and Proceedings of the Palaeontological Society of Japan, New Series, 85: 280−292.

Sato, T., and G. E. G. Westermann. 1991. Japan and South-East Asia. pp. 81−108 *in* G. E. G. Westermann and A. C. Riccardi (eds.), Jurassic Taxa Ranges and Correlation Charts for the Circum Pacific 4, Newsletters on Stratigraphy 24. Schweizerbart Science Publishers, Stuttgart.

Scotese, C., and W. McKerrow. 1990. Revised world maps and introduction; pp. 1−21 *in* W. S. McKerrow and C. R. Scotese (eds.), Palaeozoic Palaeogeography and Biogeography, Geological Society Memoir 12. Geological Society, London.

Shibata, K., and K. Ozawa. 1992. Ordovician arc ophiolite, Hayachine and Miyamori complexes, Kitakami Mountains, Northeast Japan: Isotopic ages and geochemistry. Geochemical Journal 26: 85−97.

Shiida, I. 1940. On the Geology in the environs of Kesennuma, Miyagi Prefecture. Contributions from the Institute of Geology and Paleontology, Tohoku University 33: 1−72.*

Shimizu, S. 1930. On some Anisic ammonites from the *Hollandites* beds of the Kitakami Mountainland. Science Report of the Tohoku Imperial University, Series 2, 14: 63−74.

Shimojo, M., S. Otoh, S. Yanai, T. Hirata, T. and S. Maruyama. 2010. LA-ICP-MS U-Pb age of some older rocks of the South Kitakami Belt, Northeast Japan. Journal of Geography 119: 257−269.**

Soreghan, M. J., and G. E. Gehrels (eds.). 2000. Paleozoic and Triassic Paleogeography and Tectonics of Western Nevada and Northern California. Geological Society of America Special Paper 347. Geological Society of America, Boulder, 252 pp.

Tachibana, K. 1950. Devonian plants first discovered in Japan. Proceedings of the Japan Academy 26: 54−60.

Tachibana, K. 1952. On the Tobigamori Group of the Nagasaka district, Kitakami Mountainland. Journal of the Geological Society of Japan 58: 353−360.**

Takahashi, H. 1969. Stratigraphy and ammonite fauna of the Jurassic System of the Southern Kitakami Massif, northeast Honshu, Japan. Science Report of the Tohoku University, Series 2, 41: 1−93.

Takizawa, F. 1970. Ayukawa Formation of the Ojika Peninsula, Miyagi Prefecture, northeast Japan. Bulletin of the Geological Survey of Japan 21: 567−578.

Takizawa, F. 1977. Some Aspects of the Mesozoic sedimentary basins in the South Kitakami Belt, Northeast Japan. Monograph of the Association for the Geological Collaboration in Japan 20: 61−73.**

Takizawa, F. 1985. Jurassic sedimentation in the South Kitakami Belt, Northeast Japan. Bulletin of the Geological Survey of Japan 36: 203−320.

Takizawa, F., N. Isshiki and M. Katada. 1974. Geology of the Kinkasan District, Quadrangle Series, Scale 1:50,000. Geological Survey of Japan, Kawasaki, 62 pp.**

Tamura, M. 1987. Chapter 4: Distribution of Japanese Triassic bivalve faunas and sedimentary environment of megalodont limestone in Japan; pp. 97−110 *in* A. Taira and M. Tashiro (eds.), Historical Biogeography and Plate Tectonic Evolution of Japan and Eastern Asia. TERRAPUB, Tokyo.

Tashiro, M., and T. Kozai. 1989. Bivalve faunal correlation of the Cretaceous System of Northeast Japan with that of Southwest Japan. Earth Science (Chikyu Kagaku) 43: 129−139.**

Tazawa, J. 1991. Middle Permian brachiopod biogeography of Japan and adjacent regions in East Asia; pp. 213–230 *in* K. Ishii, X. Liu, K. Ichikawa and B. Huang (eds.), Pre-Jurassic Geology of Inner Mongolia, China: Report of China-Japan Cooperative Research Group, 1987–1989. Matsuya Insatsu, Osaka.

Tazawa, J. 1996. *Rotaia* (Rhynchonellida, Brachiopoda) from the Lower Carboniferous of northeast Japan and its palaeobiogeographical significance. Scientific Papers of Niigata University, Series E (Geology), 11: 1–11.

Tazawa, J. 2001. Middle Permian brachiopod faunas of Japan and South Primorye, Far East Russia: Their palaeobiogeographic and tectonic implications. Geosciences Journal 5: 19–26.

Tazawa, J., and X. Chen. 2001. Middle Devonian brachiopods from the Nakazato Formation, South Kitakami Belt, northeast Japan and their palaeobiogeographical affinity with those of western Inner Mongolia. Journal of the Geological Society of Japan 107: 706–710.**

Tazawa, J., K. Sasaki and A. Yokota. 2006. *Leptophloeum* from the Ainosawa Formation of the Soma area, Fukushima Prefecture, northeast Japan, and the tectono-sedimentary setting of the *Leptophloeum*-bearing Upper Devonian in Japan. Earth Science (Chikyu Kagaku) 60: 69–72.**

Tsutsumi, Y., A. Miyashita, K. Horie and K. Shiraishi. 2012. Existence of multiple units with different accretionary and metamorphic ages in the Sanbagawa Belt, Sakuma–Tenryu area, central Japan. The Island Arc 21: 317–326.

Tsutsumi, Y., A. Miyashita, K. Terada and H. Hidaka. 2009. SHRIMP U-Pb dating of detrital zircons from the Sanbagawa Belt, Kanto Mountains, Japan: Need to revise the framework of the belt. Journal of Mineralogical and Petrological Sciences 104: 12–24.

Tsutsumi, Y., K. Yokoyama, K. Horie, K. Terada and H. Hidaka. 2006. SHRIMP U-Pb dating of detrital zircons in paragneiss from Oki-Dogo Island, western Japan. Journal of Mineralogical and Petrological Sciences 101: 289–298.

Tsutsumi, Y., K. Yokoyama, K. Terada and H. Hidaka. 2011. SHRIMP Dating of detrital zircons from the Sangun-Renge Belt of Sangun Metamorphic Rocks, northern Kyushu, Southwest Japan. Bulletin of the National Museum of Nature and Science, Series C, 37: 5–16.

Tsutsumi, Y., K. Yokoyama, K. Terada and Y. Sano. 2000. SHRIMP U-Pb dating of zircons in the sedimentary rocks from the Akiyoshi and Suo zones, Southwest Japan. Journal of Mineralogical and Petrological Sciences 95: 216–227.

Tsutsumi, Y., K. Yokoyama, K. Terada and Y. Sano. 2003. SHRIMP U-Pb dating of detrital zircons in metamorphic rocks from northern Kyushu, western Japan. Journal of Mineralogical and Petrological Sciences 98: 181–193.

Turner, S. A. 2010. Sedimentary record of late Neoproterozoic rifting in the NW Tarim Basin, China. Precambrian Research 181: 85–96.

Wang, T., Y. Zheng, T. Li and Y. Gao. 2004. Mesozoic granitic magmatism in extensional tectonics near the Mongolian border in China and its implications for crustal growth. Journal of Asian Earth Sciences 23: 715–729.

Watanabe, T., C. M. Fanning, K. Uruno and H. Kano. 1995. Pre-Middle Silurian granitic magmatism and associated metamorphism in northern Japan: SHRIMP U-Pb zircon chronology. Geological Journal 30: 273–280.

Wiedenbeck, M., P. Allé, F. Corfu, W. L. Griffin, M. Meier, F. Oberli, A. von Quadt, J. C. Roddick and W. Spiegel. 1995. Three natural zircon standards for U-Th-Pb, Lu-Hf, trace element and REE analyses. Geostandards Newsletter 19: 1–23.

Yabe, H. 1949. A new Triassic ammonite from Yanaizu, north of Inai, near Isinomaki, Miyagi Prefecture. Proceedings of the Japan Academy 24: 168–174.

Yamashita, N. 1957. The Mesozoic I. Geoscience Series 10, Association for Geological Collaboration of Japan, Tokyo, 94 pp.*

Yamazaki, M., K. Okami, M. Ehiro and M. Oishi. 1984. The Silurian in the vicinity of Orikabe-Pass, northern marginal part of the Southern Kitakami Mountains. Earth Science (Chikyu Kagaku) 38. 268–272.*

Yao, J., L. Shu and M. Santosh. 2011. Detrital zircon U-Pb geochronology, Hf-isotopes and geochemistry—New clues for the Precambrian crustal evolution of the Cathaysia Block, South China. Gondwana Research 20. 553–567.

Yao, J., L. Shu, M. Santosh and J. Li. 2012. Precambrian crustal evolution of the South China Block and its relation to supercontinent history: Constraints from U-Pb ages, Lu-Hf isotopes and REE geochemistry of zircons from sandstones and granodiorite. Precambrian Research 208–211: 19–48.

Yin, A., and S. Nie. 1996. A Phanerozoic palinspastic reconstruction of China and its neighboring region; pp. 442–485 *in* A. Yin and T. M. Harrison (eds.), The tectonic evolution of Asia. Cambridge University Press, Cambridge.

Zhao, G., M. Sun, S. A. Wilde and S. Li. 2004. A Paleo–Mesoproterozoic supercontinent: Assembly, growth and breakup. Earth-Science Reviews 67: 91–123.

Zhao, G., M. Sun, S. A. Wilde and S. Li. 2005. Late Archean to Paleoproterozoic evolution of the North China Craton: Key issues revisited. Precambrian Research 136: 177–202.

* : in Japanese
** : in Japanese with English abstract
*** : in Korean

＜　地名・地層名　＞

Arahama Beach …………………… 荒浜
Arato Formation ……………… 荒砥層
Aratozaki Formation ……… 荒砥崎層
Arisu Formation ………………… 有住層
Ayukawa Formation ………… 鮎川層
Ayukawa Port ………………… 鮎川港
Cape Bentenzaki …………… 弁天崎
Chonomori Formation …… 長の森層
Domeki Sandstone Member ………… ……………………ドウメキ砂岩部層
Fukiura Shale and Sandstone Member … …………………福貴浦頁岩砂岩部層
Fukkoshi Formation ………… 風越層
Funagawara Formation …… 船河原層
Futawatashi Shale Member …………… …………………………長渡頁岩部層
Hakoneyama Formation…… 箱根山層
Hanamaki City ……………… 花巻市
Hashiura ………………………… 橋浦
Hayachine Complex … 早池峰複合岩類
Hijochi Formation ………… 飛定地層
Hikami Granite ………… 氷上花崗岩
Hikoroichi …………………… 日頃市
Hiraiso Formation …………… 平磯層
Hoinyashiki ……………… 法印屋敷
Hosoura Formation ………… 細浦層
Ichinoseki City ……………… 一関市
Inai Group ………………… 稲井層群
Isatomae Formation ……… 伊里前層
Ishinomaki City ……………… 石巻市
Ishiwaritoge Formation ……石割峠層
Isokusa Formation …………… 磯草層
Iwaizaki Limestones 岩井崎石灰岩層
Iwate Prefecture …………… 岩手県
Jusanhama Group ……… 十三浜層群
Kamaishi City ……………… 釜石市
Kanaegaura Formation ……… 鼎浦層
Kanokura Formation ………… 叶倉層
Karakuwa ………………………… 唐桑
Karaumedate Formation ……唐梅館層
Kawauchi Formation ………… 川内層
Kesaiso Coast …………… 今朝磯海岸
Kesennuma City ………… 気仙沼市

Kitakamigawa River ………… 北上川
Kitsunezaki Sandstone and Shale Member ………………… 狐崎砂岩頁岩部層
Kiyosaki Sandstone Member ………… …………………………清崎砂岩部層
Kobitawatashi Sandstone and Shale Member …………………小長渡砂岩頁岩部層
Kobosoura Formation ……… 小細浦層
Kogoshio Formation ……… 小々汐層
Kosaba Formation …………… 小鯖層
Kowaragi Formation ……… 小原木層
Kozumi Shale Member 小積頁岩部層
Kukunarihama Beach……… 十三成浜
Kurosegawa ………………… 黒瀬川
Maehama Coast …………… 前浜海岸
Makinohama Sandstone Member …… ………………………牧の浜砂岩部層
Minamisanriku Town ……… 南三陸町
Miyagi Prefecture …………… 宮城県
Miyako City ………………… 宮古市
Miyamori ……………………… 宮守
Mone Formation ………………舞根層
Monobegawa Group ……物部川層群
Morioka City ………………… 盛岡市
Motoyoshi ……………………… 本吉
Mt. Hayachinesan ………… 早池峰山
Mt. Hikamisan ……………… 氷上山
Mt. Karaumedateyama …… 唐梅館山
Myojinmae Formation …… 明神前層
Nagaiwa Formation ………… 長岩層
Nagao Formation …………… 長尾層
Nagasaka ……………………… 長坂
Nakahara Formation ………… 中原層
Nakazato Formation ………… 中里層
Nameirizawa Formation… 名目入沢層
Nameirizawa River ……… 名目入沢
Natsuyama Logging Road … 夏山林道
Niranohama Formation …… 韮の浜層
Nishikori Formation ………… 錦織層
Northern Chichibu Belt … 北部秩父帯
Notsuchi Formation ………… 野土層
Odagoe Formation ………… 小田越層
Odaira Formation …………… 大平層

Ofunato Group ………… 大船渡層群
Oginohama Formation …… 荻の浜層
Ohachimori Amphibolite …………… …………………………大鉢森角閃岩
Onimaru Formation …………鬼丸層
Ono Formation ……………… 大野層
Orikabetoge Formation …… 折壁峠層
Osawa Formation …………… 大沢層
Oshika Group …………… 牡鹿層群
Oshima Group …………… 大島層群
Rodai Formation …………… 楼台層
Ryoseki ………………………… 領石
Sakamotozawa Formation … 坂本沢層
Saragai Group …………… 皿貝層群
Saragaizaka Slope …………… 皿貝坂
Sendai City ………………… 仙台市
Setamai ……………………… 世田米
Shindate Formation ………… 新館層
Shittakasawa Formation … 尻高沢層
Shizugawa …………………… 志津川
Sodenohama Beach ………… 袖の浜
South Kitakami Belt（SKB）………… ……………………………南部北上帯
Southern Chichibu Belt … 南部秩父帯
Southwest Japan ………… 西南日本
Takonoura Formation …… 蛸浦層群
Tategami Formation ………… 立神層
Tenjinnoki Formation … 天神ノ木層
Tobigamori Formation …… 鳶ヶ森層
Tome City …………………… 登米市
Torinosu-type Limestone …………… …………………………鳥巣式石灰岩
Toyoma Formation ……………登米層
Tsukihama Formation …………月浜層
Tsunakizaka Formation …… 綱木坂層
Tsukinoura Formation …… 月の浦層
Usuginu-type Conglomerate ………… ……………………………薄衣式礫岩
Yakushigawa River ………… 薬師川
Yamadori Formation ………… 山鳥層
Yamazaki Conglomerates 山崎礫岩層
Yokonuma Formation ……… 横沼層
Yoshihama Formation ……… 吉浜層

TABLE 1. U-Pb isotopic data for zircons from sandstone of the South Kitakami Belt. All errors are 2σ. % conc = 100•($^{206}Pb/^{238}U$ age)/($^{207}Pb/^{235}U$ age) is a measure of concordance between $^{206}Pb/^{238}U$ and $^{207}Pb/^{235}U$ ages. Analyses shown in italics are discordant and are not included in the probability density plot and histogram.

Grain	$^{206}Pb/^{238}U$	$^{207}Pb/^{235}U$	$^{206}Pb/^{238}U$ age (Ma)	$^{207}Pb/^{235}U$ age (Ma)	% conc	Th/U
Silurian Nameirizawa Formation (08331-9; N39°32'55.8", E141°20'20.2")						
NM-1	0.0767 ± 0.0025	0.663 ± 0.036	477 ± 15	517 ± 22	92.3	0.50
NM-2	0.0808 ± 0.0027	0.714 ± 0.039	501 ± 16	547 ± 23	91.5	0.46
NM-3	0.524 ± 0.017	14.15 ± 0.77	2715 ± 73	2760 ± 52	98.4	0.57
NM-4	0.0713 ± 0.0024	0.582 ± 0.032	444 ± 14	466 ± 20	95.3	0.81
NM-5	0.327 ± 0.011	5.24 ± 0.29	1825 ± 52	1860 ± 46	98.1	0.51
NM-6	0.2085 ± 0.0069	2.23 ± 0.12	1221 ± 37	1191 ± 38	102.5	0.63
NM-7	0.0717 ± 0.0024	0.556 ± 0.030	446 ± 14	449 ± 20	99.4	0.90
NM-8	*0.0714 ± 0.0024*	*0.636 ± 0.035*	*445 ± 14*	*500 ± 21*	*88.9*	*0.45*
NM-9	0.0704 ± 0.0023	0.540 ± 0.029	439 ± 14	438 ± 19	100.0	0.54
NM-10	0.0725 ± 0.0026	0.619 ± 0.030	451 ± 16	489 ± 19	92.2	0.50
NM-11	0.0717 ± 0.0026	0.609 ± 0.029	447 ± 15	483 ± 18	92.4	0.83
NM-12	0.0688 ± 0.0025	0.511 ± 0.024	429 ± 15	419 ± 16	102.3	0.61
NM-13	0.1951 ± 0.0070	2.23 ± 0.11	1149 ± 38	1189 ± 33	96.6	0.80
NM-14	0.1080 ± 0.0039	0.975 ± 0.047	661 ± 23	691 ± 24	95.7	0.40
NM-15	0.1105 ± 0.0040	0.984 ± 0.047	675 ± 23	695 ± 24	97.1	0.46
NM-16	0.283 ± 0.010	3.28 ± 0.16	1605 ± 51	1476 ± 37	108.7	0.66
NM-17	0.0730 ± 0.0026	0.578 ± 0.028	454 ± 16	463 ± 18	98.1	0.70
NM-17-2	0.0710 ± 0.0025	0.608 ± 0.029	442 ± 15	482 ± 18	91.7	0.65
NM-18	0.0676 ± 0.0030	0.529 ± 0.045	422 ± 18	431 ± 30	97.8	0.75
NM-19	0.230 ± 0.010	2.55 ± 0.22	1335 ± 54	1287 ± 63	103.8	0.59
NM-20	0.2163 ± 0.0097	2.42 ± 0.21	1263 ± 51	1249 ± 62	101.1	0.79
NM-21	0.0736 ± 0.0033	0.597 ± 0.051	458 ± 20	475 ± 33	96.2	0.52
NM-21-2	0.0732 ± 0.0033	0.560 ± 0.048	456 ± 20	452 ± 31	100.9	0.58
NM-22	0.0718 ± 0.0032	0.525 ± 0.045	447 ± 19	429 ± 30	104.3	0.50
NM-23	*0.0699 ± 0.0031*	*0.616 ± 0.053*	*436 ± 19*	*488 ± 33*	*89.4*	*0.68*
NM-24	0.0689 ± 0.0031	0.533 ± 0.046	429 ± 19	434 ± 30	99.0	1.0
NM-25	0.1654 ± 0.0074	1.68 ± 0.14	987 ± 41	1002 ± 55	98.5	0.48
NM-26	0.0686 ± 0.0028	0.524 ± 0.029	428 ± 17	428 ± 19	100.1	0.84
NM-27	0.0705 ± 0.0029	0.570 ± 0.032	439 ± 17	458 ± 21	95.8	0.93
NM-28	0.0747 ± 0.0031	0.605 ± 0.034	464 ± 18	480 ± 21	96.6	0.48
NM-29	0.0976 ± 0.0040	0.877 ± 0.049	600 ± 23	639 ± 26	93.9	0.24
NM-30	0.0722 ± 0.0030	0.558 ± 0.031	450 ± 18	450 ± 20	99.9	0.45
NM-31	*0.0679 ± 0.0028*	*0.626 ± 0.035*	*424 ± 17*	*494 ± 22*	*85.8*	*1.0*
NM-32	*0.2082 ± 0.0085*	*2.86 ± 0.16*	*1219 ± 45*	*1371 ± 42*	*88.9*	*0.66*
NM-33	*0.06864 ± 0.00092*	*0.448 ± 0.012*	*428.0 ± 5.5*	*375.9 ± 8.1*	*113.9*	*0.55*
NM-34	0.06897 ± 0.00092	0.599 ± 0.015	429.9 ± 5.6	477 ± 10	90.2	0.56
NM-35	0.0712 ± 0.0010	0.606 ± 0.016	443.4 ± 5.7	481 ± 10	92.1	0.76
NM-36	0.1978 ± 0.0026	2.339 ± 0.060	1163 ± 14	1224 ± 18	95.0	2.2
NM-37	0.0726 ± 0.0010	0.637 ± 0.016	451.9 ± 5.8	500 ± 10	90.3	0.57
NM-38	0.3425 ± 0.0046	5.15 ± 0.13	1899 ± 22	1844 ± 22	103.0	1.6
NM-39	0.06941 ± 0.00093	0.563 ± 0.015	432.6 ± 5.6	453.7 ± 9.4	95.4	0.85
NM-40	0.0905 ± 0.0012	0.681 ± 0.018	558.6 ± 7.1	527 ± 11	106.0	0.82
NM-41	*0.2632 ± 0.0035*	*2.739 ± 0.071*	*1506 ± 18*	*1339 ± 19*	*112.5*	*0.40*
NM-42	0.3864 ± 0.0052	6.34 ± 0.16	2106 ± 24	2024 ± 23	104.1	0.22
NM-43	0.2496 ± 0.0067	3.11 ± 0.13	1437 ± 35	1436 ± 33	100.1	0.50
NM-44	0.1788 ± 0.0048	1.921 ± 0.083	1061 ± 26	1089 ± 29	97.4	0.65
NM-45	0.0701 ± 0.0019	0.547 ± 0.024	437 ± 11	443 ± 16	98.5	0.54
NM-46	0.0679 ± 0.0018	0.560 ± 0.024	423 ± 11	452 ± 16	93.8	0.46
NM-47	0.2671 ± 0.0072	3.93 ± 0.17	1526 ± 37	1621 ± 35	94.2	0.37
NM-48	0.0701 ± 0.0019	0.553 ± 0.024	437 ± 11	447 ± 16	97.8	0.69
NM-49	0.0733 ± 0.0020	0.543 ± 0.024	456 ± 12	440 ± 15	103.5	0.39

Grain	$^{206}Pb/^{238}U$	$^{207}Pb/^{235}U$	$^{206}Pb/^{238}U$ age (Ma)	$^{207}Pb/^{235}U$ age (Ma)	% conc	Th/U
NM-50	*0.0745 ± 0.0020*	*0.662 ± 0.029*	*463 ± 12*	*516 ± 18*	*89.8*	*0.41*
NM-51	0.0729 ± 0.0020	0.559 ± 0.024	453 ± 12	451 ± 16	100.6	0.39
NM-52	0.0729 ± 0.0020	0.524 ± 0.023	453 ± 12	428 ± 15	106.0	0.54
NM-53	0.3068 ± 0.0079	4.57 ± 0.23	1725 ± 39	1745 ± 42	98.9	0.29
NM-54	0.0712 ± 0.0018	0.496 ± 0.025	443 ± 11	409 ± 17	108.4	0.47
NM-55	0.0721 ± 0.0018	0.587 ± 0.030	449 ± 11	469 ± 19	95.8	0.63
NM-56	0.1699 ± 0.0044	1.720 ± 0.087	1012 ± 24	1016 ± 32	99.6	0.71
NM-57	0.0751 ± 0.0019	0.575 ± 0.029	467 ± 12	461 ± 19	101.3	0.70
NM-58	0.0695 ± 0.0018	0.486 ± 0.025	433 ± 11	402 ± 17	107.6	0.62
NM-59	*0.0762 ± 0.0020*	*0.495 ± 0.025*	*473 ± 12*	*408 ± 17*	*116.0*	*0.59*
NM-60	0.0727 ± 0.0019	0.545 ± 0.028	453 ± 11	442 ± 18	102.5	0.74
NM-61	0.0686 ± 0.0018	0.490 ± 0.025	427 ± 11	405 ± 17	105.6	0.66
NM-62	0.0701 ± 0.0018	0.545 ± 0.028	437 ± 11	442 ± 18	98.9	0.60
NM-63	0.0667 ± 0.0021	0.482 ± 0.024	416 ± 13	399 ± 17	104.2	0.72
NM-64	*0.0701 ± 0.0022*	*0.619 ± 0.031*	*437 ± 14*	*489 ± 20*	*89.2*	*0.88*
NM-65	0.0761 ± 0.0024	0.627 ± 0.032	473 ± 15	494 ± 20	95.6	0.24
NM-66	0.0722 ± 0.0023	0.603 ± 0.031	450 ± 14	479 ± 19	93.8	0.61
NM-67	0.1975 ± 0.0063	2.04 ± 0.10	1162 ± 34	1128 ± 34	103.0	1.1
NM-68	0.1259 ± 0.0040	1.174 ± 0.059	764 ± 23	789 ± 28	96.9	0.51
NM-69	0.0722 ± 0.0023	0.598 ± 0.030	450 ± 14	476 ± 19	94.5	0.39
NM-70	*0.1490 ± 0.0048*	*1.053 ± 0.053*	*896 ± 27*	*731 ± 26*	*122.6*	*0.32*
NM-71	0.0744 ± 0.0024	0.554 ± 0.028	462 ± 14	448 ± 18	103.3	0.91
NM-72	*0.0752 ± 0.0046*	*0.683 ± 0.054*	*467 ± 28*	*529 ± 32*	*88.4*	*0.55*
NM-73	*0.0704 ± 0.0043*	*0.644 ± 0.050*	*439 ± 26*	*505 ± 31*	*87.0*	*0.52*
NM-74	0.0693 ± 0.0043	0.491 ± 0.038	432 ± 26	406 ± 26	106.4	0.65
NM-75	0.0739 ± 0.0045	0.563 ± 0.044	460 ± 27	454 ± 29	101.4	0.44
NM-75-2	0.0690 ± 0.0042	0.527 ± 0.041	430 ± 26	430 ± 27	100.1	0.33
NM-76	0.0897 ± 0.0055	0.761 ± 0.060	554 ± 33	575 ± 34	96.3	0.46
NM-77	0.548 ± 0.034	16.3 ± 1.3	2815 ± 140	2894 ± 75	97.3	0.49
NM-78	0.0734 ± 0.0045	0.579 ± 0.045	457 ± 27	464 ± 29	98.4	0.63
NM-79	0.0900 ± 0.0055	0.774 ± 0.061	555 ± 33	582 ± 35	95.4	1.5
NM-80	0.263 ± 0.016	3.55 ± 0.28	1507 ± 83	1538 ± 62	98.0	0.42
NM-81	0.0933 ± 0.0049	0.782 ± 0.051	575 ± 29	586 ± 29	98.0	0.65
NM-82	0.592 ± 0.031	20.1 ± 1.3	2998 ± 125	3098 ± 63	96.8	0.71
NM-83	0.0755 ± 0.0040	0.580 ± 0.038	469 ± 24	465 ± 24	101.0	0.44
NM-84	0.0783 ± 0.0041	0.580 ± 0.038	486 ± 25	464 ± 24	104.7	0.46
NM-85	0.0701 ± 0.0037	0.536 ± 0.035	437 ± 22	436 ± 23	100.2	0.53
NM-86	0.0772 ± 0.0040	0.631 ± 0.041	480 ± 24	497 ± 26	96.5	0.68
NM-87	0.0744 ± 0.0039	0.617 ± 0.040	463 ± 23	488 ± 25	94.8	0.56
NM-88	0.0750 ± 0.0039	0.646 ± 0.042	466 ± 24	506 ± 26	92.0	0.64
NM-89	0.0925 ± 0.0048	0.755 ± 0.049	570 ± 29	571 ± 28	99.8	0.68
NM-90	0.0682 ± 0.0036	0.517 ± 0.034	425 ± 22	423 ± 23	100.5	0.53
NM-91	0.0689 ± 0.0042	0.550 ± 0.048	430 ± 25	445 ± 32	96.6	0.43
NM-92	0.0725 ± 0.0044	0.525 ± 0.046	451 ± 27	428 ± 31	105.4	0.81
NM-93	0.269 ± 0.016	3.58 ± 0.32	1537 ± 83	1546 ± 70	99.4	0.75
NM-94	0.0684 ± 0.0042	0.534 ± 0.047	426 ± 25	434 ± 31	98.1	0.60
NM-95	0.0776 ± 0.0047	0.592 ± 0.052	482 ± 28	472 ± 33	102.0	0.50
NM-96	0.466 ± 0.028	10.31 ± 0.91	2466 ± 125	2463 ± 82	100.1	0.37
NM-97	0.0734 ± 0.0045	0.638 ± 0.056	457 ± 27	501 ± 35	91.1	0.83

TABLE 1. (*Continued*)

Grain	$^{206}Pb/^{238}U$	$^{207}Pb/^{235}U$	$^{206}Pb/^{238}U$ age (Ma)	$^{207}Pb/^{235}U$ age (Ma)	% conc	Th/U
Silurian Yakushigawa Formation (08331-3; N39°32'06.8", E141°37'30.5")						
YKS-1	0.0637 ± 0.0022	0.519 ± 0.031	398 ± 13	425 ± 21	93.8	0.56
YKS-2	0.1691 ± 0.0058	1.643 ± 0.097	1007 ± 32	987 ± 37	102.1	0.55
YKS-3	0.1394 ± 0.0048	1.202 ± 0.071	841 ± 27	802 ± 33	105.0	0.33
YKS-4	0.0712 ± 0.0024	0.539 ± 0.032	443 ± 15	438 ± 21	101.2	0.74
YKS-5	0.0695 ± 0.0024	0.523 ± 0.031	433 ± 14	427 ± 21	101.3	0.38
YKS-6	0.1673 ± 0.0057	1.82 ± 0.11	997 ± 32	1052 ± 39	94.8	0.93
YKS-7	0.0727 ± 0.0025	0.627 ± 0.037	453 ± 15	494 ± 23	91.5	0.59
YKS-8	0.0762 ± 0.0026	0.661 ± 0.039	474 ± 16	515 ± 24	92.0	0.43
YKS-9	0.294 ± 0.010	4.87 ± 0.29	1661 ± 50	1797 ± 50	92.4	0.30
YKS-10	0.0689 ± 0.0025	0.540 ± 0.037	430 ± 15	438 ± 24	98.0	0.49
YKS-11	0.1802 ± 0.0066	2.00 ± 0.14	1068 ± 36	1114 ± 46	95.8	0.11
YKS-12	0.546 ± 0.020	13.98 ± 0.96	2807 ± 83	2748 ± 65	102.2	0.39
YKS-13	0.0732 ± 0.0027	0.569 ± 0.039	455 ± 16	458 ± 25	99.5	0.48
YKS-14	0.1289 ± 0.0047	1.161 ± 0.079	782 ± 27	782 ± 37	99.9	0.35
YKS-15	0.2377 ± 0.0087	2.89 ± 0.20	1375 ± 45	1378 ± 52	99.7	0.36
YKS-16	0.0722 ± 0.0026	0.619 ± 0.042	449 ± 16	489 ± 27	91.8	0.69
YKS-17	0.2333 ± 0.0085	2.98 ± 0.20	1352 ± 45	1404 ± 52	96.3	0.48
YKS-18	0.1619 ± 0.0059	1.68 ± 0.12	967 ± 33	1002 ± 44	96.6	0.58
YKS-19	0.0884 ± 0.0041	0.691 ± 0.054	546 ± 25	534 ± 33	102.3	1.2
YKS-20	0.0680 ± 0.0032	0.589 ± 0.046	424 ± 19	470 ± 30	90.2	0.39
YKS-21	0.0718 ± 0.0034	0.509 ± 0.040	447 ± 20	418 ± 27	107.0	0.53
YKS-22	0.0682 ± 0.0032	0.560 ± 0.044	425 ± 19	451 ± 29	94.2	0.75
YKS-23	0.0681 ± 0.0032	0.490 ± 0.039	425 ± 19	405 ± 26	105.0	0.53
YKS-24	0.0670 ± 0.0031	0.506 ± 0.040	418 ± 19	416 ± 27	100.6	0.52
YKS-25	0.2012 ± 0.0094	2.24 ± 0.18	1182 ± 51	1193 ± 55	99.1	0.99
YKS-26	0.0709 ± 0.0033	0.607 ± 0.048	442 ± 20	482 ± 30	91.7	0.51
YKS-27	0.0682 ± 0.0028	0.551 ± 0.036	425 ± 17	445 ± 24	95.5	0.69
YKS-28	0.279 ± 0.012	3.83 ± 0.25	1588 ± 59	1598 ± 53	99.4	0.68
YKS-29	0.0730 ± 0.0030	0.587 ± 0.039	454 ± 18	469 ± 25	96.8	0.59
YKS-30	0.470 ± 0.020	12.87 ± 0.85	2484 ± 86	2670 ± 62	93.0	1.5
YKS-31	0.0720 ± 0.0030	0.574 ± 0.038	448 ± 18	461 ± 24	97.3	0.56
YKS-32	0.503 ± 0.021	12.78 ± 0.84	2625 ± 90	2664 ± 62	98.5	1.0
YKS-33	0.354 ± 0.015	6.50 ± 0.43	1953 ± 70	2045 ± 58	95.5	0.27
YKS-34	0.0706 ± 0.0010	0.541 ± 0.013	440.0 ± 6.0	439.4 ± 8.3	100.1	0.74
YKS-35	0.0699 ± 0.0010	0.518 ± 0.012	435.4 ± 6.0	423.6 ± 8.1	102.8	0.59
YKS-36	0.0766 ± 0.0011	0.598 ± 0.014	475.7 ± 6.5	476.1 ± 8.9	99.9	0.52
YKS-37	0.1702 ± 0.0024	1.550 ± 0.036	1013 ± 13	951 ± 14	106.6	0.32
YKS-38	0.3378 ± 0.0048	4.86 ± 0.11	1876 ± 23	1795 ± 20	104.5	0.93
YKS-39	0.0784 ± 0.0011	0.627 ± 0.015	486.8 ± 6.7	494.4 ± 9.2	98.5	0.45
YKS-40	0.1002 ± 0.0038	0.868 ± 0.041	615 ± 22	635 ± 22	97.0	0.28
YKS-41	0.0929 ± 0.0035	0.778 ± 0.036	573 ± 21	584 ± 21	98.0	1.8
YKS-42	0.0944 ± 0.0035	0.770 ± 0.036	582 ± 21	580 ± 21	100.4	0.62
YKS-43	0.0780 ± 0.0029	0.602 ± 0.028	484 ± 17	478 ± 18	101.2	0.66
YKS-44	0.0758 ± 0.0028	0.568 ± 0.027	471 ± 17	457 ± 17	103.2	0.84
YKS-45	0.1792 ± 0.0067	2.025 ± 0.095	1063 ± 37	1124 ± 32	94.6	0.88
YKS-46	0.0744 ± 0.0028	0.594 ± 0.028	462 ± 17	473 ± 18	97.7	0.68
YKS-47	0.0706 ± 0.0026	0.526 ± 0.025	440 ± 16	429 ± 16	102.4	0.54
YKS-48	0.0734 ± 0.0028	0.604 ± 0.028	457 ± 17	479 ± 18	95.2	0.58
YKS-49	0.0675 ± 0.0043	0.561 ± 0.044	421 ± 26	452 ± 28	93.1	0.65
YKS-50	0.241 ± 0.015	3.13 ± 0.24	1390 ± 79	1439 ± 60	96.6	0.61
YKS-51	0.0778 ± 0.0049	0.596 ± 0.046	483 ± 30	475 ± 29	101.7	0.54
YKS-52	0.1325 ± 0.0084	1.168 ± 0.091	802 ± 48	786 ± 43	102.1	0.56
YKS-53	0.172 ± 0.011	1.69 ± 0.13	1025 ± 60	1003 ± 50	102.2	0.50
YKS-54	0.354 ± 0.022	6.65 ± 0.52	1952 ± 107	2067 ± 69	94.5	0.15
YKS-55	0.222 ± 0.014	2.82 ± 0.22	1294 ± 74	1360 ± 58	95.2	0.37
YKS-56	0.177 ± 0.011	1.91 ± 0.15	1052 ± 62	1085 ± 52	96.9	0.39
YKS-57	0.1492 ± 0.0095	1.49 ± 0.12	896 ± 53	928 ± 47	96.6	0.21
YKS-58	0.386 ± 0.028	7.49 ± 0.64	2106 ± 128	2172 ± 77	97.0	0.56
YKS-59	0.0715 ± 0.0051	0.500 ± 0.043	445 ± 31	412 ± 29	108.1	0.58
YKS-60	0.1243 ± 0.0089	1.155 ± 0.099	755 ± 51	780 ± 47	96.9	0.19
YKS-61	0.319 ± 0.023	4.98 ± 0.43	1787 ± 111	1816 ± 73	98.4	0.30
YKS-62	0.0713 ± 0.0051	0.611 ± 0.053	444 ± 31	484 ± 33	91.7	0.51
YKS-63	0.0660 ± 0.0047	0.480 ± 0.041	412 ± 29	398 ± 28	103.5	0.48
YKS-64	0.254 ± 0.018	3.49 ± 0.30	1458 ± 93	1524 ± 68	95.6	1.4
YKS-65	0.0682 ± 0.0049	0.555 ± 0.048	425 ± 29	448 ± 31	94.9	0.72
YKS-66	0.302 ± 0.022	4.59 ± 0.39	1699 ± 107	1747 ± 72	97.2	0.28
YKS-67	0.0698 ± 0.0039	0.504 ± 0.038	435 ± 24	415 ± 26	105.0	0.67
YKS-68	0.488 ± 0.027	12.35 ± 0.93	2561 ± 119	2631 ± 71	97.3	0.42
YKS-69	0.180 ± 0.010	1.81 ± 0.14	1067 ± 55	1050 ± 49	101.6	0.42
YKS-70	0.0728 ± 0.0041	0.554 ± 0.042	453 ± 25	448 ± 27	101.2	0.71
YKS-71	0.1483 ± 0.0083	1.49 ± 0.11	891 ± 47	927 ± 46	96.2	0.35
YKS-72	0.0711 ± 0.0040	0.568 ± 0.043	443 ± 24	457 ± 28	96.9	0.70
YKS-73	0.0681 ± 0.0038	0.511 ± 0.039	425 ± 23	419 ± 26	101.4	0.45
YKS-74	0.0781 ± 0.0038	0.633 ± 0.043	485 ± 23	498 ± 27	97.3	0.71
YKS-75	0.326 ± 0.016	5.01 ± 0.34	1820 ± 77	1821 ± 57	99.9	0.72
YKS-76	0.0726 ± 0.0035	0.548 ± 0.037	452 ± 21	444 ± 24	101.8	0.85
YKS-77	0.0748 ± 0.0037	0.545 ± 0.037	465 ± 22	442 ± 24	105.2	0.45
YKS-78	0.236 ± 0.012	2.66 ± 0.18	1364 ± 60	1319 ± 50	103.4	1.6
YKS-79	0.1106 ± 0.0054	0.967 ± 0.066	676 ± 31	687 ± 34	98.4	0.26
YKS-80	0.1375 ± 0.0067	1.225 ± 0.083	830 ± 38	812 ± 38	102.2	0.29
YKS-81	0.0762 ± 0.0037	0.540 ± 0.037	473 ± 22	438 ± 24	108.0	0.99
YKS-82	0.513 ± 0.025	13.18 ± 0.79	2667 ± 108	2693 ± 57	99.1	0.87
YKS-83	0.0704 ± 0.0035	0.571 ± 0.034	439 ± 21	459 ± 22	95.6	0.54
YKS-84	0.395 ± 0.020	7.83 ± 0.47	2147 ± 91	2211 ± 54	97.1	0.65
YKS-85	0.0977 ± 0.0048	0.773 ± 0.047	601 ± 28	581 ± 27	103.3	0.32
YKS-86	0.0925 ± 0.0046	0.748 ± 0.045	570 ± 27	567 ± 26	100.5	0.55
YKS-87	0.273 ± 0.014	3.83 ± 0.23	1557 ± 69	1600 ± 49	97.3	0.84
YKS-88	0.0755 ± 0.0037	0.571 ± 0.034	469 ± 22	459 ± 22	102.3	0.69
YKS-89	0.0727 ± 0.0036	0.579 ± 0.035	452 ± 22	464 ± 22	97.5	0.74
YKS-90	0.1815 ± 0.0090	1.87 ± 0.11	1075 ± 49	1072 ± 40	100.3	0.61
YKS-91	0.0739 ± 0.0032	0.582 ± 0.036	459 ± 19	466 ± 23	98.6	0.70
YKS-92	0.0741 ± 0.0032	0.554 ± 0.035	461 ± 19	448 ± 23	103.0	0.60
YKS-93	0.0737 ± 0.0032	0.534 ± 0.033	458 ± 19	434 ± 22	105.5	0.91
YKS-94	0.0752 ± 0.0032	0.588 ± 0.037	468 ± 19	470 ± 23	99.5	0.46
YKS-95	0.1183 ± 0.0051	1.135 ± 0.071	721 ± 29	770 ± 34	93.6	0.35
YKS-96	0.0746 ± 0.0032	0.551 ± 0.034	464 ± 19	446 ± 22	104.2	0.63
YKS-97	0.0766 ± 0.0033	0.607 ± 0.038	476 ± 20	481 ± 24	98.8	0.54
YKS-98	0.0757 ± 0.0033	0.560 ± 0.035	471 ± 20	451 ± 23	104.3	0.47
YKS-99	0.0702 ± 0.0030	0.527 ± 0.033	438 ± 18	430 ± 22	101.8	0.60
YKS-100	0.0719 ± 0.0031	0.589 ± 0.037	448 ± 19	470 ± 23	95.2	0.43

TABLE 1. (*Continued*)

Grain	$^{206}Pb/^{238}U$	$^{207}Pb/^{235}U$	$^{206}Pb/^{238}U$ age (Ma)	$^{207}Pb/^{235}U$ age (Ma)	% conc	Th/U
Devonian Tobigamori Formation (08429-5; N39°04'02.0", E141°14'37.0")						
TGM-1	0.0700 ± 0.0035	0.564 ± 0.044	436 ± 21	454 ± 29	96.0	0.47
TGM-2	0.0617 ± 0.0031	0.506 ± 0.040	386 ± 19	416 ± 27	92.9	0.34
TGM-3	0.1953 ± 0.0097	2.15 ± 0.17	1150 ± 52	1165 ± 55	98.7	0.57
TGM-4	0.239 ± 0.012	3.11 ± 0.25	1384 ± 62	1436 ± 61	96.4	0.93
TGM-5	0.1828 ± 0.0091	1.99 ± 0.16	1082 ± 49	1111 ± 53	97.4	0.33
TGM-6	0.1388 ± 0.0069	1.38 ± 0.11	838 ± 39	882 ± 47	95.0	0.21
TGM-7	0.0660 ± 0.0033	0.471 ± 0.037	412 ± 20	392 ± 26	105.2	0.53
TGM-8	0.0694 ± 0.0034	0.591 ± 0.047	432 ± 21	471 ± 30	91.7	0.81
TGM-9	0.247 ± 0.012	3.22 ± 0.25	1425 ± 63	1462 ± 61	97.5	1.8
TGM-10	0.0709 ± 0.0033	0.576 ± 0.031	442 ± 20	462 ± 20	95.7	0.38
TGM-11	0.0697 ± 0.0032	0.490 ± 0.026	434 ± 20	405 ± 18	107.3	0.59
TGM-12	0.0691 ± 0.0032	0.539 ± 0.029	431 ± 19	438 ± 19	98.4	0.50
TGM-13	0.0709 ± 0.0033	0.621 ± 0.033	442 ± 20	490 ± 21	90.1	0.74
TGM-14	0.0776 ± 0.0036	0.628 ± 0.034	482 ± 22	495 ± 21	97.4	0.44
TGM-15	0.0673 ± 0.0031	0.493 ± 0.027	420 ± 19	407 ± 18	103.2	0.80
TGM-16	0.0702 ± 0.0033	0.588 ± 0.032	437 ± 20	470 ± 20	93.1	0.56
TGM-17	0.0647 ± 0.0027	0.523 ± 0.029	404 ± 16	427 ± 19	94.6	0.59
TGM-18	0.0686 ± 0.0028	0.549 ± 0.030	427 ± 17	444 ± 20	96.3	1.0
TGM-19	0.0932 ± 0.0038	0.693 ± 0.038	575 ± 23	535 ± 23	107.5	2.2
TGM-20	0.481 ± 0.020	11.78 ± 0.65	2534 ± 86	2587 ± 52	97.9	0.69
TGM-21	0.0674 ± 0.0020	0.499 ± 0.025	420 ± 12	411 ± 17	102.3	0.70
TGM-22	0.1068 ± 0.0032	0.935 ± 0.046	654 ± 19	670 ± 24	97.6	0.63
TGM-23	0.1544 ± 0.0047	1.523 ± 0.076	925 ± 26	940 ± 30	98.5	0.53
TGM-24	0.611 ± 0.018	21.6 ± 1.1	3072 ± 74	3166 ± 48	97.0	0.76
TGM-25	0.0671 ± 0.0020	0.519 ± 0.026	419 ± 12	425 ± 17	98.7	0.55
TGM-26	0.0680 ± 0.0021	0.517 ± 0.026	424 ± 12	423 ± 17	100.2	0.56
TGM-27	0.0659 ± 0.0020	0.535 ± 0.027	412 ± 12	435 ± 18	94.7	0.65
TGM-28	0.2021 ± 0.0061	2.09 ± 0.10	1187 ± 33	1144 ± 34	103.7	0.92
TGM-29	0.0686 ± 0.0021	0.473 ± 0.023	428 ± 13	393 ± 16	108.8	0.78
TGM-30	0.0636 ± 0.0042	0.513 ± 0.045	398 ± 26	420 ± 30	94.6	0.54
TGM-31	0.553 ± 0.037	15.1 ± 1.3	2839 ± 153	2823 ± 84	100.6	0.25
TGM-32	0.0700 ± 0.0047	0.517 ± 0.046	436 ± 28	423 ± 31	103.1	0.62
TGM-33	0.0667 ± 0.0044	0.475 ± 0.042	416 ± 27	394 ± 29	105.5	0.57
TGM-34	0.0695 ± 0.0046	0.541 ± 0.048	433 ± 28	439 ± 31	98.6	0.46
TGM-35	0.1040 ± 0.0069	0.971 ± 0.086	638 ± 41	689 ± 44	92.6	0.23
TGM-36	0.1024 ± 0.0068	0.931 ± 0.082	629 ± 40	668 ± 43	94.1	0.20
TGM-37	0.197 ± 0.013	2.08 ± 0.18	1157 ± 71	1144 ± 61	101.1	0.52
Lower Carboniferous Karaumedate Formation (120611-2; N39°0'25.10", E141°15'57.06")						
120611-2-1	0.1826 ± 0.0036	1.961 ± 0.054	1081 ± 21	1102 ± 30	98.1	0.58
120611-2-2	0.0587 ± 0.0012	0.457 ± 0.015	367.8 ± 7.3	382 ± 13	96.3	0.48
120611-2-3	0.0567 ± 0.0011	0.424 ± 0.015	355.7 ± 7.2	359 ± 13	99.1	0.40
120611-2-4	0.2397 ± 0.0035	2.993 ± 0.099	1385 ± 20	1406 ± 46	98.5	0.24
120611-2-5	0.05688 ± 0.00083	0.434 ± 0.015	356.6 ± 5.2	366 ± 13	97.5	0.49
120611-2-6	0.0824 ± 0.0012	0.663 ± 0.022	510.3 ± 7.5	516 ± 18	98.8	0.54
120611-2-7	0.05879 ± 0.00089	0.448 ± 0.017	368.2 ± 5.6	376 ± 15	98.0	0.45
120611-2-8	0.0583 ± 0.0015	0.445 ± 0.017	365.0 ± 9.3	374 ± 15	97.6	0.47
120611-2-9	0.0577 ± 0.0015	0.433 ± 0.016	361.7 ± 9.2	365 ± 13	99.1	0.59
120611-2-10	0.0578 ± 0.0015	0.431 ± 0.017	362.2 ± 9.3	364 ± 14	99.5	0.63
120611-2-11	0.0592 ± 0.0015	0.443 ± 0.017	370.5 ± 9.5	373 ± 15	99.5	0.51
120611-2-12	0.0595 ± 0.0016	0.453 ± 0.022	373 ± 10	380 ± 19	98.1	0.35
120611-2-13	0.0655 ± 0.0018	0.512 ± 0.025	409 ± 11	420 ± 21	97.4	0.75
120611-2-14	0.0734 ± 0.0020	0.597 ± 0.031	457 ± 12	476 ± 25	96.1	0.33
120611-2-15	0.0570 ± 0.0015	0.456 ± 0.023	357.3 ± 9.7	382 ± 19	93.6	0.68
120611-2-16	0.2584 ± 0.0069	3.49 ± 0.15	1482 ± 40	1525 ± 67	97.2	0.93
120611-2-17	0.2871 ± 0.0026	4.053 ± 0.089	1627 ± 15	1645 ± 36	98.9	0.30
120611-2-18	0.05741 ± 0.00060	0.423 ± 0.014	359.9 ± 3.8	358 ± 12	100.5	0.69
120611-2-19	0.05832 ± 0.00062	0.427 ± 0.014	365.4 ± 3.9	361 ± 12	101.3	1.2
120611-2-20	0.05613 ± 0.00059	0.415 ± 0.014	352.1 ± 3.7	353 ± 12	99.8	0.56
120611-2-21	0.06587 ± 0.00065	0.526 ± 0.014	411.2 ± 4.0	429 ± 12	95.8	0.67
120611-2-22	0.2314 ± 0.0021	2.891 ± 0.064	1342 ± 12	1380 ± 30	97.2	0.53
120611-2-23	0.4869 ± 0.0045	12.49 ± 0.27	2557 ± 23	2642 ± 58	96.8	0.35
120611-2-24	0.0564 ± 0.0010	0.430 ± 0.019	353.4 ± 6.5	363 ± 16	97.4	0.65
120611-2-25	0.0576 ± 0.0011	0.451 ± 0.020	360.8 ± 6.6	378 ± 17	95.5	0.46
120611-2-26	0.0565 ± 0.0011	0.459 ± 0.024	354.6 ± 6.8	384 ± 20	92.4	0.58
120611-2-27	0.2465 ± 0.0043	3.08 ± 0.11	1420 ± 25	1428 ± 51	99.5	0.31
120611-2-28	0.0558 ± 0.0010	0.430 ± 0.019	350.2 ± 6.4	363 ± 16	96.4	0.53
120611-2-29	0.2434 ± 0.0042	3.20 ± 0.11	1404 ± 24	1456 ± 51	96.5	0.33
120611-2-30	0.0673 ± 0.0012	0.507 ± 0.019	419.7 ± 7.4	416 ± 16	100.8	0.55
120611-2-31	0.0584 ± 0.0010	0.439 ± 0.017	366.2 ± 6.4	370 ± 14	99.1	0.61
120611-2-32	0.05848 ± 0.00064	0.439 ± 0.014	366.4 ± 4.0	370 ± 12	99.1	0.63
120611-2-33	0.06830 ± 0.00070	0.531 ± 0.015	425.9 ± 4.4	433 ± 12	98.5	0.71
120611-2-34	0.05735 ± 0.00066	0.449 ± 0.016	359.5 ± 4.2	376 ± 14	95.5	0.81
120611-2-35	0.05746 ± 0.00062	0.443 ± 0.014	360.1 ± 3.9	372 ± 12	96.8	0.74
120611-2-36	0.05820 ± 0.00065	0.437 ± 0.015	364.7 ± 4.1	368 ± 13	99.1	0.70
120611-2-37	0.3370 ± 0.0034	5.58 ± 0.14	1872 ± 19	1912 ± 48	97.9	0.75
120611-2-38	0.2497 ± 0.0025	3.127 ± 0.081	1437 ± 14	1439 ± 37	99.8	0.76
120611-2-39	0.1741 ± 0.0017	2.041 ± 0.053	1034 ± 10	1129 ± 29	91.6	0.25
120611-2-40	0.07107 ± 0.00071	0.574 ± 0.014	442.6 ± 4.4	461 ± 11	96.1	1.0
120611-2-41	0.05738 ± 0.00072	0.442 ± 0.019	359.7 ± 4.5	372 ± 16	96.7	0.58
120611-2-42	0.06157 ± 0.00067	0.450 ± 0.014	385.2 ± 4.2	377 ± 12	102.2	0.93
120611-2-43	0.05825 ± 0.00055	0.439 ± 0.009	364.9 ± 3.5	369.6 ± 7.7	98.8	0.35
120611-2-44	0.06554 ± 0.00070	0.493 ± 0.015	409.3 ± 4.4	407 ± 12	100.5	0.52
120611-2-45	0.07487 ± 0.00071	0.587 ± 0.012	465.4 ± 4.4	469 ± 10	99.2	0.62
120611-2-46	0.05818 ± 0.00062	0.441 ± 0.014	364.6 ± 3.9	371 ± 11	98.3	0.95
120611-2-47	0.0994 ± 0.0020	0.850 ± 0.036	611 ± 13	625 ± 26	97.8	0.77
120611-2-48	0.0602 ± 0.0012	0.465 ± 0.020	377.0 ± 7.8	388 ± 17	97.3	0.99
120611-2-49	0.0584 ± 0.0012	0.436 ± 0.018	365.8 ± 7.4	367 ± 15	99.6	0.94
120611-2-50	0.0659 ± 0.0014	0.489 ± 0.025	411.4 ± 8.8	404 ± 20	101.8	0.73
120611-2-51	0.0599 ± 0.0012	0.449 ± 0.018	374.9 ± 7.6	376 ± 15	99.7	0.39
120611-2-52	0.0568 ± 0.0013	0.437 ± 0.028	356.0 ± 8.1	368 ± 24	96.7	0.97
120611-2-53	*0.0726 ± 0.0014*	*0.652 ± 0.022*	*452.0 ± 8.7*	*510 ± 17*	*88.7*	*0.46*
120611-2-54	0.0575 ± 0.0011	0.458 ± 0.017	360.1 ± 7.0	383 ± 14	94.1	0.57
120611-2-55	0.0558 ± 0.0011	0.421 ± 0.018	350.1 ± 7.0	357 ± 15	98.2	0.40
120611-2-56	0.0578 ± 0.0013	0.464 ± 0.028	362.1 ± 7.9	387 ± 23	93.6	0.35
120611-2-57	0.0684 ± 0.0011	0.532 ± 0.016	426.2 ± 6.9	433 ± 13	98.5	0.67
120611-2-58	0.05601 ± 0.00094	0.436 ± 0.017	351.3 ± 5.9	367 ± 14	95.6	0.41
120611-2-59	0.0688 ± 0.0011	0.542 ± 0.017	428.9 ± 7.0	440 ± 14	97.5	0.41
120611-2-60	0.0662 ± 0.0012	0.540 ± 0.029	413.0 ± 7.7	438 ± 23	94.3	0.55
120611-2-61	0.0583 ± 0.0017	0.445 ± 0.018	365 ± 11	373 ± 15	97.7	0.61
120611-2-62	0.0597 ± 0.0018	0.444 ± 0.016	374 ± 11	373 ± 13	100.2	1.2
120611-2-63	*0.0584 ± 0.0018*	*0.584 ± 0.024*	*366 ± 11*	*467 ± 19*	*78.4*	*0.64*

TABLE 1. (*Continued*)

Grain	$^{206}Pb/^{238}U$	$^{207}Pb/^{235}U$	$^{206}Pb/^{238}U$ age (Ma)	$^{207}Pb/^{235}U$ age (Ma)	% conc	Th/U
120611-2-64	0.0572 ± 0.0011	0.459 ± 0.016	358.5 ± 7.0	384 ± 13	93.5	0.72
120611-2-65	0.0715 ± 0.0014	0.549 ± 0.016	445.1 ± 8.4	444 ± 13	100.2	0.35
120611-2-66	0.0576 ± 0.0011	0.432 ± 0.015	360.9 ± 7.0	365 ± 13	99.0	0.88
120611-2-67	0.0587 ± 0.0013	0.461 ± 0.019	367.9 ± 8.2	385 ± 15	95.5	0.74
120611-2-68	0.0707 ± 0.0015	0.553 ± 0.019	440.6 ± 9.6	447 ± 15	98.6	0.56
120611-2-69	0.0691 ± 0.0015	0.529 ± 0.020	431.0 ± 9.5	431 ± 16	100.0	0.60
120611-2-70	*0.0573 ± 0.0015*	*0.482 ± 0.024*	*359.3 ± 9.1*	*400 ± 20*	*89.9*	*0.69*
120611-2-71	*0.0584 ± 0.0015*	*0.497 ± 0.023*	*366.0 ± 9.2*	*410 ± 19*	*89.4*	*0.59*
120611-2-72	0.0685 ± 0.0017	0.552 ± 0.021	427 ± 10	446 ± 17	95.8	0.56
120611-2-73	*0.0554 ± 0.0015*	*0.467 ± 0.029*	*347.4 ± 9.3*	*389 ± 24*	*89.2*	*0.58*
120611-2-74	0.2446 ± 0.0059	3.05 ± 0.11	1411 ± 34	1421 ± 51	99.3	0.40
120611-2-75	0.0566 ± 0.0013	0.435 ± 0.016	354.7 ± 8.0	367 ± 14	96.7	1.1
120611-2-76	0.0556 ± 0.0012	0.420 ± 0.014	348.9 ± 7.8	356 ± 12	97.9	0.63
120611-2-77	0.2039 ± 0.0045	2.554 ± 0.080	1197 ± 27	1288 ± 41	92.9	0.23
120611-2-78	0.0577 ± 0.0013	0.452 ± 0.016	361.6 ± 8.1	379 ± 14	95.5	0.86
Lower Permian Nishikori Formation (120611-8; N38°41'14.17", E141°17'24.39")						
120611-8-1	*0.0438 ± 0.0017*	*0.362 ± 0.045*	*276 ± 11*	*314 ± 39*	*88.2*	*0.35*
120611-8-2	0.0489 ± 0.0030	0.384 ± 0.093	308 ± 19	330 ± 80	93.2	0.55
120611-8-3	*0.0427 ± 0.0026*	*0.360 ± 0.083*	*270 ± 16*	*312 ± 72*	*86.4*	*0.36*
120611-8-4	0.0468 ± 0.0016	0.326 ± 0.031	295 ± 10	287 ± 27	102.8	1.2
120611-8-5	0.0440 ± 0.0025	0.286 ± 0.069	278 ± 16	255 ± 62	108.9	0.57
120611-8-6	0.0455 ± 0.0025	0.307 ± 0.069	287 ± 16	272 ± 61	105.4	0.45
120611-8-7	0.0478 ± 0.0028	0.345 ± 0.083	301 ± 18	301 ± 72	100.1	0.51
120611-8-8	0.0449 ± 0.0017	0.330 ± 0.040	283 ± 11	290 ± 35	97.8	0.49
120611-8-9	0.0446 ± 0.0026	0.308 ± 0.072	282 ± 17	273 ± 64	103.3	0.56
120611-8-10	*0.0460 ± 0.0019*	*0.277 ± 0.030*	*290 ± 12*	*248 ± 27*	*116.7*	*0.77*
120611-8-11	0.0481 ± 0.0025	0.337 ± 0.062	303 ± 16	295 ± 54	102.6	0.49
120611-8-12	0.0436 ± 0.0023	0.328 ± 0.058	275 ± 14	288 ± 51	95.5	0.31
120611-8-13	*0.0439 ± 0.0023*	*0.377 ± 0.063*	*277 ± 14*	*325 ± 54*	*85.2*	*0.38*
120611-8-14	0.0450 ± 0.0022	0.326 ± 0.054	284 ± 14	287 ± 47	98.9	0.34
120611-8-15	0.0434 ± 0.0018	0.297 ± 0.035	274 ± 12	264 ± 31	103.6	0.61
120611-8-16	0.0436 ± 0.0027	0.281 ± 0.084	275 ± 17	252 ± 75	109.4	0.52
120611-8-17	*0.0443 ± 0.0019*	*0.269 ± 0.053*	*279 ± 12*	*242 ± 48*	*115.2*	*0.76*
120611-8-18	0.0434 ± 0.0017	0.318 ± 0.051	274 ± 11	281 ± 45	97.6	0.54
120611-8-19	*0.0481 ± 0.0027*	*0.290 ± 0.080*	*303 ± 17*	*258 ± 71*	*117.3*	*0.35*
120611-8-20	0.0464 ± 0.0017	0.353 ± 0.052	292 ± 11	307 ± 45	95.1	0.48
120611-8-21	0.0420 ± 0.0017	0.325 ± 0.054	265 ± 11	285 ± 48	93.0	0.35
120611-8-22	0.0421 ± 0.0017	0.287 ± 0.049	266 ± 10	256 ± 44	103.6	0.39
120611-8-23	0.0426 ± 0.0024	0.296 ± 0.076	269 ± 15	263 ± 68	102.2	0.67
120611-8-24	0.0439 ± 0.0013	0.309 ± 0.041	276.9 ± 8.4	273 ± 36	101.4	0.45
120611-8-25	*0.0437 ± 0.0018*	*0.232 ± 0.052*	*276 ± 11*	*212 ± 47*	*130.2*	*0.64*
120611-8-26	0.0473 ± 0.0015	0.330 ± 0.048	298 ± 10	290 ± 42	102.9	0.48
120611-8-27	0.0438 ± 0.0014	0.337 ± 0.047	276.1 ± 8.9	295 ± 41	93.5	0.43
120611-8-28	0.0438 ± 0.0018	0.290 ± 0.056	276 ± 11	259 ± 50	106.8	0.48
120611-8-29	0.0465 ± 0.0017	0.348 ± 0.057	293 ± 11	303 ± 50	96.6	0.38
120611-8-30	0.0466 ± 0.0018	0.325 ± 0.056	293 ± 11	285 ± 50	102.8	0.42
120611-8-31	0.0433 ± 0.0013	0.327 ± 0.042	273.2 ± 8.3	287 ± 37	95.1	0.59
120611-8-32	0.0494 ± 0.0020	0.362 ± 0.062	311 ± 13	314 ± 54	99.2	0.35
120611-8-33	0.0438 ± 0.0018	0.332 ± 0.054	276 ± 11	291 ± 48	95.0	0.67
120611-8-34	0.0436 ± 0.0019	0.332 ± 0.062	275 ± 12	291 ± 54	94.4	0.64
120611-8-35	0.0448 ± 0.0015	0.341 ± 0.046	282 ± 10	298 ± 40	94.8	0.50
120611-8-36	0.0462 ± 0.0017	0.307 ± 0.048	291 ± 11	272 ± 43	107.1	0.76
120611-8-37	*0.0431 ± 0.0019*	*0.274 ± 0.054*	*272 ± 12*	*246 ± 48*	*110.6*	*0.62*
120611-8-38	*0.0429 ± 0.0017*	*0.362 ± 0.057*	*271 ± 11*	*314 ± 50*	*86.2*	*0.55*
120611-8-39	0.0428 ± 0.0012	0.317 ± 0.033	270.1 ± 7.7	279 ± 29	96.6	0.51
120611-8-40	0.0444 ± 0.0012	0.313 ± 0.035	280.0 ± 7.8	276 ± 31	101.4	0.58
120611-8-41	*0.0421 ± 0.0028*	*0.246 ± 0.085*	*266 ± 18*	*223 ± 77*	*119.1*	*0.37*
120611-8-42	0.0433 ± 0.0015	0.280 ± 0.043	273.4 ± 9.4	250 ± 38	109.2	0.59
120611-8-43	0.0463 ± 0.0015	0.348 ± 0.048	292 ± 10	303 ± 42	96.1	0.51
120611-8-44	0.0445 ± 0.0010	0.329 ± 0.025	280.5 ± 6.2	289 ± 22	97.1	0.91
120611-8-45	*0.0437 ± 0.0013*	*0.353 ± 0.039*	*275.9 ± 8.0*	*307 ± 34*	*89.9*	*0.76*
120611-8-46	0.0441 ± 0.0016	0.350 ± 0.051	278 ± 10	305 ± 45	91.2	0.45
120611-8-47	*0.0445 ± 0.0015*	*0.280 ± 0.042*	*280.4 ± 9.4*	*251 ± 38*	*111.8*	*0.34*
120611-8-48	0.0463 ± 0.0024	0.344 ± 0.078	292 ± 15	300 ± 68	97.2	0.52
120611-8-49	0.0416 ± 0.0013	0.307 ± 0.039	263.0 ± 8.4	272 ± 34	96.8	0.54
120611-8-50	0.0452 ± 0.0014	0.346 ± 0.041	284.8 ± 8.7	302 ± 35	94.4	0.46
120611-8-51	0.0422 ± 0.0019	0.295 ± 0.058	266 ± 12	262 ± 52	101.6	0.35
120611-8-52	*0.0431 ± 0.0022*	*0.408 ± 0.081*	*272 ± 14*	*347 ± 69*	*78.4*	*0.46*
120611-8-53	0.0452 ± 0.0016	0.329 ± 0.049	285 ± 10	288 ± 43	98.7	0.34
120611-8-54	0.0449 ± 0.0017	0.325 ± 0.053	283 ± 11	286 ± 46	99.1	0.43
120611-8-55	0.0439 ± 0.0016	0.334 ± 0.049	277 ± 10	292 ± 43	94.7	0.46
120611-8-56	0.0490 ± 0.0017	0.361 ± 0.043	308 ± 11	313 ± 37	98.5	0.75
120611-8-57	0.0480 ± 0.0020	0.363 ± 0.059	302 ± 13	315 ± 52	96.1	0.49
120611-8-58	0.0460 ± 0.0020	0.352 ± 0.061	290 ± 13	306 ± 53	94.7	0.36
120611-8-59	0.0489 ± 0.0020	0.338 ± 0.055	308 ± 13	296 ± 48	104.1	0.68
120611-8-60	0.0449 ± 0.0020	0.356 ± 0.062	283 ± 13	309 ± 54	91.7	0.51
120611-8-61	0.0463 ± 0.0015	0.317 ± 0.035	291.7 ± 9.4	280 ± 31	104.2	0.51
120611-8-62	*0.0463 ± 0.0020*	*0.377 ± 0.061*	*292 ± 12*	*325 ± 53*	*89.9*	*0.42*
120611-8-63	*0.0452 ± 0.0016*	*0.380 ± 0.044*	*285 ± 10*	*327 ± 37*	*87.2*	*0.57*
120611-8-64	0.0448 ± 0.0015	0.341 ± 0.039	282.8 ± 9.2	298 ± 34	95.0	0.51
120611-8-65	0.0437 ± 0.0017	0.298 ± 0.048	276 ± 11	265 ± 42	104.1	0.60
120611-8-66	*0.0433 ± 0.0016*	*0.354 ± 0.051*	*273 ± 10*	*308 ± 44*	*88.8*	*0.57*
120611-8-67	0.0458 ± 0.0022	0.343 ± 0.073	289 ± 14	299 ± 64	96.4	0.59
120611-8-68	0.0463 ± 0.0023	0.347 ± 0.077	292 ± 15	303 ± 67	96.3	0.48
120611-8-69	*0.0420 ± 0.0014*	*0.338 ± 0.041*	*265.1 ± 9.0*	*295 ± 36*	*89.7*	*0.49*
120611-8-70	0.0478 ± 0.0019	0.345 ± 0.056	301 ± 12	301 ± 48	100.1	0.51
120611-8-71	0.0448 ± 0.0017	0.342 ± 0.046	283 ± 11	299 ± 40	94.6	0.38
120611-8-72	0.0475 ± 0.0019	0.338 ± 0.052	299 ± 12	295 ± 46	101.3	0.45
120611-8-73	0.0449 ± 0.0018	0.327 ± 0.051	283 ± 12	287 ± 44	98.5	0.43
120611-8-74	*0.0445 ± 0.0022*	*0.389 ± 0.073*	*281 ± 14*	*334 ± 62*	*84.2*	*0.64*
120611-8-75	*0.0454 ± 0.0020*	*0.395 ± 0.062*	*286 ± 13*	*338 ± 53*	*84.8*	*0.41*
120611-8-76	0.0475 ± 0.0019	0.337 ± 0.051	299 ± 12	295 ± 45	101.4	0.58
120611-8-77	*0.0450 ± 0.0025*	*0.377 ± 0.082*	*284 ± 15*	*325 ± 70*	*87.3*	*0.46*
Upper Permian Toyoma Formation (101001-1; N38°48'02.3", E141°33'04.0")						
101001-1-1	0.03919 ± 0.00056	0.286 ± 0.013	247.8 ± 3.6	256 ± 11	96.9	0.44
101001-1-2	0.0724 ± 0.0010	0.559 ± 0.019	450.9 ± 6.0	451 ± 16	100.1	0.57
101001-1-3	0.06872 ± 0.00094	0.595 ± 0.021	428.4 ± 5.8	474 ± 17	90.4	0.53
101001-1-4	0.1293 ± 0.0018	1.200 ± 0.041	784 ± 11	801 ± 27	98.0	1.0
101001-1-5	0.03767 ± 0.00052	0.284 ± 0.011	238.4 ± 3.3	253.9 ± 9.8	93.9	1.1
101001-1-6	0.03949 ± 0.00051	0.2896 ± 0.0070	249.7 ± 3.2	258.2 ± 6.3	96.7	0.37

TABLE 1. (*Continued*)

Grain	$^{206}Pb/^{238}U$	$^{207}Pb/^{235}U$	$^{206}Pb/^{238}U$ age (Ma)	$^{207}Pb/^{235}U$ age (Ma)	% conc	Th/U
101001-1-7	0.1263 ± 0.0016	1.152 ± 0.019	766.9 ± 9.6	778 ± 13	98.5	0.56
101001-1-8	0.1551 ± 0.0038	1.522 ± 0.044	929 ± 23	939 ± 27	98.9	0.34
101001-1-9	0.0413 ± 0.0011	0.302 ± 0.021	260.9 ± 6.8	268 ± 18	97.4	0.68
101001-1-10	0.0394 ± 0.0010	0.286 ± 0.012	249.0 ± 6.2	255 ± 11	97.5	0.43
101001-1-11	*0.0403 ± 0.0011*	*0.329 ± 0.025*	*254.8 ± 6.8*	*289 ± 22*	*88.2*	*0.41*
101001-1-12	*0.0419 ± 0.0011*	*0.347 ± 0.021*	*264.8 ± 6.9*	*303 ± 18*	*87.4*	*0.89*
101001-1-13	0.04046 ± 0.00056	0.289 ± 0.011	255.7 ± 3.5	257.9 ± 9.4	99.2	0.68
101001-1-14	0.03938 ± 0.00052	0.3127 ± 0.0081	249.0 ± 3.3	276.3 ± 7.2	90.1	1.8
101001-1-15	0.05875 ± 0.00091	0.430 ± 0.027	368.0 ± 5.7	363 ± 23	101.4	0.69
101001-1-16	0.03914 ± 0.00054	0.287 ± 0.011	247.5 ± 3.4	256.3 ± 9.7	96.6	0.57
101001-1-17	0.03862 ± 0.00052	0.2802 ± 0.0094	244.3 ± 3.3	250.8 ± 8.4	97.4	0.38
101001-1-18	0.04039 ± 0.00059	0.287 ± 0.014	255.3 ± 3.7	256 ± 13	99.7	0.77
101001-1-19	0.03916 ± 0.00054	0.281 ± 0.010	247.6 ± 3.4	251.8 ± 9.1	98.3	0.37
101001-1-20	0.03859 ± 0.00054	0.280 ± 0.011	244.1 ± 3.4	251 ± 10	97.2	1.1
101001-1-21	0.04008 ± 0.00085	0.297 ± 0.013	253.3 ± 5.4	264 ± 12	95.9	0.47
101001-1-22	*0.03832 ± 0.00081*	*0.314 ± 0.012*	*242.4 ± 5.1*	*277 ± 11*	*87.4*	*1.0*
101001-1-23	0.0454 ± 0.0010	0.343 ± 0.015	286.1 ± 6.1	300 ± 13	95.5	0.48
101001-1-24	0.03936 ± 0.00085	0.287 ± 0.015	248.9 ± 5.4	257 ± 13	97.0	0.58
101001-1-25	0.0822 ± 0.0019	0.613 ± 0.033	509 ± 12	485 ± 26	105.0	0.24
101001-1-26	0.0830 ± 0.0019	0.649 ± 0.028	514 ± 12	508 ± 22	101.2	0.47
101001-1-27	0.0409 ± 0.0011	0.315 ± 0.022	258.3 ± 6.6	278 ± 20	93.0	0.77
101001-1-28	0.0415 ± 0.0010	0.311 ± 0.018	262.1 ± 6.3	275 ± 16	95.3	0.47
101001-1-29	0.0405 ± 0.0013	0.275 ± 0.033	255.9 ± 8.2	247 ± 29	103.6	0.41
101001-1-30	0.0475 ± 0.0014	0.334 ± 0.035	298.9 ± 9.0	292 ± 30	102.2	0.46
101001-1-31	0.0431 ± 0.0011	0.299 ± 0.021	272.3 ± 6.9	266 ± 18	102.5	0.49
101001-1-32	0.0406 ± 0.0012	0.287 ± 0.025	256.7 ± 7.6	256 ± 22	100.2	0.58
101001-1-33	0.0403 ± 0.0011	0.297 ± 0.022	254.7 ± 7.2	264 ± 20	96.5	0.72
101001-1-34	0.0417 ± 0.0012	0.293 ± 0.022	263.4 ± 7.4	261 ± 20	100.8	0.53
101001-1-35	0.0434 ± 0.0021	0.290 ± 0.074	274 ± 13	258 ± 66	105.9	0.74
101001-1-36	0.0422 ± 0.0012	0.308 ± 0.024	266.6 ± 7.6	272 ± 21	97.9	0.45
101001-1-37	0.0435 ± 0.0013	0.310 ± 0.029	274.7 ± 8.3	274 ± 25	100.3	0.54
101001-1-38	*0.0496 ± 0.0013*	*0.408 ± 0.022*	*312.0 ± 8.1*	*347 ± 18*	*89.8*	*0.46*
101001-1-39	0.1792 ± 0.0018	1.998 ± 0.067	1063 ± 11	1115 ± 37	95.3	0.19
101001-1-40	0.04388 ± 0.00070	0.315 ± 0.022	276.8 ± 4.4	278 ± 19	99.5	1.0
101001-1-41	0.04313 ± 0.00064	0.325 ± 0.020	272.2 ± 4.0	286 ± 17	95.2	0.59
101001-1-42	0.0741 ± 0.0011	0.577 ± 0.037	460.7 ± 7.1	463 ± 29	99.6	0.41
101001-1-43	0.04192 ± 0.00071	0.289 ± 0.022	264.7 ± 4.5	258 ± 19	102.7	0.38
101001-1-44	0.04151 ± 0.00060	0.288 ± 0.017	262.2 ± 3.8	257 ± 16	102.1	0.53
101001-1-45	0.04291 ± 0.00094	0.285 ± 0.029	270.8 ± 5.9	254 ± 26	106.5	0.84
101001-1-46	0.03984 ± 0.00078	0.315 ± 0.026	251.8 ± 4.9	278 ± 23	90.7	0.55
101001-1-47	0.0433 ± 0.0012	0.343 ± 0.026	273.0 ± 7.5	299 ± 23	91.2	0.48
101001-1-48	0.0428 ± 0.0011	0.335 ± 0.021	270.2 ± 6.9	293 ± 18	92.2	0.43
101001-1-49	*0.0429 ± 0.0013*	*0.349 ± 0.033*	*270.6 ± 8.2*	*304 ± 29*	*89.1*	*0.33*
101001-1-50	*0.0487 ± 0.0016*	*0.315 ± 0.040*	*306 ± 10*	*278 ± 35*	*110.3*	*0.55*
101001-1-51	*0.0426 ± 0.0012*	*0.452 ± 0.034*	*269.0 ± 7.6*	*379 ± 28*	*71.0*	*0.46*
101001-1-52	0.0392 ± 0.0010	0.281 ± 0.019	247.7 ± 6.4	251 ± 17	98.6	0.46
101001-1-53	0.03989 ± 0.00078	0.284 ± 0.018	252.1 ± 5.0	254 ± 16	99.3	0.65
101001-1-54	0.0439 ± 0.0014	0.306 ± 0.041	276.8 ± 8.8	271 ± 36	102.1	0.71
101001-1-55	0.0379 ± 0.0013	0.248 ± 0.036	239.9 ± 8.0	225 ± 33	106.8	0.92
101001-1-56	*0.03891 ± 0.00083*	*0.323 ± 0.023*	*246.1 ± 5.2*	*284 ± 20*	*86.5*	*0.35*
101001-1-57	*0.04009 ± 0.00068*	*0.344 ± 0.015*	*253.4 ± 4.3*	*300 ± 13*	*84.4*	*0.50*
101001-1-58	0.03597 ± 0.00068	0.254 ± 0.015	227.8 ± 4.3	230 ± 14	99.0	0.39
101001-1-59	0.0408 ± 0.0011	0.297 ± 0.027	257.7 ± 7.0	264 ± 24	97.6	0.51
101001-1-60	0.03774 ± 0.00085	0.267 ± 0.015	238.8 ± 5.4	240 ± 14	99.3	0.70

Grain	$^{206}Pb/^{238}U$	$^{207}Pb/^{235}U$	$^{206}Pb/^{238}U$ age (Ma)	$^{207}Pb/^{235}U$ age (Ma)	% conc	Th/U
101001-1-61	0.0422 ± 0.0012	0.318 ± 0.030	266.3 ± 7.4	280 ± 26	95.0	0.82
101001-1-62	0.0538 ± 0.0015	0.403 ± 0.035	337.9 ± 9.1	344 ± 30	98.3	0.46
101001-1-63	0.0838 ± 0.0018	0.672 ± 0.028	519 ± 11	522 ± 22	99.4	0.35
101001-1-64	0.0454 ± 0.0012	0.359 ± 0.029	286.0 ± 7.5	312 ± 25	91.7	0.83
101001-1-65	0.3520 ± 0.0074	5.53 ± 0.19	1944 ± 41	1905 ± 66	102.0	0.25
101001-1-66	0.0477 ± 0.0012	0.354 ± 0.024	300.7 ± 7.3	308 ± 21	97.6	1.0
101001-1-67	*0.0421 ± 0.0015*	*0.342 ± 0.028*	*265.9 ± 9.4*	*298 ± 25*	*89.1*	*0.99*
101001-1-68	0.0502 ± 0.0017	0.353 ± 0.028	316 ± 11	307 ± 25	102.8	0.44
101001-1-69	0.0393 ± 0.0013	0.313 ± 0.019	*248.3 ± 8.1*	*277 ± 17*	*89.8*	*0.55*
101001-1-70	*0.0418 ± 0.0014*	*0.300 ± 0.018*	263.8 ± 8.6	266 ± 16	99.2	0.56
Lower Triassic Osawa Formation (120612-3; N38°31’56.7”, E141°32’2.43”)						
120612-3-1	0.0439 ± 0.0021	0.302 ± 0.035	277 ± 13	268 ± 31	103.4	0.49
120612-3-2	0.0418 ± 0.0024	0.307 ± 0.058	264 ± 15	272 ± 51	96.9	0.62
120612-3-3	0.0455 ± 0.0021	0.343 ± 0.034	287 ± 14	299 ± 30	95.8	0.63
120612-3-4	0.0430 ± 0.0020	0.294 ± 0.026	271 ± 12	262 ± 23	103.5	0.67
120612-3-5	0.0453 ± 0.0020	0.324 ± 0.025	286 ± 13	285 ± 22	100.2	0.81
120612-3-6	*0.0425 ± 0.0021*	*0.254 ± 0.031*	*268 ± 13*	*230 ± 28*	*116.5*	*0.49*
120612-3-7	0.0412 ± 0.0020	0.302 ± 0.036	260 ± 13	268 ± 32	97.1	0.50
120612-3-8	0.0441 ± 0.0020	0.312 ± 0.025	278 ± 13	276 ± 22	100.8	0.70
120612-3-9	0.0429 ± 0.0014	0.315 ± 0.031	270.7 ± 8.8	278 ± 28	97.4	0.51
120612-3-10	0.0414 ± 0.0014	0.295 ± 0.034	261.3 ± 9.1	262 ± 30	99.7	0.54
120612-3-11	0.0424 ± 0.0014	0.311 ± 0.032	268.0 ± 8.9	275 ± 28	97.5	0.58
120612-3-12	0.0433 ± 0.0020	0.320 ± 0.058	273 ± 13	282 ± 51	96.9	0.82
120612-3-13	0.0424 ± 0.0012	0.294 ± 0.022	267.6 ± 7.8	262 ± 20	102.2	0.66
120612-3-14	0.0454 ± 0.0017	0.311 ± 0.042	286 ± 11	275 ± 37	104.0	0.60
120612-3-15	0.0461 ± 0.0017	0.355 ± 0.046	291 ± 11	308 ± 40	94.3	0.53
120612-3-16	*0.0442 ± 0.0016*	*0.273 ± 0.036*	*279 ± 10*	*245 ± 33*	*113.9*	*0.59*
120612-3-17	0.0443 ± 0.0012	0.310 ± 0.021	279.4 ± 7.4	274 ± 19	101.9	0.62
120612-3-18	0.0404 ± 0.0012	0.268 ± 0.026	255.4 ± 7.5	241 ± 23	105.9	0.97
120612-3-19	0.0433 ± 0.0015	0.286 ± 0.038	273.6 ± 9.3	256 ± 34	107.1	0.79
120612-3-20	0.0412 ± 0.0013	0.308 ± 0.032	260.2 ± 8.1	273 ± 28	95.4	0.49
120612-3-21	0.0428 ± 0.0014	0.303 ± 0.033	269.9 ± 8.5	269 ± 30	100.4	0.70
120612-3-22	0.0472 ± 0.0015	0.355 ± 0.036	297.3 ± 9.2	309 ± 32	96.3	0.55
120612-3-23	0.0448 ± 0.0016	0.348 ± 0.046	282.5 ± 9.9	303 ± 40	93.2	0.84
120612-3-24	0.0446 ± 0.0015	0.330 ± 0.031	281.6 ± 9.3	290 ± 27	97.1	0.91
120612-3-25	0.0469 ± 0.0017	0.357 ± 0.042	295 ± 11	310 ± 36	95.3	0.58
120612-3-26	0.0429 ± 0.0014	0.286 ± 0.027	270.6 ± 8.9	255 ± 24	106.0	0.88
120612-3-27	0.0438 ± 0.0016	0.293 ± 0.038	276 ± 10	261 ± 34	105.8	0.71
120612-3-28	*0.0393 ± 0.0013*	*0.315 ± 0.029*	*248.2 ± 8.3*	*278 ± 26*	*89.3*	*0.79*
120612-3-29	0.0440 ± 0.0014	0.309 ± 0.028	277.4 ± 9.0	273 ± 24	101.4	0.69
120612-3-30	0.0436 ± 0.0014	0.315 ± 0.028	275.1 ± 8.9	278 ± 24	99.0	1.1
120612-3-31	0.0448 ± 0.0016	0.303 ± 0.037	283 ± 10	269 ± 33	105.2	0.69
120612-3-32	0.0405 ± 0.0013	0.294 ± 0.025	255.7 ± 8.2	262 ± 23	97.7	1.1
120612-3-33	0.0454 ± 0.0018	0.300 ± 0.033	286 ± 12	267 ± 30	107.4	0.74
120612-3-34	0.0434 ± 0.0017	0.336 ± 0.033	274 ± 11	294 ± 29	93.1	0.57
120612-3-35	0.0470 ± 0.0020	0.359 ± 0.043	296 ± 13	312 ± 37	94.9	0.89
120612-3-36	0.0442 ± 0.0018	0.349 ± 0.038	279 ± 11	304 ± 33	91.8	0.47
120612-3-37	0.0423 ± 0.0016	0.294 ± 0.026	267 ± 10	262 ± 23	102.2	0.64
120612-3-38	0.0431 ± 0.0016	0.329 ± 0.024	272 ± 10	289 ± 21	94.2	0.63
120612-3-39	0.0447 ± 0.0021	0.314 ± 0.049	282 ± 13	277 ± 43	101.8	0.75

TABLE 1. (*Continued*)

Grain	$^{206}Pb/^{238}U$	$^{207}Pb/^{235}U$	$^{206}Pb/^{238}U$ age (Ma)	$^{207}Pb/^{235}U$ age (Ma)	% conc	Th/U
120612-3-40	0.0461 ± 0.0019	0.325 ± 0.036	291 ± 12	286 ± 32	101.6	0.54
120612-3-41	0.0438 ± 0.0011	0.307 ± 0.022	276.5 ± 6.9	272 ± 20	101.6	0.55
120612-3-42	0.0442 ± 0.0013	0.333 ± 0.032	278.5 ± 8.0	292 ± 28	95.4	0.65
120612-3-43	0.0393 ± 0.0012	0.298 ± 0.033	248.7 ± 7.7	265 ± 29	93.8	0.51
120612-3-44	0.0458 ± 0.0015	0.342 ± 0.043	288.5 ± 9.7	299 ± 38	96.6	0.60
120612-3-45	0.0440 ± 0.0012	0.335 ± 0.030	277.3 ± 7.7	294 ± 27	94.4	0.53
120612-3-46	0.0426 ± 0.0013	0.335 ± 0.035	269.1 ± 8.2	293 ± 31	91.8	0.76
120612-3-47	0.0458 ± 0.0016	0.337 ± 0.045	289 ± 10	295 ± 40	97.9	0.58
120612-3-48	*0.0426 ± 0.0017*	*0.379 ± 0.055*	*269 ± 11*	*327 ± 47*	*82.4*	*0.43*
120612-3-49	0.0408 ± 0.0012	0.288 ± 0.031	257.9 ± 7.8	257 ± 28	100.4	0.54
120612-3-50	0.0414 ± 0.0012	0.312 ± 0.036	261.5 ± 7.6	276 ± 32	94.8	0.63
120612-3-51	0.03931 ± 0.00090	0.295 ± 0.024	248.6 ± 5.7	263 ± 22	94.7	0.75
120612-3-52	0.03951 ± 0.00089	0.267 ± 0.022	249.8 ± 5.6	241 ± 20	103.8	0.79
120612-3-53	0.0422 ± 0.0011	0.272 ± 0.030	266.7 ± 7.1	244 ± 27	109.3	0.64
120612-3-54	*0.0457 ± 0.0017*	*0.396 ± 0.058*	*288 ± 11*	*339 ± 50*	*85.0*	*0.54*
120612-3-55	0.0431 ± 0.0011	0.292 ± 0.029	271.7 ± 6.8	260 ± 26	104.4	0.57
120612-3-56	0.04204 ± 0.00090	0.300 ± 0.022	265.4 ± 5.7	266 ± 20	99.6	0.73
120612-3-57	0.0446 ± 0.0015	0.328 ± 0.047	281.5 ± 9.6	288 ± 41	97.7	0.54
120612-3-58	*0.0435 ± 0.0015*	*0.263 ± 0.043*	*274.6 ± 9.6*	*237 ± 39*	*115.7*	*0.68*
120612-3-59	*0.0440 ± 0.0018*	*0.359 ± 0.032*	*278 ± 11*	*311 ± 28*	*89.2*	*0.72*
120612-3-60	0.0406 ± 0.0021	0.290 ± 0.052	256 ± 13	258 ± 46	99.3	0.62
120612-3-61	0.0467 ± 0.0020	0.372 ± 0.041	294 ± 13	321 ± 36	91.6	0.69
120612-3-62	*0.0421 ± 0.0018*	*0.418 ± 0.044*	*266 ± 12*	*355 ± 37*	*75.0*	*0.85*
120612-3-63	0.0418 ± 0.0018	0.311 ± 0.031	264 ± 11	275 ± 28	96.1	0.58
120612-3-64	0.0430 ± 0.0018	0.318 ± 0.032	272 ± 11	281 ± 28	96.8	0.97
120612-3-65	0.0431 ± 0.0018	0.298 ± 0.029	272 ± 11	265 ± 26	102.6	0.71
120612-3-66	0.0422 ± 0.0027	0.304 ± 0.078	266 ± 17	269 ± 69	98.9	0.54
120612-3-67	0.0410 ± 0.0014	0.307 ± 0.028	259.0 ± 8.7	272 ± 25	95.3	0.63
120612-3-68	*0.0413 ± 0.0014*	*0.333 ± 0.032*	*260.6 ± 9.0*	*292 ± 28*	*89.3*	*0.78*
120612-3-69	0.0449 ± 0.0014	0.327 ± 0.023	283.0 ± 8.8	287 ± 20	98.6	0.67
120612-3-70	0.0409 ± 0.0015	0.276 ± 0.034	258.2 ± 9.6	247 ± 30	104.5	0.91
120612-3-71	0.0416 ± 0.0015	0.319 ± 0.033	262.9 ± 9.3	281 ± 29	93.5	0.51
120612-3-72	0.0415 ± 0.0015	0.325 ± 0.035	261.9 ± 9.4	286 ± 30	91.6	0.80
120612-3-73	0.0434 ± 0.0016	0.298 ± 0.033	274.1 ± 9.8	265 ± 29	103.6	0.77
120612-3-74	0.0435 ± 0.0015	0.294 ± 0.032	274.4 ± 9.7	261 ± 29	105.0	0.52
120612-3-75	0.0419 ± 0.0017	0.288 ± 0.049	264 ± 11	257 ± 44	102.8	0.66
120612-3-76	*0.0453 ± 0.0019*	*0.368 ± 0.059*	*286 ± 12*	*318 ± 51*	*89.8*	*0.64*
120612-3-77	0.0445 ± 0.0012	0.330 ± 0.027	280.8 ± 7.9	290 ± 24	96.8	0.83
120612-3-78	0.0438 ± 0.0012	0.317 ± 0.024	276.6 ± 7.5	280 ± 22	98.9	1.0
120612-3-79	0.0427 ± 0.0012	0.307 ± 0.025	269.7 ± 7.5	272 ± 22	99.3	0.53
120612-3-80	0.0429 ± 0.0012	0.302 ± 0.025	270.6 ± 7.5	268 ± 22	101.0	0.69
120612-3-81	0.0429 ± 0.0012	0.336 ± 0.029	271.0 ± 7.8	294 ± 26	92.2	0.57
120612-3-82	*0.0479 ± 0.0016*	*0.305 ± 0.040*	*302 ± 10*	*271 ± 35*	*111.4*	*0.82*
120612-3-83	0.0414 ± 0.0011	0.278 ± 0.020	261.5 ± 6.9	249 ± 18	105.1	0.45
120612-3-84	0.0438 ± 0.0013	0.341 ± 0.030	276.1 ± 8.1	298 ± 26	92.8	0.74
120612-3-85	0.0410 ± 0.0012	0.295 ± 0.026	259.2 ± 7.5	262 ± 23	98.8	0.66
120612-3-86	0.0418 ± 0.0012	0.279 ± 0.023	264.0 ± 7.4	250 ± 21	105.8	0.84
120612-3-87	0.0459 ± 0.0015	0.323 ± 0.036	289.0 ± 9.3	284 ± 32	101.7	0.59
120612-3-88	0.0448 ± 0.0013	0.300 ± 0.027	282.3 ± 8.2	266 ± 24	105.9	0.59
120612-3-89	0.0420 ± 0.0011	0.301 ± 0.020	265.1 ± 7.0	268 ± 18	99.1	0.50
120612-3-90	0.0419 ± 0.0011	0.281 ± 0.018	264.6 ± 7.1	251 ± 16	105.3	0.78
120612-3-91	0.0428 ± 0.0013	0.277 ± 0.027	270.1 ± 8.3	248 ± 24	108.8	0.58
120612-3-92	0.0408 ± 0.0012	0.298 ± 0.023	257.8 ± 7.6	264 ± 20	97.5	0.85
120612-3-93	0.0422 ± 0.0013	0.313 ± 0.024	266.7 ± 8.0	276 ± 21	96.5	0.67
120612-3-94	0.0439 ± 0.0013	0.312 ± 0.022	276.9 ± 8.0	276 ± 19	100.5	0.74
120612-3-95	0.0421 ± 0.0015	0.334 ± 0.039	266.1 ± 9.6	293 ± 34	91.0	0.57
120612-3-96	*0.0447 ± 0.0015*	*0.285 ± 0.031*	*281.6 ± 9.4*	*254 ± 28*	*110.8*	*0.51*
120612-3-97	0.0450 ± 0.0015	0.315 ± 0.032	283.7 ± 9.3	278 ± 28	102.0	0.48
120612-3-98	0.0419 ± 0.0015	0.312 ± 0.037	264.7 ± 9.5	276 ± 33	95.9	0.48
120612-3-99	0.0462 ± 0.0015	0.339 ± 0.031	290.9 ± 9.2	297 ± 27	98.1	0.64
120612-3-100	0.0441 ± 0.0015	0.335 ± 0.036	278.0 ± 9.5	294 ± 32	94.7	0.55
120612-3-101	0.0464 ± 0.0018	0.339 ± 0.039	292 ± 11	296 ± 34	98.7	0.66
120612-3-102	*0.0422 ± 0.0015*	*0.396 ± 0.033*	*266.3 ± 9.3*	*339 ± 28*	*78.6*	*0.85*
120612-3-103	0.0423 ± 0.0016	0.274 ± 0.031	267.0 ± 9.8	246 ± 28	108.6	0.52
120612-3-104	*0.0416 ± 0.0014*	*0.369 ± 0.031*	*262.6 ± 9.1*	*319 ± 26*	*82.4*	*0.64*
120612-3-105	0.0444 ± 0.0017	0.334 ± 0.039	280 ± 11	293 ± 34	95.8	0.55
120612-3-106	0.0456 ± 0.0016	0.366 ± 0.034	287 ± 10	317 ± 29	90.7	0.64
120612-3-107	*0.0440 ± 0.0016*	*0.426 ± 0.039*	*278 ± 10*	*360 ± 33*	*77.0*	*1.1*
120612-3-108	0.0428 ± 0.0012	0.304 ± 0.023	270.3 ± 7.4	269 ± 21	100.4	0.91
120612-3-109	0.0457 ± 0.0015	0.368 ± 0.042	287.8 ± 9.7	318 ± 36	90.4	0.53
120612-3-110	0.0493 ± 0.0017	0.386 ± 0.047	310 ± 11	332 ± 41	93.5	0.56
120612-3-111	0.0458 ± 0.0013	0.307 ± 0.028	288.5 ± 8.3	272 ± 24	106.2	0.42
120612-3-112	0.0419 ± 0.0014	0.279 ± 0.034	264.7 ± 8.9	250 ± 31	106.0	0.67
120612-3-113	0.0463 ± 0.0012	0.316 ± 0.023	291.9 ± 7.8	279 ± 20	104.8	0.72
120612-3-114	*0.0503 ± 0.0016*	*0.460 ± 0.045*	*316 ± 10*	*384 ± 38*	*82.3*	*0.74*
120612-3-115	0.0443 ± 0.0013	0.333 ± 0.029	279.7 ± 8.1	292 ± 25	95.9	0.71
120612-3-116	0.0394 ± 0.0010	0.277 ± 0.028	248.9 ± 6.3	249 ± 25	100.1	0.66
120612-3-117	0.0417 ± 0.0010	0.322 ± 0.029	263.4 ± 6.4	284 ± 26	92.9	0.91
120612-3-118	0.04212 ± 0.00090	0.300 ± 0.024	265.9 ± 5.7	266 ± 21	99.9	0.64
120612-3-119	0.0434 ± 0.0011	0.294 ± 0.030	273.7 ± 6.9	262 ± 27	104.6	0.75
120612-3-120	0.04286 ± 0.00092	0.285 ± 0.023	270.5 ± 5.8	254 ± 21	106.3	0.56
120612-3-121	0.0428 ± 0.0013	0.339 ± 0.042	270.4 ± 8.2	296 ± 36	91.2	0.59
120612-3-122	0.0404 ± 0.0010	0.283 ± 0.027	255.1 ± 6.2	253 ± 24	100.8	0.62
120612-3-123	0.0401 ± 0.0010	0.276 ± 0.028	253.7 ± 6.4	248 ± 25	102.4	0.61
120612-3-124	0.04014 ± 0.00081	0.279 ± 0.020	253.7 ± 5.1	250 ± 18	101.6	0.59
120612-3-125	0.0499 ± 0.0017	0.382 ± 0.053	314 ± 11	329 ± 45	95.4	0.46
120612-3-126	0.0421 ± 0.0010	0.318 ± 0.026	265.8 ± 6.4	280 ± 23	94.9	0.61
120612-3-127	0.0416 ± 0.0010	0.310 ± 0.024	262.8 ± 6.0	274 ± 21	95.8	0.78
120612-3-128	*0.0412 ± 0.0011*	*0.336 ± 0.031*	*260.5 ± 6.8*	*294 ± 27*	*88.5*	*0.49*
120612-3-129	0.0412 ± 0.0015	0.314 ± 0.047	260.4 ± 9.5	278 ± 41	93.8	0.81
120612-3-130	0.0454 ± 0.0011	0.318 ± 0.026	286.5 ± 6.8	281 ± 23	102.1	0.61
120612-3-131	*0.0467 ± 0.0011*	*0.301 ± 0.025*	*294.5 ± 6.9*	*267 ± 23*	*110.3*	*0.67*
120612-3-132	0.0444 ± 0.0018	0.332 ± 0.058	280 ± 12	291 ± 51	96.2	0.46

TABLE 1. (*Continued*)

Grain	$^{206}Pb/^{238}U$	$^{207}Pb/^{235}U$	$^{206}Pb/^{238}U$ age (Ma)	$^{207}Pb/^{235}U$ age (Ma)	% conc	Th/U
Lower Triassic Fukkoshi Formation (120613-2; N38°45’28.5”, E141°31’39.19”)						
120613-2-1	0.0420 ± 0.0011	0.311 ± 0.022	265.0 ± 6.6	275 ± 20	96.3	0.3
120613-2-2	0.0418 ± 0.0011	0.283 ± 0.021	264.1 ± 6.7	253 ± 19	104.4	0.67
120613-2-3	0.0410 ± 0.0011	0.288 ± 0.023	258.8 ± 6.7	257 ± 21	100.6	0.49
120613-2-4	0.0418 ± 0.0012	0.285 ± 0.028	263.8 ± 7.5	255 ± 25	103.5	0.60
120613-2-5	0.0412 ± 0.0016	0.271 ± 0.044	260 ± 10	243 ± 40	106.9	0.71
120613-2-6	0.0434 ± 0.0014	0.290 ± 0.036	273.9 ± 9.0	259 ± 32	105.9	0.72
120613-2-7	0.0408 ± 0.0014	0.293 ± 0.035	257.7 ± 8.7	261 ± 31	98.7	0.53
120613-2-8	0.0450 ± 0.0013	0.307 ± 0.029	283.6 ± 8.2	272 ± 25	104.3	0.58
120613-2-9	0.0449 ± 0.0013	0.316 ± 0.031	283.0 ± 8.2	279 ± 28	101.6	0.58
120613-2-10	0.0414 ± 0.0011	0.318 ± 0.025	261.3 ± 6.7	280 ± 22	93.3	0.76
120613-2-11	0.0433 ± 0.0013	0.316 ± 0.035	273.0 ± 8.5	279 ± 31	97.9	0.48
120613-2-12	0.0422 ± 0.0019	0.329 ± 0.059	266 ± 12	289 ± 52	92.1	0.67
120613-2-13	0.0405 ± 0.0014	0.312 ± 0.042	255.9 ± 9.1	276 ± 37	92.7	0.86
120613-2-14	0.0397 ± 0.0012	0.305 ± 0.033	251.1 ± 7.9	270 ± 30	92.9	0.63
120613-2-15	0.0410 ± 0.0011	0.314 ± 0.029	259.3 ± 7.2	278 ± 26	93.4	0.52
120613-2-16	0.0418 ± 0.0011	0.296 ± 0.023	264.0 ± 6.6	263 ± 20	100.4	0.66
120613-2-17	0.0463 ± 0.0015	0.321 ± 0.037	291.9 ± 9.2	282 ± 33	103.3	0.37
120613-2-18	0.0396 ± 0.0013	0.285 ± 0.033	250.4 ± 7.9	255 ± 30	98.3	0.64
120613-2-19	0.0424 ± 0.0017	0.309 ± 0.049	268 ± 11	273 ± 43	98.0	0.53
120613-2-20	0.0434 ± 0.0012	0.319 ± 0.028	273.8 ± 7.4	281 ± 25	97.5	0.80
120613-2-21	0.0478 ± 0.0022	0.355 ± 0.066	301 ± 14	309 ± 57	97.5	0.43
120613-2-22	0.0472 ± 0.0019	0.332 ± 0.055	297 ± 12	291 ± 48	102.3	0.39
120613-2-23	0.0436 ± 0.0026	0.336 ± 0.051	275 ± 17	294 ± 44	93.4	0.44
120613-2-24	0.0456 ± 0.0030	0.325 ± 0.064	288 ± 19	286 ± 56	100.7	0.51
120613-2-25	0.0430 ± 0.0025	0.290 ± 0.039	271 ± 16	259 ± 35	105.0	0.57
120613-2-26	0.0409 ± 0.0023	0.288 ± 0.037	259 ± 15	257 ± 33	100.6	0.52
120613-2-27	0.0422 ± 0.0025	0.280 ± 0.039	267 ± 15	251 ± 35	106.2	0.55
120613-2-28	0.0427 ± 0.0024	0.292 ± 0.030	270 ± 15	260 ± 27	103.8	0.42
120613-2-29	0.0413 ± 0.0023	0.307 ± 0.037	261 ± 15	272 ± 33	96.0	0.57
120613-2-30	0.0434 ± 0.0022	0.307 ± 0.057	274 ± 14	272 ± 50	100.8	0.48
120613-2-31	0.0462 ± 0.0028	0.308 ± 0.083	291 ± 18	273 ± 73	106.7	0.41
120613-2-32	0.0437 ± 0.0018	0.301 ± 0.033	276 ± 11	267 ± 30	103.3	0.72
120613-2-33	0.0421 ± 0.0018	0.292 ± 0.039	266 ± 11	260 ± 34	102.0	0.55
120613-2-34	*0.0421 ± 0.0020*	*0.769 ± 0.091*	*266 ± 13*	*579 ± 69*	*45.9*	*0.69*
120613-2-35	0.0415 ± 0.0017	0.273 ± 0.030	262 ± 10	245 ± 27	107.1	0.70
120613-2-36	0.0414 ± 0.0018	0.271 ± 0.038	262 ± 11	243 ± 34	107.5	0.50
120613-2-37	0.0413 ± 0.0020	0.322 ± 0.054	261 ± 13	284 ± 48	92.0	0.49
120613-2-38	0.0413 ± 0.0013	0.321 ± 0.033	261.1 ± 8.2	283 ± 29	92.3	0.55
120613-2-39	*0.0460 ± 0.0014*	*0.290 ± 0.029*	*290.1 ± 8.6*	*259 ± 26*	*112.2*	*0.40*
120613-2-40	0.0436 ± 0.0019	0.299 ± 0.053	275 ± 12	265 ± 48	103.7	0.55
120613-2-41	0.0398 ± 0.0016	0.312 ± 0.048	252 ± 10	275 ± 43	91.4	0.62
120613-2-42	0.0389 ± 0.0011	0.285 ± 0.024	246.2 ± 7.0	255 ± 22	96.6	0.66
120613-2-43	0.0411 ± 0.0012	0.280 ± 0.025	259.9 ± 7.4	250 ± 22	103.8	0.60
120613-2-44	0.0440 ± 0.0015	0.350 ± 0.041	277.5 ± 9.4	305 ± 35	91.0	0.57
120613-2-45	0.0427 ± 0.0018	0.314 ± 0.034	269 ± 12	277 ± 30	97.3	0.69
120613-2-46	0.0445 ± 0.0018	0.308 ± 0.030	281 ± 12	272 ± 26	103.1	0.55
120613-2-47	*0.0440 ± 0.0021*	*0.545 ± 0.064*	*277 ± 13*	*442 ± 52*	*62.8*	*0.51*
120613-2-48	0.0415 ± 0.0017	0.289 ± 0.030	262 ± 11	258 ± 27	101.5	0.68
120613-2-49	0.0397 ± 0.0018	0.289 ± 0.034	251 ± 11	258 ± 31	97.4	0.57
120613-2-50	0.0485 ± 0.0021	0.318 ± 0.035	305 ± 13	280 ± 31	109.0	0.67
120613-2-51	0.0425 ± 0.0019	0.319 ± 0.038	268 ± 12	281 ± 34	95.6	0.69
120613-2-52	0.0430 ± 0.0022	0.318 ± 0.053	271 ± 14	281 ± 47	96.7	0.50
120613-2-53	*0.0403 ± 0.0022*	*0.255 ± 0.053*	*255 ± 14*	*230 ± 48*	*110.6*	*0.57*
120613-2-54	0.0438 ± 0.0018	0.298 ± 0.054	276 ± 11	265 ± 48	104.3	0.71
120613-2-55	0.0415 ± 0.0013	0.283 ± 0.035	262.4 ± 8.1	253 ± 31	103.6	0.84
120613-2-56	0.0437 ± 0.0011	0.320 ± 0.028	276.0 ± 6.9	282 ± 24	98.0	0.63
120613-2-57	0.0453 ± 0.0014	0.294 ± 0.037	285.6 ± 8.8	262 ± 33	109.0	0.41
120613-2-58	0.0467 ± 0.0014	0.322 ± 0.039	294.4 ± 9.0	283 ± 35	104.0	0.58
120613-2-59	*0.0452 ± 0.0013*	*0.285 ± 0.031*	*284.8 ± 7.9*	*255 ± 28*	*111.7*	*0.56*
120613-2-60	0.0425 ± 0.0011	0.314 ± 0.029	268.5 ± 7.1	277 ± 26	96.8	0.56
120613-2-61	0.0453 ± 0.0012	0.334 ± 0.033	285.9 ± 7.9	292 ± 29	97.8	0.54
120613-2-62	0.0416 ± 0.0014	0.308 ± 0.032	262.8 ± 9.0	273 ± 28	96.3	0.50
120613-2-63	0.0441 ± 0.0015	0.306 ± 0.034	278.4 ± 9.6	271 ± 30	102.7	0.79
120613-2-64	0.0439 ± 0.0014	0.303 ± 0.027	277.0 ± 8.8	268 ± 24	103.2	0.66
120613-2-65	0.0516 ± 0.0019	0.359 ± 0.045	324 ± 12	312 ± 39	104.0	0.62
120613-2-66	0.0454 ± 0.0019	0.341 ± 0.053	286 ± 12	298 ± 47	96.1	0.72
120613-2-67	*0.0455 ± 0.0020*	*0.278 ± 0.050*	*287 ± 13*	*249 ± 45*	*115.2*	*0.53*
120613-2-68	0.0434 ± 0.0017	0.305 ± 0.042	274 ± 11	270 ± 37	101.4	0.46
120613-2-69	*0.0421 ± 0.0020*	*0.404 ± 0.068*	*266 ± 13*	*344 ± 58*	*77.3*	*0.54*
120613-2-70	0.0430 ± 0.0013	0.300 ± 0.024	271.7 ± 8.3	267 ± 21	101.9	0.62
120613-2-71	0.0426 ± 0.0012	0.295 ± 0.029	269.1 ± 7.3	263 ± 26	102.4	0.51
120613-2-72	0.0404 ± 0.0014	0.294 ± 0.039	255.3 ± 8.7	262 ± 35	97.5	0.52
120613-2-73	*0.0422 ± 0.0016*	*0.263 ± 0.044*	*266 ± 10*	*237 ± 40*	*112.4*	*0.73*
120613-2-74	0.0414 ± 0.0011	0.286 ± 0.027	261.6 ± 6.9	255 ± 24	102.4	0.60
120613-2-75	*0.0482 ± 0.0017*	*0.417 ± 0.056*	*303 ± 11*	*354 ± 48*	*85.8*	*0.43*
120613-2-76	0.0391 ± 0.0010	0.255 ± 0.022	247.1 ± 6.1	231 ± 19	107.0	0.87
120613-2-77	0.0458 ± 0.0012	0.359 ± 0.033	288.6 ± 7.8	311 ± 29	92.6	0.52
120613-2-78	*0.0426 ± 0.0013*	*0.357 ± 0.039*	*269.0 ± 8.2*	*310 ± 34*	*86.9*	*0.50*
120613-2-79	0.0452 ± 0.0023	0.297 ± 0.065	285 ± 14	264 ± 58	107.9	0.56
120613-2-80	0.0430 ± 0.0015	0.306 ± 0.037	271.2 ± 9.4	271 ± 33	100.0	0.61
120613-2-81	0.0427 ± 0.0014	0.318 ± 0.037	269.3 ± 9.1	281 ± 32	96.0	0.63
120613-2-82	0.0424 ± 0.0014	0.336 ± 0.038	267.8 ± 9.1	294 ± 33	91.1	0.82
120613-2-83	*0.0404 ± 0.0014*	*0.331 ± 0.039*	*255.3 ± 9.0*	*290 ± 34*	*88.1*	*0.54*
120613-2-84	0.0410 ± 0.0017	0.269 ± 0.046	259 ± 11	242 ± 41	107.0	0.72
120613-2-85	*0.0442 ± 0.0014*	*0.380 ± 0.035*	*278.6 ± 8.6*	*327 ± 30*	*85.2*	*0.70*
120613-2-86	*0.0416 ± 0.0018*	*0.245 ± 0.044*	*263 ± 11*	*223 ± 40*	*118.0*	*0.77*
120613-2-87	0.0440 ± 0.0018	0.351 ± 0.039	277 ± 11	305 ± 34	90.9	0.66
120613-2-88	0.0449 ± 0.0029	0.297 ± 0.082	283 ± 19	264 ± 73	107.0	0.44
120613-2-89	*0.0408 ± 0.0017*	*0.351 ± 0.039*	*258 ± 11*	*305 ± 34*	*84.6*	*0.33*
120613-2-90	0.0423 ± 0.0022	0.310 ± 0.057	267 ± 14	275 ± 50	97.2	0.34
120613-2-91	0.0379 ± 0.0016	0.289 ± 0.036	240 ± 10	258 ± 32	93.1	0.58
120613-2-92	0.0415 ± 0.0018	0.303 ± 0.040	262 ± 11	269 ± 36	97.5	0.55
120613-2-93	0.0420 ± 0.0017	0.304 ± 0.032	265 ± 11	269 ± 28	98.6	0.53
120613-2-94	0.0453 ± 0.0016	0.308 ± 0.039	286 ± 10	273 ± 34	104.7	0.51
120613-2-95	*0.0470 ± 0.0021*	*0.297 ± 0.056*	*296 ± 13*	*264 ± 50*	*112.0*	*0.55*
120613-2-96	0.0435 ± 0.0018	0.343 ± 0.051	274 ± 11	300 ± 44	91.5	0.37
120613-2-97	*0.0408 ± 0.0020*	*0.336 ± 0.062*	*258 ± 12*	*294 ± 54*	*87.7*	*0.49*
120613-2-98	0.0435 ± 0.0016	0.332 ± 0.043	274 ± 10	291 ± 38	94.3	0.57
120613-2-99	*0.0414 ± 0.0015*	*0.491 ± 0.053*	*261.3 ± 9.5*	*406 ± 44*	*64.4*	*0.58*
120613-2-100	0.0394 ± 0.0013	0.278 ± 0.029	248.9 ± 8.2	249 ± 26	100.0	0.77
120613-2-101	0.0429 ± 0.0017	0.317 ± 0.057	270 ± 11	279 ± 50	96.8	0.55
120613-2-102	0.0437 ± 0.0017	0.317 ± 0.053	276 ± 11	280 ± 47	98.6	0.65
120613-2-103	0.0422 ± 0.0013	0.276 ± 0.038	266.7 ± 8.3	248 ± 34	107.6	0.66
120613-2-104	0.0415 ± 0.0017	0.281 ± 0.054	262 ± 11	252 ± 48	104.2	0.33
120613-2-105	0.0454 ± 0.0013	0.330 ± 0.038	286.2 ± 8.0	289 ± 33	98.9	0.72
120613-2-106	0.0389 ± 0.0013	0.306 ± 0.043	245.8 ± 8.3	271 ± 38	90.7	0.50
120613-2-107	0.0401 ± 0.0010	0.290 ± 0.030	253.4 ± 6.5	258 ± 27	98.1	0.75

TABLE 1. (*Continued*)

Grain	$^{206}Pb/^{238}U$	$^{207}Pb/^{235}U$	$^{206}Pb/^{238}U$ age (Ma)	$^{207}Pb/^{235}U$ age (Ma)	% conc	Th/U
Middle Triassic Isatomae Formation (130612-7; N38°42'48.27", E141°31'25.91")						
120612-7-1	0.0389 ± 0.0014	0.269 ± 0.037	246.2 ± 9.1	241 ± 33	102.0	0.47
120612-7-2	0.0381 ± 0.0010	0.301 ± 0.018	241.2 ± 6.4	267 ± 16	90.2	0.86
120612-7-3	0.0405 ± 0.0012	0.279 ± 0.026	256.1 ± 7.8	250 ± 24	102.5	0.52
120612-7-4	*0.0402 ± 0.0015*	*0.376 ± 0.043*	*253.8 ± 9.2*	*324 ± 37*	*78.3*	*0.57*
120612-7-5	0.0403 ± 0.0012	0.288 ± 0.025	254.9 ± 7.6	257 ± 22	99.3	0.68
120612-7-6	0.03852 ± 0.00080	0.268 ± 0.022	243.6 ± 5.0	241 ± 20	100.9	0.57
120612-7-7	*0.0408 ± 0.0011*	*0.329 ± 0.034*	*257.5 ± 6.7*	*288 ± 30*	*89.3*	*0.51*
120612-7-8	0.03987 ± 0.00092	0.313 ± 0.028	252.0 ± 5.8	276 ± 25	91.2	0.54
120612-7-9	0.0398 ± 0.0011	0.308 ± 0.036	251.3 ± 7.1	272 ± 32	92.3	0.70
120612-7-10	0.03830 ± 0.00081	0.289 ± 0.024	242.3 ± 5.1	258 ± 21	93.9	0.37
120612-7-11	0.0404 ± 0.0010	0.306 ± 0.032	255.2 ± 6.6	271 ± 29	94.0	0.52
120612-7-12	0.04242 ± 0.00091	0.306 ± 0.026	267.8 ± 5.7	271 ± 23	98.8	0.41
120612-7-13	0.03830 ± 0.00085	0.272 ± 0.025	242.3 ± 5.4	244 ± 22	99.2	0.80
120612-7-14	0.03773 ± 0.00091	0.279 ± 0.022	238.7 ± 5.7	250 ± 20	95.6	0.70
120612-7-15	*0.0389 ± 0.0013*	*0.328 ± 0.041*	*246.2 ± 8.1*	*288 ± 36*	*85.5*	*0.58*
120612-7-16	*0.0379 ± 0.0013*	*0.320 ± 0.042*	*239.5 ± 8.3*	*282 ± 37*	*84.9*	*0.57*
120612-7-17	0.0398 ± 0.0012	0.299 ± 0.034	251.7 ± 7.5	266 ± 30	94.8	0.66
120612-7-18	0.0389 ± 0.0011	0.306 ± 0.030	245.8 ± 6.8	271 ± 27	90.8	0.55
120612-7-19	0.0442 ± 0.0012	0.321 ± 0.030	278.6 ± 7.3	282 ± 27	98.6	0.72
120612-7-20	*0.0457 ± 0.0013*	*0.496 ± 0.046*	*288.3 ± 8.3*	*409 ± 38*	*70.5*	*0.89*
120612-7-21	0.0434 ± 0.0011	0.302 ± 0.026	273.6 ± 6.8	268 ± 23	102.1	0.87
120612-7-22	0.0415 ± 0.0010	0.314 ± 0.019	262.0 ± 6.2	277 ± 17	94.6	0.65
120612-7-23	0.0399 ± 0.0010	0.291 ± 0.021	252.4 ± 6.3	259 ± 19	97.4	0.60
120612-7-24	0.0462 ± 0.0011	0.350 ± 0.024	291.4 ± 7.2	305 ± 21	95.7	0.60
120612-7-25	0.0395 ± 0.0010	0.287 ± 0.024	249.7 ± 6.6	256 ± 21	97.4	0.38
120612-7-26	0.0398 ± 0.0010	0.292 ± 0.022	251.6 ± 6.4	260 ± 20	96.7	0.42
120612-7-27	0.0395 ± 0.0010	0.311 ± 0.020	250.0 ± 6.1	275 ± 18	91.0	0.54
120612-7-28	0.0418 ± 0.0010	0.303 ± 0.021	264.1 ± 6.4	269 ± 18	98.2	0.45
120612-7-29	*0.0410 ± 0.0014*	*0.368 ± 0.046*	*258.9 ± 9.1*	*318 ± 40*	*81.3*	*0.43*
120612-7-30	*0.0417 ± 0.0011*	*0.387 ± 0.031*	*263.4 ± 7.1*	*332 ± 26*	*79.3*	*0.62*
120612-7-31	0.0382 ± 0.0011	0.290 ± 0.029	241.9 ± 7.1	258 ± 26	93.6	0.59
120612-7-32	*0.0389 ± 0.0011*	*0.341 ± 0.032*	*246.0 ± 7.2*	*298 ± 28*	*82.7*	*0.52*
120612-7-33	0.0398 ± 0.0011	0.263 ± 0.025	251.3 ± 7.1	237 ± 23	105.9	0.47
120612-7-34	0.0401 ± 0.0011	0.289 ± 0.026	253.7 ± 6.9	258 ± 23	98.5	0.76
120612-7-35	*0.0370 ± 0.0010*	*0.300 ± 0.027*	*234.3 ± 6.5*	*267 ± 24*	*87.9*	*0.59*
120612-7-36	0.0441 ± 0.0014	0.341 ± 0.040	278.0 ± 9.0	298 ± 35	93.3	0.47
120612-7-37	0.0417 ± 0.0010	0.310 ± 0.019	263.3 ± 6.2	274 ± 17	96.0	0.65
120612-7-38	*0.0424 ± 0.0015*	*0.508 ± 0.058*	*267.7 ± 9.6*	*417 ± 47*	*64.2*	*0.46*
120612-7-39	0.0417 ± 0.0010	0.306 ± 0.022	263.2 ± 6.6	271 ± 19	97.2	0.39
120612-7-40	0.0382 ± 0.0014	0.293 ± 0.037	241.9 ± 8.7	261 ± 33	92.6	0.65
120612-7-41	0.0409 ± 0.0011	0.312 ± 0.019	258.2 ± 6.9	276 ± 17	93.6	0.70
120612-7-42	*0.0382 ± 0.0016*	*0.326 ± 0.048*	*241.9 ± 9.9*	*286 ± 42*	*84.5*	*0.78*
120612-7-43	0.0418 ± 0.0015	0.325 ± 0.040	264.1 ± 9.5	286 ± 35	92.4	0.75
120612-7-44	0.0403 ± 0.0015	0.272 ± 0.037	254.8 ± 9.3	244 ± 33	104.3	0.56
120612-7-45	0.0394 ± 0.0010	0.287 ± 0.016	248.8 ± 6.5	256 ± 15	97.3	1.0
120612-7-46	0.0405 ± 0.0013	0.298 ± 0.030	255.6 ± 8.1	265 ± 26	96.6	0.50
120612-7-47	0.0389 ± 0.0011	0.285 ± 0.023	246.3 ± 7.1	255 ± 20	96.6	0.60
120612-7-48	0.0384 ± 0.0010	0.293 ± 0.019	243.0 ± 6.6	261 ± 17	93.2	0.62
120612-7-49	*0.0402 ± 0.0013*	*0.349 ± 0.030*	*254.1 ± 8.3*	*304 ± 26*	*83.6*	*0.60*
120612-7-50	0.0387 ± 0.0012	0.293 ± 0.023	244.5 ± 7.6	261 ± 21	93.8	0.49
120612-7-51	0.0401 ± 0.0016	0.303 ± 0.040	253.3 ± 9.8	268 ± 36	94.4	0.90
120612-7-52	0.0406 ± 0.0015	0.317 ± 0.037	256.8 ± 9.4	279 ± 33	92.0	0.49
120612-7-53	0.0476 ± 0.0016	0.353 ± 0.036	300 ± 10	307 ± 31	97.5	0.95
120612-7-54	0.0434 ± 0.0018	0.341 ± 0.048	274 ± 11	298 ± 42	91.9	0.81
120612-7-55	0.03751 ± 0.00084	0.274 ± 0.018	237.4 ± 5.3	246 ± 17	96.5	0.68
120612-7-56	0.03792 ± 0.00084	0.287 ± 0.019	239.9 ± 5.3	256 ± 17	93.6	0.70
120612-7-57	0.0435 ± 0.0012	0.335 ± 0.034	274.4 ± 7.7	293 ± 29	93.6	0.58
120612-7-58	*0.0391 ± 0.0013*	*0.331 ± 0.039*	*247.3 ± 8.0*	*290 ± 34*	*85.2*	*0.53*
120612-7-59	0.03632 ± 0.00081	0.285 ± 0.018	230.0 ± 5.1	255 ± 16	90.3	0.68
120612-7-60	0.0380 ± 0.0010	0.291 ± 0.028	240.7 ± 6.6	259 ± 25	92.8	0.53
120612-7-61	0.0413 ± 0.0012	0.294 ± 0.034	260.6 ± 7.9	261 ± 30	99.7	0.49
120612-7-62	0.0414 ± 0.0010	0.320 ± 0.030	261.8 ± 6.3	282 ± 27	92.9	0.63
120612-7-63	0.04054 ± 0.00089	0.306 ± 0.026	256.2 ± 5.6	271 ± 23	94.5	0.56
120612-7-64	0.03933 ± 0.00085	0.280 ± 0.024	248.7 ± 5.4	251 ± 22	99.2	0.46
120612-7-65	0.0417 ± 0.0010	0.334 ± 0.030	263.6 ± 6.1	292 ± 26	90.2	0.48
120612-7-66	*0.0436 ± 0.0015*	*0.366 ± 0.051*	*274.8 ± 9.3*	*316 ± 44*	*86.8*	*0.56*
120612-7-67	0.04048 ± 0.00078	0.291 ± 0.021	255.8 ± 4.9	259 ± 19	98.6	0.46
120612-7-68	0.0401 ± 0.0010	0.283 ± 0.031	253.7 ± 6.6	253 ± 28	100.2	0.96
120612-7-69	*0.0406 ± 0.0013*	*0.404 ± 0.051*	*256.5 ± 8.5*	*344 ± 44*	*74.5*	*0.58*
120612-7-70	0.0407 ± 0.0013	0.303 ± 0.028	257.3 ± 8.2	269 ± 25	95.8	0.50
120612-7-71	*0.0389 ± 0.0013*	*0.338 ± 0.032*	*245.8 ± 8.1*	*296 ± 28*	*83.1*	*0.54*
120612-7-72	0.0372 ± 0.0011	0.268 ± 0.020	235.2 ± 6.9	241 ± 18	97.7	0.69
120612-7-73	*0.0420 ± 0.0016*	*0.382 ± 0.048*	*265 ± 10*	*329 ± 41*	*80.8*	*0.57*
120612-7-74	0.0382 ± 0.0013	0.301 ± 0.030	241.9 ± 8.1	267 ± 27	90.7	0.52
120612-7-75	0.0408 ± 0.0018	0.310 ± 0.050	258 ± 11	274 ± 44	94.1	0.79
120612-7-76	0.0391 ± 0.0012	0.306 ± 0.023	247.2 ± 7.3	271 ± 20	91.1	1.2
120612-7-77	0.0413 ± 0.0013	0.318 ± 0.030	260.9 ± 8.4	281 ± 26	93.0	0.59
120612-7-78	0.03735 ± 0.00089	0.271 ± 0.020	236.4 ± 5.6	243 ± 18	97.2	0.67
120612-7-79	0.0396 ± 0.0011	0.315 ± 0.033	250.3 ± 7.3	278 ± 29	90.0	0.56
120612-7-80	0.04014 ± 0.00092	0.304 ± 0.020	253.7 ± 5.8	269 ± 18	94.2	0.53
120612-7-81	0.03895 ± 0.00085	0.277 ± 0.017	246.3 ± 5.4	248 ± 15	99.2	0.75
120612-7-82	0.0405 ± 0.0013	0.287 ± 0.038	256.1 ± 8.4	256 ± 34	100.0	0.51
120612-7-83	0.0395 ± 0.0010	0.282 ± 0.023	249.7 ± 6.1	252 ± 20	99.0	1.0
120612-7-84	0.0384 ± 0.0010	0.269 ± 0.024	242.9 ± 6.2	242 ± 22	100.3	0.46
120612-7-85	*0.0424 ± 0.0015*	*0.396 ± 0.054*	*267.5 ± 9.7*	*339 ± 46*	*78.9*	*0.51*
120612-7-86	0.0424 ± 0.0012	0.290 ± 0.033	267.6 ± 7.9	259 ± 29	103.4	0.75
Upper Triassic Shindate Formation (120612-8; N38°42'33.27", E141°30'36.32")						
120612-8-1	0.0429 ± 0.0013	0.321 ± 0.030	270.6 ± 7.9	282 ± 26	95.9	1.1
120612-8-2	0.0421 ± 0.0018	0.287 ± 0.052	266 ± 12	256 ± 46	103.6	0.62
120612-8-3	*0.0462 ± 0.0021*	*0.410 ± 0.071*	*291 ± 13*	*349 ± 60*	*83.5*	*0.46*
120612-8-4	0.0397 ± 0.0011	0.301 ± 0.025	251.3 ± 7.0	267 ± 22	94.0	0.67
120612-8-5	0.0437 ± 0.0014	0.307 ± 0.033	275.5 ± 8.6	272 ± 29	101.2	0.55
120612-8-6	0.0357 ± 0.0010	0.257 ± 0.024	226.0 ± 6.6	233 ± 21	97.1	0.43
120612-8-7	*0.0430 ± 0.0014*	*0.355 ± 0.038*	*271.4 ± 8.9*	*308 ± 33*	*88.0*	*0.84*
120612-8-8	0.0422 ± 0.0011	0.282 ± 0.029	266.4 ± 7.0	252 ± 26	105.6	0.49
120612-8-9	0.0345 ± 0.0014	0.224 ± 0.040	218.9 ± 8.8	205 ± 37	106.5	1.3
120612-8-10	*0.0334 ± 0.0016*	*0.262 ± 0.053*	*212 ± 10*	*237 ± 47*	*89.5*	*1.1*
120612-8-11	0.0424 ± 0.0013	0.320 ± 0.038	267.7 ± 8.1	282 ± 34	95.0	0.51
120612-8-12	*0.0454 ± 0.0018*	*0.286 ± 0.051*	*286 ± 11*	*256 ± 46*	*112.0*	*0.67*
120612-8-13	0.0421 ± 0.0010	0.287 ± 0.025	265.8 ± 6.2	256 ± 22	103.7	0.55
120612-8-14	0.0418 ± 0.0015	0.268 ± 0.041	264.2 ± 9.3	241 ± 37	109.6	0.62
120612-8-15	*0.0352 ± 0.0020*	*0.341 ± 0.076*	*223 ± 13*	*298 ± 66*	*74.8*	*0.70*
120612-8-16	0.04053 ± 0.00090	0.302 ± 0.023	256.1 ± 5.7	268 ± 21	95.6	0.52

TABLE 1. (*Continued*)

Grain	$^{206}Pb/^{238}U$	$^{207}Pb/^{235}U$	$^{206}Pb/^{238}U$ age (Ma)	$^{207}Pb/^{235}U$ age (Ma)	% conc	Th/U
120612-8-17	0.0417 ± 0.0019	0.275 ± 0.053	263 ± 12	247 ± 48	106.6	0.61
120612-8-18	0.0451 ± 0.0019	0.305 ± 0.052	284 ± 12	270 ± 46	105.3	0.55
120612-8-19	*0.0380 ± 0.0017*	*0.666 ± 0.082*	*241 ± 11*	*518 ± 64*	*46.5*	*0.94*
120612-8-20	0.0441 ± 0.0018	0.341 ± 0.053	278 ± 11	298 ± 46	93.5	0.58
120612-8-21	0.0412 ± 0.0016	0.319 ± 0.044	260 ± 10	281 ± 39	92.5	0.72
120612-8-22	*0.0352 ± 0.0018*	*0.526 ± 0.084*	*223 ± 11*	*429 ± 69*	*51.9*	*0.48*
120612-8-23	0.0421 ± 0.0015	0.315 ± 0.039	266.0 ± 9.4	278 ± 34	95.5	0.95
120612-8-24	0.0413 ± 0.0016	0.298 ± 0.041	261.0 ± 9.8	265 ± 37	98.7	0.63
120612-8-25	*0.0452 ± 0.0018*	*0.407 ± 0.058*	*285 ± 11*	*347 ± 49*	*82.2*	*0.63*
120612-8-26	*0.0384 ± 0.0030*	*0.337 ± 0.052*	*243 ± 19*	*295 ± 45*	*82.3*	*0.54*
120612-8-27	0.0408 ± 0.0030	0.315 ± 0.031	258 ± 19	278 ± 28	92.8	0.52
120612-8-28	*0.0332 ± 0.0030*	*0.307 ± 0.078*	*211 ± 19*	*272 ± 69*	*77.4*	*0.89*
120612-8-29	0.0344 ± 0.0028	0.250 ± 0.050	218 ± 18	227 ± 45	96.2	0.40
120612-8-30	*0.0431 ± 0.0031*	*0.475 ± 0.048*	*272 ± 20*	*395 ± 40*	*68.9*	*0.52*
120612-8-31	0.0400 ± 0.0031	0.306 ± 0.051	253 ± 20	271 ± 45	93.4	0.65
120612-8-32	*0.0435 ± 0.0034*	*0.276 ± 0.047*	*275 ± 21*	*247 ± 42*	*111.0*	*0.52*
120612-8-33	0.0424 ± 0.0034	0.284 ± 0.059	267 ± 22	254 ± 52	105.2	0.55
120612-8-34	*0.0421 ± 0.0016*	*0.420 ± 0.057*	*266 ± 10*	*356 ± 49*	*74.6*	*0.62*
120612-8-35	0.0422 ± 0.0017	0.285 ± 0.048	266 ± 11	255 ± 43	104.6	0.60
120612-8-36	0.0412 ± 0.0012	0.305 ± 0.032	260.0 ± 7.7	270 ± 28	96.2	0.78
120612-8-37	0.0411 ± 0.0013	0.292 ± 0.035	260.0 ± 8.3	260 ± 32	99.9	0.54
120612-8-38	0.0433 ± 0.0017	0.323 ± 0.051	273 ± 11	284 ± 45	96.3	0.82
120612-8-39	0.0435 ± 0.0016	0.340 ± 0.048	274 ± 10	297 ± 42	92.3	0.70
120612-8-40	0.0406 ± 0.0012	0.300 ± 0.032	256.4 ± 7.6	266 ± 28	96.3	0.67
120612-8-41	*0.0346 ± 0.0020*	*0.310 ± 0.079*	*220 ± 13*	*274 ± 70*	*80.1*	*0.80*
120612-8-42	0.0349 ± 0.0016	0.250 ± 0.050	220.9 ± 9.9	227 ± 45	97.4	0.94
120612-8-43	0.0443 ± 0.0011	0.302 ± 0.022	279.6 ± 6.7	268 ± 20	104.4	0.53
120612-8-44	*0.0361 ± 0.0017*	*0.302 ± 0.058*	*229 ± 11*	*268 ± 52*	*85.3*	*1.2*
120612-8-45	0.0442 ± 0.0016	0.292 ± 0.046	279 ± 10	260 ± 41	107.1	0.73
120612-8-46	*0.0356 ± 0.0018*	*0.314 ± 0.064*	*226 ± 11*	*277 ± 56*	*81.5*	*0.64*
120612-8-47	0.0424 ± 0.0018	0.306 ± 0.033	268 ± 11	271 ± 29	98.7	0.76
120612-8-48	0.0411 ± 0.0016	0.289 ± 0.023	260 ± 10	258 ± 21	100.6	0.48
120612-8-49	0.0411 ± 0.0018	0.294 ± 0.035	259 ± 11	262 ± 31	99.1	0.45
120612-8-50	0.0436 ± 0.0022	0.332 ± 0.056	275 ± 14	291 ± 49	94.5	0.73
120612-8-51	*0.0363 ± 0.0025*	*0.337 ± 0.086*	*230 ± 16*	*295 ± 75*	*78.0*	*1.0*
120612-8-52	0.0368 ± 0.0015	0.273 ± 0.028	233.2 ± 9.6	245 ± 25	95.1	0.70
120612-8-53	0.0429 ± 0.0020	0.292 ± 0.043	271 ± 13	260 ± 39	104.0	0.70
120612-8-54	0.0432 ± 0.0019	0.281 ± 0.036	272 ± 12	251 ± 32	108.4	0.54
120612-8-55	0.0420 ± 0.0016	0.294 ± 0.023	265 ± 10	262 ± 20	101.3	0.72
120612-8-56	0.0439 ± 0.0018	0.334 ± 0.050	277 ± 11	293 ± 44	94.7	0.47
120612-8-57	0.0428 ± 0.0016	0.317 ± 0.041	270 ± 10	280 ± 36	96.6	0.56
120612-8-58	*0.0447 ± 0.0019*	*0.285 ± 0.047*	*282 ± 12*	*254 ± 42*	*110.9*	*0.60*
120612-8-59	0.0423 ± 0.0014	0.322 ± 0.032	266.8 ± 8.8	283 ± 28	94.1	0.61
120612-8-60	*0.0424 ± 0.0016*	*0.345 ± 0.042*	*267.7 ± 9.9*	*301 ± 37*	*88.9*	*0.40*
120612-8-61	0.0412 ± 0.0014	0.300 ± 0.034	260.2 ± 9.1	266 ± 30	97.7	0.58
120612-8-62	0.0355 ± 0.0020	0.239 ± 0.057	225 ± 12	218 ± 52	103.2	0.86
120612-8-63	0.0413 ± 0.0014	0.305 ± 0.034	260.7 ± 9.1	271 ± 30	96.4	0.56
120612-8-64	0.0396 ± 0.0013	0.271 ± 0.028	250.5 ± 8.3	243 ± 25	103.0	0.48
120612-8-65	*0.0350 ± 0.0018*	*0.301 ± 0.064*	*222 ± 11*	*267 ± 57*	*83.0*	*0.95*
120612-8-66	0.0329 ± 0.0015	0.239 ± 0.050	208.7 ± 9.7	217 ± 45	96.0	0.91
120612-8-67	0.0397 ± 0.0013	0.311 ± 0.042	250.8 ± 8.3	275 ± 37	91.1	0.54
120612-8-68	*0.0332 ± 0.0022*	*0.277 ± 0.079*	*210 ± 14*	*248 ± 71*	*84.7*	*0.75*
120612-8-69	0.0359 ± 0.0016	0.248 ± 0.051	227 ± 10	225 ± 46	101.1	0.72
120612-8-70	0.04244 ± 0.00084	0.312 ± 0.022	267.9 ± 5.3	276 ± 19	97.2	0.76
120612-8-71	0.03224 ± 0.00076	0.217 ± 0.020	204.6 ± 4.8	199 ± 19	102.6	0.40
120612-8-72	*0.0393 ± 0.0017*	*0.674 ± 0.074*	*248 ± 11*	*523 ± 57*	*47.5*	*0.39*
120612-8-73	0.0439 ± 0.0017	0.343 ± 0.040	277 ± 11	299 ± 35	92.6	0.60
120612-8-74	0.0392 ± 0.0015	0.294 ± 0.031	247.6 ± 9.3	261 ± 27	94.7	0.48
120612-8-75	0.0386 ± 0.0016	0.286 ± 0.037	244.4 ± 9.9	256 ± 33	95.7	0.57
120612-8-76	*0.0347 ± 0.0017*	*0.281 ± 0.051*	*220 ± 11*	*251 ± 46*	*87.6*	*0.66*
120612-8-77	0.0405 ± 0.0016	0.275 ± 0.037	256 ± 10	247 ± 33	103.7	0.57
120612-8-78	0.0399 ± 0.0014	0.292 ± 0.027	252.3 ± 9.0	260 ± 24	97.1	0.69
120612-8-79	0.0424 ± 0.0019	0.280 ± 0.046	268 ± 12	251 ± 41	106.9	0.69
120612-8-80	0.0398 ± 0.0015	0.290 ± 0.033	251.4 ± 9.6	258 ± 29	97.3	0.47
120612-8-81	0.0404 ± 0.0015	0.282 ± 0.030	255.0 ± 9.2	252 ± 27	101.3	0.56
120612-8-82	0.0420 ± 0.0015	0.288 ± 0.028	265.3 ± 9.2	257 ± 25	103.1	0.93
120612-8-83	0.0415 ± 0.0017	0.286 ± 0.040	262 ± 11	255 ± 36	102.8	0.54
120612-8-84	0.0338 ± 0.0022	0.250 ± 0.070	214 ± 14	226 ± 64	94.6	0.76
120612-8-85	0.0404 ± 0.0016	0.263 ± 0.036	255 ± 10	237 ± 33	107.4	0.53
120612-8-86	0.0418 ± 0.0020	0.278 ± 0.050	264 ± 12	249 ± 45	105.8	0.54
120612-8-87	0.0422 ± 0.0016	0.311 ± 0.037	266 ± 10	275 ± 33	96.7	0.57
120612-8-88	0.0408 ± 0.0014	0.310 ± 0.029	257.9 ± 9.1	274 ± 25	94.1	0.65
120612-8-89	*0.0372 ± 0.0024*	*0.201 ± 0.062*	*236 ± 15*	*186 ± 57*	*126.6*	*0.93*
120612-8-90	0.0428 ± 0.0012	0.329 ± 0.035	270.1 ± 7.7	289 ± 31	93.6	0.50
120612-8-91	*0.03890 ± 0.00086*	*0.314 ± 0.023*	*246.0 ± 5.5*	*278 ± 20*	*88.6*	*0.58*
120612-8-92	0.0432 ± 0.0017	0.293 ± 0.051	273 ± 11	261 ± 45	104.6	0.47
120612-8-93	0.0458 ± 0.0011	0.330 ± 0.030	288.6 ± 7.2	289 ± 27	99.7	0.54
120612-8-94	*0.0422 ± 0.0015*	*0.387 ± 0.051*	*266.7 ± 9.5*	*332 ± 44*	*80.3*	*0.47*
120612-8-95	0.04216 ± 0.00094	0.298 ± 0.023	266.2 ± 5.9	265 ± 20	100.4	0.52
120612-8-96	0.0428 ± 0.0017	0.338 ± 0.051	270 ± 11	295 ± 45	91.4	0.49
120612-8-97	0.0425 ± 0.0015	0.304 ± 0.039	268.2 ± 9.5	269 ± 35	99.6	0.87
120612-8-98	0.0424 ± 0.0014	0.296 ± 0.034	267.4 ± 8.8	263 ± 30	101.7	0.48
120612-8-99	0.0346 ± 0.0022	0.270 ± 0.073	219 ± 14	242 ± 66	90.6	0.81
120612-8-100	0.0399 ± 0.0012	0.273 ± 0.028	252.4 ± 7.8	245 ± 25	102.9	0.42
120612-8-101	0.0352 ± 0.0010	0.241 ± 0.022	222.8 ± 6.5	219 ± 20	101.6	0.55
120612-8-102	0.0346 ± 0.0017	0.236 ± 0.051	219 ± 11	215 ± 47	101.9	1.1
120612-8-103	*0.0411 ± 0.0015*	*0.354 ± 0.045*	*259.5 ± 9.5*	*308 ± 39*	*84.2*	*0.57*
120612-8-104	*0.0425 ± 0.0017*	*0.380 ± 0.055*	*268 ± 11*	*327 ± 48*	*82.0*	*0.57*
120612-8-105	0.0400 ± 0.0012	0.301 ± 0.033	252.5 ± 7.5	267 ± 30	94.5	0.76
120612-8-106	0.0398 ± 0.0010	0.273 ± 0.023	251.5 ± 6.2	245 ± 21	102.5	0.54
120612-8-107	*0.0321 ± 0.0021*	*0.300 ± 0.079*	*203 ± 13*	*266 ± 70*	*76.4*	*0.77*
120612-8-108	0.0409 ± 0.0013	0.262 ± 0.033	258.3 ± 8.0	236 ± 30	109.4	0.57
120612-8-109	0.0419 ± 0.0013	0.282 ± 0.036	264.6 ± 8.3	252 ± 32	104.8	0.61
120612-8-110	0.0330 ± 0.0019	0.223 ± 0.062	209 ± 12	204 ± 57	102.5	0.80
120612-8-111	*0.0331 ± 0.0018*	*0.266 ± 0.064*	*210 ± 12*	*240 ± 58*	*87.6*	*0.65*
120612-8-112	0.0307 ± 0.0015	0.223 ± 0.049	195.1 ± 9.6	204 ± 45	95.6	1.1
120612-8-113	0.0376 ± 0.0014	0.279 ± 0.042	237.7 ± 8.8	250 ± 38	95.3	0.49
120612-8-114	0.0402 ± 0.0015	0.293 ± 0.033	254.1 ± 9.4	261 ± 30	97.5	0.51
120612-8-115	0.0418 ± 0.0018	0.319 ± 0.048	264 ± 11	281 ± 43	93.9	0.57
120612-8-116	0.0426 ± 0.0018	0.321 ± 0.045	269 ± 11	283 ± 40	95.2	0.48
120612-8-117	0.0409 ± 0.0018	0.290 ± 0.047	258 ± 11	259 ± 42	99.9	0.50
120612-8-118	0.0365 ± 0.0024	0.235 ± 0.071	231 ± 15	215 ± 64	107.8	0.77
120612-8-119	*0.0372 ± 0.0023*	*0.304 ± 0.075*	*236 ± 15*	*270 ± 66*	*87.4*	*0.88*
120612-8-120	0.0427 ± 0.0015	0.301 ± 0.033	269.6 ± 9.7	267 ± 29	100.9	0.46
120612-8-121	0.0415 ± 0.0018	0.299 ± 0.046	262 ± 11	265 ± 41	98.7	0.70

TABLE 1. (*Continued*)

Grain	$^{206}Pb/^{238}U$	$^{207}Pb/^{235}U$	$^{206}Pb/^{238}U$ age (Ma)	$^{207}Pb/^{235}U$ age (Ma)	% conc	Th/U
Lower–Middle Jurassic Niranohama Formation (101001-2; N38°41’35.3”, E141°30’05.0”)						
101001-2-1	0.03754 ± 0.00064	0.2634 ± 0.0080	237.6 ± 4.0	237.4 ± 7.2	100.1	0.76
101001-2-2	0.03902 ± 0.00066	0.2784 ± 0.0079	246.8 ± 4.2	249.4 ± 7.1	98.9	0.74
101001-2-3	0.03839 ± 0.00064	0.2717 ± 0.0073	242.9 ± 4.1	244.1 ± 6.5	99.5	0.55
101001-2-4	0.04036 ± 0.00071	0.293 ± 0.011	255.0 ± 4.5	261 ± 10	97.9	0.70
101001-2-5	0.03908 ± 0.00066	0.2782 ± 0.0083	247.1 ± 4.2	249.3 ± 7.4	99.1	0.68
101001-2-6	0.04058 ± 0.00068	0.2928 ± 0.0077	256.4 ± 4.3	260.8 ± 6.8	98.3	0.79
101001-2-7	0.04170 ± 0.00070	0.3025 ± 0.0077	263.4 ± 4.4	268.3 ± 6.8	98.2	0.75
101001-2-8	0.04070 ± 0.00071	0.293 ± 0.010	257.1 ± 4.5	260.9 ± 8.8	98.6	0.56
101001-2-9	0.04092 ± 0.00078	0.275 ± 0.016	258.5 ± 4.9	247 ± 14	104.7	0.69
101001-2-10	0.0446 ± 0.0011	0.323 ± 0.011	281.4 ± 6.8	284.3 ± 9.8	99.0	0.46
101001-2-11	0.0431 ± 0.0010	0.3052 ± 0.0094	272.2 ± 6.5	270.4 ± 8.3	100.7	0.59
101001-2-12	0.0440 ± 0.0010	0.3001 ± 0.0084	277.6 ± 6.5	266.5 ± 7.4	104.2	0.83
101001-2-13	0.0437 ± 0.0010	0.326 ± 0.010	275.5 ± 6.5	286.7 ± 8.7	96.1	0.77
101001-2-14	0.0635 ± 0.0015	0.489 ± 0.019	396.6 ± 9.7	404 ± 16	98.2	0.65
101001-2-15	0.04065 ± 0.00096	0.2948 ± 0.0089	256.9 ± 6.1	262.3 ± 8.0	97.9	0.64
101001-2-16	0.03985 ± 0.00096	0.276 ± 0.010	251.9 ± 6.1	247.5 ± 9.0	101.8	0.93
101001-2-17	0.0421 ± 0.0011	0.308 ± 0.016	266.1 ± 6.8	272 ± 14	97.7	0.78
101001-2-18	0.04046 ± 0.00046	0.2815 ± 0.0083	255.7 ± 2.9	251.9 ± 7.5	101.5	0.59
101001-2-19	0.04153 ± 0.00044	0.3077 ± 0.0064	262.3 ± 2.8	272.4 ± 5.7	96.3	1.2
101001-2-20	*0.0428 ± 0.0014*	*0.372 ± 0.017*	*270.0 ± 8.8*	*321 ± 15*	*84.1*	*0.88*
101001-2-21	0.0412 ± 0.0013	0.283 ± 0.013	260.1 ± 8.5	253 ± 12	102.8	0.55
101001-2-22	0.0434 ± 0.0014	0.311 ± 0.013	274.2 ± 8.8	275 ± 12	99.8	0.52
101001-2-23	0.0411 ± 0.0013	0.306 ± 0.016	259.7 ± 8.5	271 ± 14	95.7	0.78
101001-2-24	0.0410 ± 0.0013	0.312 ± 0.015	258.8 ± 8.4	276 ± 13	93.9	1.2
101001-2-25	0.0424 ± 0.0014	0.318 ± 0.014	267.5 ± 8.6	280 ± 12	95.4	1.3
101001-2-26	0.0418 ± 0.0014	0.292 ± 0.013	263.8 ± 8.5	260 ± 12	101.4	0.52
101001-2-27	0.0414 ± 0.0013	0.297 ± 0.010	261.3 ± 8.4	264.0 ± 9.3	99.0	0.85
101001-2-28	0.0432 ± 0.0013	0.308 ± 0.014	272.3 ± 8.4	273 ± 12	99.9	0.59
101001-2-29	0.0427 ± 0.0013	0.308 ± 0.015	269.3 ± 8.4	273 ± 13	98.8	0.60
101001-2-30	0.0416 ± 0.0012	0.314 ± 0.016	262.7 ± 7.8	277 ± 14	94.8	0.85
101001-2-31	0.0404 ± 0.0012	0.287 ± 0.013	255.1 ± 7.5	256 ± 12	99.6	0.42
101001-2-32	0.0392 ± 0.0012	0.301 ± 0.020	247.8 ± 7.6	267 ± 18	92.7	0.58
101001-2-33	0.0406 ± 0.0012	0.294 ± 0.011	256.6 ± 7.6	262 ± 10	97.9	0.59
101001-2-34	0.0405 ± 0.0012	0.289 ± 0.012	255.7 ± 7.6	257 ± 11	99.3	0.76
101001-2-35	0.0401 ± 0.0012	0.275 ± 0.016	253.3 ± 7.8	247 ± 14	102.6	0.98
101001-2-36	0.0415 ± 0.0012	0.304 ± 0.012	262.2 ± 7.8	270 ± 11	97.2	0.58
101001-2-37	0.0416 ± 0.0012	0.292 ± 0.011	262.7 ± 7.8	260.0 ± 9.9	101.0	0.67
101001-2-38	0.0413 ± 0.0013	0.287 ± 0.016	260.7 ± 8.0	256 ± 14	101.9	0.96
101001-2-39	0.0408 ± 0.0012	0.306 ± 0.015	258.1 ± 7.8	271 ± 13	95.2	0.69
101001-2-40	0.0404 ± 0.0012	0.290 ± 0.012	255.3 ± 7.6	259 ± 11	98.7	0.59
101001-2-41	0.0411 ± 0.0012	0.309 ± 0.012	259.8 ± 7.7	274 ± 11	94.9	1.1
101001-2-42	*0.0408 ± 0.0012*	*0.348 ± 0.022*	*257.6 ± 7.7*	*303 ± 19*	*85.0*	*0.47*
101001-2-43	0.0408 ± 0.0012	0.317 ± 0.017	257.9 ± 7.5	280 ± 15	92.3	0.98
101001-2-44	0.0418 ± 0.0012	0.300 ± 0.014	263.9 ± 7.5	267 ± 12	98.9	0.92
101001-2-45	0.0417 ± 0.0012	0.311 ± 0.012	263.5 ± 7.4	275 ± 11	95.9	0.63
101001-2-46	0.0436 ± 0.0012	0.313 ± 0.015	275.3 ± 7.9	276 ± 13	99.7	0.58
101001-2-47	0.0417 ± 0.0012	0.310 ± 0.012	263.4 ± 7.4	274 ± 11	96.2	1.0
101001-2-48	0.0409 ± 0.0011	0.300 ± 0.011	258.7 ± 7.3	267 ± 10	97.0	0.78
101001-2-49	0.04034 ± 0.00085	0.294 ± 0.012	254.9 ± 5.3	262 ± 11	97.4	1.1
101001-2-50	0.04159 ± 0.00087	0.303 ± 0.012	262.7 ± 5.5	269 ± 11	97.7	0.43
101001-2-51	0.04011 ± 0.00083	0.284 ± 0.011	253.5 ± 5.2	254.1 ± 9.7	99.8	0.83
101001-2-52	0.0511 ± 0.0011	0.400 ± 0.019	321.4 ± 6.9	342 ± 16	94.0	0.52
101001-2-53	0.04026 ± 0.00083	0.293 ± 0.011	254.5 ± 5.3	261 ± 10	97.5	0.56
101001-2-54	0.04090 ± 0.00086	0.298 ± 0.013	258.4 ± 5.4	265 ± 11	97.5	0.74
101001-2-55	0.04095 ± 0.00085	0.306 ± 0.012	258.7 ± 5.3	271 ± 10	95.6	0.73
101001-2-56	0.04023 ± 0.00086	0.291 ± 0.014	254.2 ± 5.4	260 ± 12	97.9	0.62
101001-2-57	*0.0434 ± 0.0012*	*0.467 ± 0.028*	*274.1 ± 7.7*	*389 ± 23*	*70.4*	*0.56*
101001-2-58	0.0401 ± 0.0011	0.313 ± 0.015	253.4 ± 6.8	277 ± 14	91.6	0.89
101001-2-59	0.0395 ± 0.0010	0.286 ± 0.012	249.6 ± 6.6	255 ± 11	97.9	0.26
101001-2-60	0.0400 ± 0.0011	0.296 ± 0.014	252.7 ± 6.8	263 ± 12	95.9	0.66
101001-2-61	0.0408 ± 0.0011	0.294 ± 0.013	258.0 ± 6.8	261 ± 11	98.7	0.72
101001-2-62	0.0406 ± 0.0011	0.285 ± 0.012	256.6 ± 6.8	254 ± 11	101.0	0.56
101001-2-63	0.0413 ± 0.0011	0.300 ± 0.015	260.7 ± 7.0	266 ± 13	97.9	0.95
101001-2-64	0.0426 ± 0.0012	0.328 ± 0.018	269.2 ± 7.4	288 ± 16	93.3	0.91
101001-2-65	0.0419 ± 0.0011	0.316 ± 0.015	264.3 ± 7.1	278 ± 13	94.9	0.78
101001-2-66	0.0399 ± 0.0013	0.292 ± 0.012	252.3 ± 7.9	260 ± 11	97.1	0.65
101001-2-67	0.0433 ± 0.0014	0.325 ± 0.015	273.2 ± 8.6	286 ± 13	95.6	0.96
101001-2-68	0.0416 ± 0.0013	0.312 ± 0.014	262.9 ± 8.3	275 ± 12	95.4	0.85
101001-2-69	0.0411 ± 0.0013	0.296 ± 0.019	259.8 ± 8.4	264 ± 17	98.6	0.42
101001-2-70	*0.0425 ± 0.0013*	*0.369 ± 0.016*	*268.6 ± 8.5*	*319 ± 14*	*84.3*	*1.1*
101001-2-71	0.0402 ± 0.0013	0.288 ± 0.012	254.3 ± 8.0	257 ± 11	99.0	0.69
101001-2-72	0.0427 ± 0.0013	0.319 ± 0.013	269.8 ± 8.5	281 ± 11	96.0	0.75
Middle Jurassic Aratozaki Formation (120612-4; N38°41’46.27”, E141°29’54.69”)						
120612-4-1	0.0431 ± 0.0019	0.292 ± 0.045	272 ± 12	260 ± 40	104.4	0.41
120612-4-2	*0.0414 ± 0.0019*	*0.263 ± 0.045*	*261 ± 12*	*237 ± 40*	*110.3*	*0.70*
120612-4-3	*0.0416 ± 0.0024*	*0.388 ± 0.080*	*262 ± 15*	*333 ± 69*	*78.9*	*0.39*
120612-4-4	0.0415 ± 0.0016	0.291 ± 0.033	262 ± 10	260 ± 30	101.0	0.49
120612-4-5	0.0324 ± 0.0012	0.241 ± 0.021	205.4 ± 7.5	219 ± 19	93.8	0.43
120612-4-6	0.0290 ± 0.0010	0.194 ± 0.017	184.4 ± 6.7	180 ± 16	102.4	0.57
120612-4-7	0.0281 ± 0.0011	0.205 ± 0.019	178.8 ± 6.7	189 ± 18	94.4	0.54
120612-4-8	0.0399 ± 0.0014	0.288 ± 0.022	252.2 ± 9.0	257 ± 20	98.1	0.37
120612-4-9	0.0429 ± 0.0015	0.337 ± 0.047	270.7 ± 9.2	295 ± 41	91.8	0.45
120612-4-10	0.03124 ± 0.00072	0.212 ± 0.019	198.3 ± 4.6	195 ± 17	101.6	0.40
120612-4-11	0.04485 ± 0.00089	0.292 ± 0.020	282.8 ± 5.6	260 ± 18	108.7	0.99
120612-4-12	0.0463 ± 0.0017	0.323 ± 0.052	292 ± 11	284 ± 46	102.9	0.46
120612-4-13	0.0438 ± 0.0011	0.344 ± 0.030	276.2 ± 6.7	300 ± 27	92.0	0.57
120612-4-14	0.03009 ± 0.00069	0.212 ± 0.018	191.1 ± 4.4	195 ± 17	97.8	0.78
120612-4-15	0.04465 ± 0.00087	0.327 ± 0.022	281.6 ± 5.5	287 ± 19	98.2	0.50
120612-4-16	*0.0475 ± 0.0018*	*0.289 ± 0.053*	*299 ± 12*	*258 ± 47*	*116.1*	*0.48*
120612-4-17	*0.03416 ± 0.00083*	*0.211 ± 0.021*	*216.5 ± 5.2*	*195 ± 19*	*111.2*	*0.34*
120612-4-18	0.0399 ± 0.0012	0.277 ± 0.023	252.3 ± 7.8	248 ± 20	101.7	0.23
120612-4-19	0.0422 ± 0.0019	0.283 ± 0.052	266 ± 12	253 ± 46	105.3	0.62
120612-4-20	0.0400 ± 0.0012	0.292 ± 0.022	252.6 ± 7.7	260 ± 20	97.1	0.49
120612-4-21	0.0439 ± 0.0015	0.305 ± 0.034	276.8 ± 9.6	270 ± 30	102.5	0.36
120612-4-22	0.0449 ± 0.0018	0.348 ± 0.048	283 ± 11	303 ± 41	93.3	0.50
120612-4-23	*0.0372 ± 0.0014*	*0.355 ± 0.042*	*235.3 ± 8.9*	*308 ± 36*	*76.4*	*0.71*
120612-4-24	0.0303 ± 0.0011	0.227 ± 0.025	192.4 ± 6.7	208 ± 22	92.6	0.64
120612-4-25	0.0327 ± 0.0010	0.222 ± 0.016	207.3 ± 6.2	204 ± 15	101.8	0.49
120612-4-26	0.0453 ± 0.0016	0.336 ± 0.040	286 ± 10	294 ± 35	97.2	0.49
120612-4-27	*0.0448 ± 0.0019*	*0.377 ± 0.063*	*282 ± 12*	*325 ± 54*	*87.0*	*0.45*
120612-4-28	0.0413 ± 0.0015	0.289 ± 0.039	260.8 ± 9.3	258 ± 35	101.2	0.80
120612-4-29	*0.0631 ± 0.0022*	*0.297 ± 0.047*	*395 ± 14*	*264 ± 42*	*149.3*	*0.82*
120612-4-30	0.0306 ± 0.0013	0.232 ± 0.040	194.5 ± 8.4	212 ± 36	91.8	0.81

TABLE 1. (*Continued*)

Grain	$^{206}Pb/^{238}U$	$^{207}Pb/^{235}U$	$^{206}Pb/^{238}U$ age (Ma)	$^{207}Pb/^{235}U$ age (Ma)	% conc	Th/U
120612-4-31	0.0458 ± 0.0019	0.321 ± 0.056	288 ± 12	283 ± 49	102.0	0.56
120612-4-32	0.0363 ± 0.0011	0.271 ± 0.026	229.9 ± 6.9	243 ± 23	94.4	0.96
120612-4-33	*0.0407 ± 0.0015*	*0.350 ± 0.047*	*257.0 ± 9.7*	*304 ± 41*	*84.4*	*0.36*
120612-4-34	0.0462 ± 0.0021	0.343 ± 0.047	291 ± 13	300 ± 41	97.1	0.35
120612-4-35	*0.2281 ± 0.0085*	*3.39 ± 0.22*	*1324 ± 50*	*1503 ± 97*	*88.1*	*0.21*
120612-4-36	0.0286 ± 0.0011	0.194 ± 0.016	181.7 ± 7.0	180 ± 15	100.9	0.23
120612-4-37	0.0472 ± 0.0029	0.321 ± 0.082	297 ± 18	283 ± 73	105.1	0.52
120612-4-38	0.0380 ± 0.0016	0.246 ± 0.028	240 ± 10	223 ± 26	107.8	0.49
120612-4-39	0.0423 ± 0.0019	0.293 ± 0.039	267 ± 12	261 ± 35	102.1	0.50
120612-4-40	0.0274 ± 0.0012	0.187 ± 0.026	174.3 ± 7.8	174 ± 24	99.9	0.59
120612-4-41	0.3361 ± 0.0131	5.12 ± 0.37	1868 ± 73	1839 ± 134	101.6	0.68
120612-4-42	0.0468 ± 0.0024	0.341 ± 0.070	295 ± 15	298 ± 61	98.9	0.49
120612-4-43	0.3302 ± 0.0090	5.31 ± 0.22	1839 ± 50	1871 ± 77	98.3	0.40
120612-4-44	*0.0623 ± 0.0022*	*0.585 ± 0.059*	*390 ± 14*	*467 ± 47*	*83.4*	*0.58*
120612-4-45	0.0287 ± 0.0012	0.198 ± 0.031	182.4 ± 7.7	183 ± 29	99.6	0.53
120612-4-46	0.0492 ± 0.0018	0.324 ± 0.041	309 ± 11	285 ± 36	108.5	0.55
120612-4-47	*0.0402 ± 0.0017*	*0.369 ± 0.050*	*254 ± 10*	*319 ± 43*	*79.6*	*0.64*
120612-4-48	0.0447 ± 0.0013	0.290 ± 0.032	281.9 ± 8.2	259 ± 28	108.9	0.23
120612-4-49	0.0426 ± 0.0013	0.335 ± 0.038	268.8 ± 8.4	293 ± 33	91.7	0.46
120612-4-50	0.02855 ± 0.00085	0.199 ± 0.022	181.5 ± 5.4	184 ± 20	98.6	0.51
120612-4-51	0.0451 ± 0.0019	0.299 ± 0.055	284 ± 12	266 ± 49	107.0	0.43
120612-4-52	*0.0320 ± 0.0010*	*0.274 ± 0.030*	*202.8 ± 6.4*	*246 ± 27*	*82.4*	*0.71*
120612-4-53	*0.0445 ± 0.0017*	*0.404 ± 0.056*	*281 ± 11*	*345 ± 48*	*81.4*	*0.59*
120612-4-54	*0.0461 ± 0.0021*	*0.296 ± 0.059*	*290 ± 13*	*263 ± 52*	*110.3*	*0.29*
120612-4-55	0.0454 ± 0.0021	0.347 ± 0.065	286 ± 13	302 ± 56	94.6	0.47
120612-4-56	0.0408 ± 0.0017	0.288 ± 0.028	258 ± 11	257 ± 25	100.5	0.85
120612-4-57	0.0440 ± 0.0020	0.294 ± 0.037	278 ± 12	262 ± 33	106.1	0.69
120612-4-58	0.374 ± 0.014	5.86 ± 0.26	2046 ± 77	1956 ± 87	104.6	0.10
120612-4-59	0.0290 ± 0.0013	0.200 ± 0.023	184.4 ± 8.0	185 ± 21	99.5	0.36
120612-4-60	*0.0355 ± 0.0015*	*0.297 ± 0.026*	*224.9 ± 9.3*	*264 ± 23*	*85.2*	*0.49*
120612-4-61	0.287 ± 0.011	4.75 ± 0.22	1627 ± 62	1777 ± 81	91.6	0.14
120612-4-62	0.0265 ± 0.0011	0.167 ± 0.018	168.8 ± 7.2	157 ± 17	107.5	0.43
120612-4-63	0.0438 ± 0.0014	0.293 ± 0.038	276.6 ± 9.1	261 ± 34	106.1	0.62
120612-4-64	0.3016 ± 0.0062	4.65 ± 0.16	1699 ± 35	1758 ± 60	96.6	0.40
120612-4-65	0.02614 ± 0.00085	0.193 ± 0.024	166.4 ± 5.4	179 ± 22	92.8	0.46
120612-4-66	*0.02826 ± 0.00089*	*0.218 ± 0.025*	*179.6 ± 5.7*	*201 ± 23*	*89.6*	*0.59*
120612-4-67	0.03333 ± 0.00079	0.223 ± 0.016	211.4 ± 5.0	205 ± 14	103.2	0.45
120612-4-68	0.3526 ± 0.0071	5.68 ± 0.18	1947 ± 39	1928 ± 61	101.0	0.43
120612-4-69	0.0290 ± 0.0010	0.190 ± 0.027	184.1 ± 6.5	176 ± 26	104.4	0.49
120612-4-70	0.0412 ± 0.0011	0.287 ± 0.028	260.5 ± 7.2	256 ± 25	101.7	0.40
120612-4-71	0.3372 ± 0.0066	5.37 ± 0.15	1873 ± 37	1880 ± 53	99.6	0.18
120612-4-72	0.02818 ± 0.00081	0.208 ± 0.022	179.1 ± 5.1	192 ± 20	93.4	0.36
120612-4-73	0.02849 ± 0.00077	0.204 ± 0.020	181.1 ± 4.9	189 ± 18	96.0	0.35
120612-4-74	0.0423 ± 0.0011	0.282 ± 0.028	267.0 ± 7.1	252 ± 25	106.0	0.63
120612-4-75	*0.0439 ± 0.0029*	*0.45 ± 0.11*	*277 ± 18*	*377 ± 95*	*73.3*	*0.44*
120612-4-76	0.0411 ± 0.0011	0.316 ± 0.028	259.8 ± 6.8	278 ± 25	93.3	0.46
120612-4-77	*0.0457 ± 0.0018*	*0.643 ± 0.077*	*288 ± 11*	*504 ± 61*	*57.2*	*0.51*
120612-4-78	0.3496 ± 0.0064	5.50 ± 0.16	1933 ± 35	1901 ± 54	101.7	0.26
120612-4-79	0.3566 ± 0.0058	5.74 ± 0.28	1966 ± 32	1937 ± 94	101.5	0.67
120612-4-80	0.0414 ± 0.0012	0.276 ± 0.034	261.4 ± 7.4	247 ± 31	105.7	0.72
120612-4-81	0.03647 ± 0.00080	0.278 ± 0.024	230.9 ± 5.1	249 ± 22	92.8	0.40
120612-4-82	0.0427 ± 0.0012	0.333 ± 0.038	269.2 ± 7.5	292 ± 34	92.2	0.64
120612-4-83	0.0456 ± 0.0012	0.301 ± 0.033	287.2 ± 7.3	267 ± 29	107.6	0.68
120612-4-84	0.03090 ± 0.00065	0.222 ± 0.019	196.2 ± 4.1	204 ± 17	96.4	1.0

Grain	$^{206}Pb/^{238}U$	$^{207}Pb/^{235}U$	$^{206}Pb/^{238}U$ age (Ma)	$^{207}Pb/^{235}U$ age (Ma)	% conc	Th/U
120612-4-85	0.0394 ± 0.0014	0.304 ± 0.044	249.2 ± 8.8	270 ± 39	92.3	0.57
Upper Jurassic Sodenohama Formation (101001-3; N38°40'22.9", E141°28'05.3")						
101001-3-1	0.04386 ± 0.00058	0.2973 ± 0.0078	276.7 ± 3.7	264.3 ± 6.9	104.7	0.45
101001-3-2	*0.02836 ± 0.00040*	*0.2194 ± 0.0086*	*180.3 ± 2.6*	*201.4 ± 7.9*	*89.5*	*0.38*
101001-3-3	0.03574 ± 0.00048	0.2372 ± 0.0071	226.4 ± 3.1	216.1 ± 6.5	104.8	1.3
101001-3-4	0.02792 ± 0.00038	0.2125 ± 0.0061	177.5 ± 2.4	195.6 ± 5.6	90.7	0.31
101001-3-5	0.02669 ± 0.00037	0.1961 ± 0.0064	169.8 ± 2.3	181.8 ± 6.0	93.4	0.56
101001-3-6	*0.02960 ± 0.00042*	*0.1812 ± 0.0073*	*188.1 ± 2.6*	*169.1 ± 6.8*	*111.2*	*0.38*
101001-3-7	0.03464 ± 0.00048	0.2317 ± 0.0082	219.5 ± 3.0	211.6 ± 7.5	103.7	0.82
101001-3-8	0.03002 ± 0.00042	0.2131 ± 0.0063	190.7 ± 2.6	196.2 ± 5.8	97.2	0.70
101001-3-9	0.03362 ± 0.00047	0.2497 ± 0.0082	213.2 ± 3.0	226.4 ± 7.5	94.2	0.74
101001-3-10	0.02836 ± 0.00051	0.1901 ± 0.0060	180.2 ± 3.2	176.7 ± 5.6	102.0	0.35
101001-3-11	0.02616 ± 0.00047	0.1804 ± 0.0052	166.5 ± 3.0	168.4 ± 4.9	98.9	0.42
101001-3-12	0.02821 ± 0.00050	0.1923 ± 0.0051	179.4 ± 3.2	178.6 ± 4.7	100.5	0.53
101001-3-13	0.02659 ± 0.00048	0.1852 ± 0.0064	169.2 ± 3.1	172.5 ± 5.9	98.1	1.5
101001-3-14	0.02908 ± 0.00053	0.1988 ± 0.0065	184.8 ± 3.3	184.1 ± 6.1	100.4	0.44
101001-3-15	0.03146 ± 0.00059	0.226 ± 0.010	199.7 ± 3.7	207.0 ± 9.3	96.5	0.99
101001-3-16	*0.1478 ± 0.0026*	*2.108 ± 0.045*	*889 ± 16*	*1151 ± 24*	*77.2*	*0.23*
101001-3-17	0.03037 ± 0.00058	0.204 ± 0.011	192.9 ± 3.7	188 ± 10	102.4	0.58
101001-3-18	*0.0883 ± 0.0016*	*1.180 ± 0.026*	*545.5 ± 9.6*	*791 ± 18*	*68.9*	*0.36*
101001-3-19	0.03251 ± 0.00049	0.2221 ± 0.0085	206.2 ± 3.1	203.7 ± 7.8	101.3	0.39
101001-3-20	0.02815 ± 0.00040	0.2002 ± 0.0059	178.9 ± 2.6	185.3 ± 5.5	96.6	0.45
101001-3-21	0.03842 ± 0.00053	0.2722 ± 0.0066	243.0 ± 3.4	244.4 ± 5.9	99.4	0.41
101001-3-22	0.0738 ± 0.0010	0.590 ± 0.013	459.0 ± 6.3	471 ± 11	97.4	1.1
101001-3-23	0.02678 ± 0.00038	0.1773 ± 0.0054	170.4 ± 2.4	165.7 ± 5.1	102.8	0.47
101001-3-24	0.03536 ± 0.00050	0.2504 ± 0.0072	224.0 ± 3.2	226.9 ± 6.5	98.7	0.58
101001-3-25	0.03591 ± 0.00050	0.2468 ± 0.0060	227.4 ± 3.2	224.0 ± 5.4	101.5	0.62
101001-3-26	0.04063 ± 0.00080	0.2910 ± 0.0090	256.8 ± 5.1	259.4 ± 8.0	99.0	0.81
101001-3-27	0.03365 ± 0.00067	0.2385 ± 0.0079	213.4 ± 4.2	217.2 ± 7.2	98.2	0.84
101001-3-28	0.03049 ± 0.00060	0.2016 ± 0.0061	193.6 ± 3.8	186.5 ± 5.6	103.8	0.56
101001-3-29	0.02879 ± 0.00057	0.2050 ± 0.0063	183.0 ± 3.6	189.4 ± 5.8	96.6	0.76
101001-3-30	0.3186 ± 0.0061	5.00 ± 0.12	1783 ± 34	1819 ± 43	98.0	0.67
101001-3-31	0.02630 ± 0.00053	0.1791 ± 0.0065	167.4 ± 3.3	167.3 ± 6.0	100.1	0.64
101001-3-32	0.02878 ± 0.00056	0.2014 ± 0.0055	182.9 ± 3.6	186.3 ± 5.1	98.2	0.53
101001-3-33	0.02685 ± 0.00052	0.1875 ± 0.0051	170.8 ± 3.3	174.5 ± 4.8	97.9	0.25
101001-3-34	0.3307 ± 0.0041	5.20 ± 0.12	1842 ± 23	1852 ± 44	99.5	0.18
101001-3-35	0.03415 ± 0.00048	0.2536 ± 0.0098	216.5 ± 3.0	229.5 ± 8.9	94.3	0.81
101001-3-36	0.03582 ± 0.00047	0.2511 ± 0.0078	226.9 ± 3.0	227.4 ± 7.1	99.8	0.60
101001-3-37	0.04121 ± 0.00052	0.2996 ± 0.0083	260.3 ± 3.3	266.1 7.3	97.9	1.1
Upper Jurassic Oginohama Formation (120416-5; N38°18'16.3", E141°29'50.2")						
100416-5-1	0.0390 ± 0.0012	0.267 ± 0.012	246.3 ± 7.8	240 ± 11	102.5	0.27
100416-5-2	0.02541 ± 0.00082	0.1713 ± 0.0086	161.7 ± 5.2	160.6 ± 8.1	100.7	0.62
100416-5-3	0.459 ± 0.014	10.46 ± 0.40	2434 ± 77	2477 ± 95	98.3	0.87
100416-5-4	0.02596 ± 0.00084	0.1761 ± 0.0090	165.2 ± 5.3	164.7 ± 8.4	100.3	0.57
100416-5-5	0.0353 ± 0.0011	0.250 ± 0.012	223.4 ± 7.1	227 ± 11	98.6	0.58
100416-5-6	0.02679 ± 0.00085	0.1762 ± 0.0080	170.4 ± 5.4	164.8 ± 7.5	103.4	0.43

TABLE 1. (*Continued*)

Grain	^{206}Pb/^{238}U	^{207}Pb/^{235}U	^{206}Pb/^{238}U age (Ma)	^{207}Pb/^{235}U age (Ma)	% conc	Th/U
100416-5-7	0.0343 ± 0.0011	0.236 ± 0.011	217.3 ± 6.9	215 ± 10	101.1	0.32
100416-5-8	0.357 ± 0.011	5.76 ± 0.20	1968 ± 62	1941 ± 66	101.4	0.40
100416-5-9	0.0379 ± 0.0012	0.264 ± 0.012	239.9 ± 7.7	238 ± 11	100.9	0.43
100416-5-10	0.0412 ± 0.0011	0.316 ± 0.037	260.0 ± 6.8	279 ± 33	93.3	0.92
100416-5-11	0.02902 ± 0.00053	0.185 ± 0.010	184.4 ± 3.4	172.4 ± 9.6	107.0	0.39
100416-5-12	*0.1592 ± 0.0025*	*2.585 ± 0.070*	*952 ± 15*	*1296 ± 35*	*73.5*	*0.20*
100416-5-13	0.02726 ± 0.00060	0.192 ± 0.017	173.4 ± 3.8	178 ± 16	97.3	0.68
100416-5-14	0.2856 ± 0.0045	4.51 ± 0.12	1619 ± 25	1733 ± 46	93.4	0.22
100416-5-15	0.02617 ± 0.00045	0.1834 ± 0.0084	166.5 ± 2.9	171.0 ± 7.9	97.4	0.58
100416-5-16	0.03816 ± 0.00062	0.2669 ± 0.0095	241.4 ± 3.9	240.2 ± 8.6	100.5	0.36
100416-5-17	*0.02467 ± 0.00042*	*0.0770 ± 0.0034*	*157.1 ± 2.7*	*75.4 ± 3.3*	*208.5*	*0.53*
100416-5-18	0.04010 ± 0.00065	0.286 ± 0.010	253.5 ± 4.1	255.3 ± 9.0	99.3	0.48
100416-5-19	0.03458 ± 0.00039	0.2403 ± 0.0073	219.1 ± 2.5	218.6 ± 6.7	100.2	0.67
100416-5-20	0.3431 ± 0.0037	5.73 ± 0.14	1901 ± 20	1935 ± 46	98.2	0.56
100416-5-21	0.03316 ± 0.00039	0.2345 ± 0.0079	210.3 ± 2.5	213.9 ± 7.2	98.3	0.55
100416-5-22	0.3476 ± 0.0037	5.93 ± 0.14	1923 ± 21	1965 ± 47	97.9	0.94
100416-5-23	0.04023 ± 0.00049	0.286 ± 0.011	254.3 ± 3.1	255.5 ± 9.6	99.5	0.37
100416-5-24	0.03377 ± 0.00041	0.2163 ± 0.0082	214.1 ± 2.6	198.8 ± 7.5	107.7	0.69
100416-5-25	0.3089 ± 0.0033	4.89 ± 0.12	1735 ± 19	1800 ± 44	96.4	0.29
100416-5-26	0.02752 ± 0.00031	0.1936 ± 0.0056	175.0 ± 2.0	179.7 ± 5.2	97.4	0.34
100416-5-27	0.03444 ± 0.00066	0.2446 ± 0.0080	218.3 ± 4.2	222.1 ± 7.2	98.3	0.54
100416-5-28	0.03461 ± 0.00067	0.2607 ± 0.0088	219.3 ± 4.2	235.3 ± 7.9	93.2	0.56
100416-5-29	0.02902 ± 0.00058	0.1965 ± 0.0086	184.4 ± 3.7	182.2 ± 8.0	101.2	0.32
100416-5-30	0.02887 ± 0.00057	0.1915 ± 0.0083	183.5 ± 3.7	177.9 ± 7.7	103.1	0.29
100416-5-31	0.03902 ± 0.00074	0.2964 ± 0.0091	246.7 ± 4.7	263.5 ± 8.1	93.6	0.92
100416-5-32	0.02735 ± 0.00054	0.1986 ± 0.0076	174.0 ± 3.4	183.9 ± 7.1	94.6	0.50
100416-5-33	0.4202 ± 0.0080	8.85 ± 0.25	2262 ± 43	2323 ± 67	97.4	0.59
100416-5-34	0.02828 ± 0.00055	0.2045 ± 0.0078	179.8 ± 3.5	188.9 ± 7.2	95.2	0.74
100416-5-35	0.03885 ± 0.00074	0.2736 ± 0.0086	245.7 ± 4.7	245.6 ± 7.7	100.1	0.21
100416-5-36	*0.02838 ± 0.00085*	*0.1581 ± 0.0070*	*180.4 ± 5.4*	*149.1 ± 6.6*	*121.0*	*0.54*
100416-5-37	*0.1043 ± 0.0031*	*1.422 ± 0.048*	*639 ± 19*	*898 ± 30*	*71.2*	*0.15*
100416-5-38	0.02727 ± 0.00081	0.1742 ± 0.0068	173.5 ± 5.2	163.0 ± 6.4	106.4	0.26
100416-5-39	0.3195 ± 0.0094	4.96 ± 0.16	1787 ± 53	1813 ± 59	98.6	0.16
100416-5-40	*0.02802 ± 0.00085*	*0.1395 ± 0.0071*	*178.2 ± 5.4*	*132.6 ± 6.7*	*134.3*	*0.55*
100416-5-41	0.346 ± 0.010	6.15 ± 0.20	1914 ± 56	1997 ± 65	95.9	0.25
100416-5-42	0.0345 ± 0.0010	0.252 ± 0.012	218.8 ± 6.6	228 ± 11	96.0	0.72
100416-5-43	0.02724 ± 0.00081	0.1868 ± 0.0077	173.2 ± 5.2	173.9 ± 7.2	99.6	0.46
100416-5-44	0.02587 ± 0.00077	0.1810 ± 0.0074	164.7 ± 4.9	168.9 ± 6.9	97.5	0.35
100416-5-45	0.02584 ± 0.00049	0.1829 ± 0.0058	164.4 ± 3.1	170.5 ± 5.4	96.4	0.54
100416-5-46	0.3065 ± 0.0057	4.89 ± 0.14	1724 ± 32	1800 ± 50	95.8	0.20
100416-5-47	0.3216 ± 0.0060	5.07 ± 0.14	1798 ± 34	1830 ± 52	98.2	0.43
100416-5-48	0.3023 ± 0.0056	4.79 ± 0.13	1703 ± 32	1783 ± 50	95.5	0.16
100416-5-49	0.03476 ± 0.00067	0.2450 ± 0.0088	220.3 ± 4.2	222.5 ± 8.0	99.0	0.59
100416-5-50	0.2802 ± 0.0053	4.46 ± 0.13	1592 ± 30	1724 ± 51	92.4	0.53
100416-5-51	0.02767 ± 0.00053	0.1949 ± 0.0071	176.0 ± 3.4	180.8 ± 6.6	97.3	0.29
100416-5-52	0.02859 ± 0.00056	0.1885 ± 0.0075	181.7 ± 3.5	175.3 ± 7.0	103.7	0.33
100416-5-53	*0.02623 ± 0.00058*	*0.1373 ± 0.0058*	*166.9 ± 3.7*	*130.6 ± 5.5*	*127.8*	*0.56*
100416-5-54	0.02680 ± 0.00060	0.1863 ± 0.0075	170.5 ± 3.8	173.5 ± 7.0	98.3	0.39
100416-5-55	0.03471 ± 0.00076	0.2438 ± 0.0093	219.9 ± 4.8	221.5 ± 8.5	99.3	0.76
100416-5-56	0.02942 ± 0.00066	0.2083 ± 0.0094	186.9 ± 4.2	192.1 ± 8.7	97.3	0.37
100416-5-57	0.3055 ± 0.0065	4.79 ± 0.14	1719 ± 37	1782 ± 53	96.4	0.29
100416-5-58	0.03357 ± 0.00077	0.221 ± 0.011	212.8 ± 4.9	203.0 ± 9.7	104.8	0.96
100416-5-59	0.3676 ± 0.0079	7.27 ± 0.22	2018 ± 43	2145 ± 64	94.1	1.1
100416-5-60	0.03368 ± 0.00073	0.2198 ± 0.0076	213.5 ± 4.6	201.7 ± 7.0	105.9	0.48
100416-5-61	*0.02784 ± 0.00062*	*0.1582 ± 0.0064*	*177.0 ± 3.9*	*149.1 ± 6.1*	*118.7*	0.38
Lower Cretaceous Yoshihama Formation (101002-1; N38°34’25.4”, E141°26’52.9”)						
101002-1-1	*0.02816 ± 0.00064*	*0.243 ± 0.010*	*179.1 ± 4.1*	*220.8 ± 9.2*	*81.1*	*0.44*
101002-1-2	*0.02905 ± 0.00065*	*0.2264 ± 0.0079*	*184.6 ± 4.1*	*207.2 ± 7.3*	*89.1*	*1.4*
101002-1-3	*0.02923 ± 0.00064*	*0.2280 ± 0.0074*	*185.7 ± 4.1*	*208.5 ± 6.8*	*89.1*	*0.32*
101002-1-4	0.02962 ± 0.00065	0.2236 ± 0.0072	188.2 ± 4.1	204.9 ± 6.6	91.8	0.39
101002-1-5	0.03437 ± 0.00076	0.2681 ± 0.0086	217.9 ± 4.8	241.1 ± 7.7	90.4	0.65
101002-1-6	*0.03858 ± 0.00086*	*0.316 ± 0.010*	*244.0 ± 5.5*	*279.1 ± 9.3*	*87.4*	*0.55*
101002-1-7	*0.02985 ± 0.00059*	*0.269 ± 0.010*	*189.6 ± 3.7*	*242.1 ± 9.1*	*78.3*	*0.47*
101002-1-8	0.03060 ± 0.00058	0.2140 ± 0.0067	194.3 ± 3.7	196.9 ± 6.2	98.7	1.1
101002-1-9	0.03905 ± 0.00075	0.290 ± 0.010	246.9 ± 4.7	258.8 ± 9.1	95.4	0.32
101002-1-10	*0.02907 ± 0.00058*	*0.2431 ± 0.0099*	*184.7 ± 3.7*	*220.9 ± 9.0*	*83.6*	*0.36*
101002-1-11	*0.03418 ± 0.00065*	*0.2762 ± 0.0091*	*216.7 ± 4.1*	*247.6 ± 8.2*	*87.5*	*0.63*
101002-1-12	*0.0335 ± 0.0011*	*0.297 ± 0.014*	*212.4 ± 7.1*	*264 ± 12*	*80.4*	*1.2*
101002-1-13	0.323 ± 0.011	5.05 ± 0.18	1802 ± 60	1828 ± 66	98.6	0.15
101002-1-14	0.02714 ± 0.00091	0.2057 ± 0.0094	172.6 ± 5.8	190.0 ± 8.7	90.9	0.45
101002-1-15	0.0325 ± 0.0011	0.243 ± 0.015	206.4 ± 7.1	221 ± 13	93.6	1.4
101002-1-16	0.02895 ± 0.00099	0.207 ± 0.012	184.0 ± 6.3	191 ± 11	96.3	0.62
101002-1-17	0.03030 ± 0.00077	0.2120 ± 0.0071	192.4 ± 4.9	195.2 ± 6.5	98.6	0.59
101002-1-18	0.02882 ± 0.00075	0.2023 ± 0.0089	183.1 ± 4.8	187.1 ± 8.3	97.9	0.69
101002-1-19	0.03620 ± 0.00092	0.2545 ± 0.0082	229.3 ± 5.8	230.2 ± 7.4	99.6	0.67
101002-1-20	0.02912 ± 0.00076	0.2127 ± 0.0095	185.0 ± 4.8	195.8 ± 8.7	94.5	0.45
101002-1-21	0.03279 ± 0.00085	0.233 ± 0.010	208.0 ± 5.4	212.4 ± 9.4	97.9	0.31
101002-1-22	0.03115 ± 0.00080	0.2387 ± 0.0092	197.7 ± 5.1	217.3 ± 8.4	91.0	0.63
101002-1-23	0.0395 ± 0.0010	0.2882 ± 0.0088	249.9 ± 6.3	257.2 ± 7.8	97.2	0.53
101002-1-24	0.2945 ± 0.0075	4.60 ± 0.13	1664 ± 42	1748 ± 51	95.2	0.43
101002-1-25	0.03018 ± 0.00075	0.2141 ± 0.0086	191.7 ± 4.8	197.0 ± 7.9	97.3	0.49
101002-1-26	*0.03207 ± 0.00079*	*0.2701 ± 0.0096*	*203.5 ± 5.0*	*242.7 ± 8.7*	*83.8*	*0.49*
101002-1-27	0.02506 ± 0.00062	0.1773 ± 0.0061	159.6 ± 3.9	165.8 ± 5.7	96.3	0.33
101002-1-28	*0.03079 ± 0.00077*	*0.2412 ± 0.0098*	*195.5 ± 4.9*	*219.4 ± 8.9*	*89.1*	*0.66*
101002-1-29	0.02524 ± 0.00062	0.1822 ± 0.0067	160.7 ± 4.0	169.9 ± 6.3	94.6	0.52
101002-1-30	0.02864 ± 0.00070	0.2195 ± 0.0074	182.0 ± 4.5	201.5 ± 6.8	90.3	0.44
101002-1-31	0.03566 ± 0.00095	0.270 ± 0.019	225.9 ± 6.0	243 ± 17	93.1	0.65
Lower Cretaceous Ayukawa Formation (100416-4; N38°17’29.8”, E141°30’36.8”)						
100416-4-1	0.391 ± 0.020	0.0523 ± 0.0024	328 ± 15	335 ± 18	98.0	0.36
100416-4-2	*0.166 ± 0.012*	*0.0204 ± 0.0010*	*130.0 ± 6.2*	*156 ± 11*	*83.4*	*1.6*
100416-4-3	*5.98 ± 0.30*	*0.298 ± 0.014*	*1682 ± 78*	*1972 ± 98*	*85.3*	*0.56*
100416-4-4	*0.1725 ± 0.0097*	*0.0221 ± 0.0010*	*140.7 ± 6.6*	*161.6 ± 9.1*	*87.1*	*1.0*
100416-4-5	*3.09 ± 0.15*	*0.2072 ± 0.0097*	*1214 ± 57*	*1431 ± 71*	*84.8*	*0.24*
100416-4-6	*0.1665 ± 0.0098*	*0.0209 ± 0.0010*	*133.5 ± 6.3*	*156 ± 9*	*85.4*	*1.1*
100416-4-7	0.262 ± 0.016	0.0367 ± 0.0017	233 ± 11	236 ± 14	98.4	0.92
100416-4-8	*0.173 ± 0.012*	*0.0206 ± 0.0010*	*131.2 ± 6.2*	*162 ± 11*	*81.1*	*1.7*
100416-4-9	0.331 ± 0.018	0.0461 ± 0.0020	291 ± 13	290 ± 16	100.1	0.14
100416-4-10	0.252 ± 0.014	0.0358 ± 0.0016	227 ± 10	228 ± 13	99.4	0.54
100416-4-11	0.1457 ± 0.0087	0.0219 ± 0.0010	140 ± 6	138 ± 8	101.0	1.2
100416-4-12	0.1520 ± 0.0090	0.02123 ± 0.00071	135.4 ± 4.5	144 ± 8	94.3	0.9

TABLE 1. (*Continued*)

Grain	$^{206}Pb/^{238}U$	$^{207}Pb/^{235}U$	$^{206}Pb/^{238}U$ age (Ma)	$^{207}Pb/^{235}U$ age (Ma)	% conc	Th/U
100416-4-13	0.1504 ± 0.0094	0.02002 ± 0.00069	127.8 ± 4.4	142.3 ± 8.9	89.8	1.1
100416-4-14	0.368 ± 0.019	0.0366 ± 0.0012	232.0 ± 7.6	318 ± 16	72.9	0.28
100416-4-15	3.28 ± 0.15	0.2178 ± 0.0070	1270 ± 41	1475 ± 68	86.1	0.1
100416-4-16	0.186 ± 0.011	0.0265 ± 0.0012	168.8 ± 7.8	174 ± 10	97.3	0.35
100416-4-17	0.145 ± 0.010	0.0211 ± 0.0010	135 ± 6	138 ± 10	98.0	1.1
100416-4-18	0.201 ± 0.011	0.0292 ± 0.0013	186 ± 9	186 ± 10	99.9	0.29
100416-4-19	1.387 ± 0.025	0.1042 ± 0.0013	639 ± 8	883 ± 16	72.3	0.24
100416-4-20	4.689 ± 0.074	0.2958 ± 0.0035	1671 ± 20	1765 ± 28	94.6	0.16
100416-4-21	4.762 ± 0.076	0.2695 ± 0.0032	1538 ± 18	1778 ± 29	86.5	0.4
100416-4-22	0.2229 ± 0.0078	0.02857 ± 0.00040	181.6 ± 2.5	204.3 ± 7.1	88.9	0.61
100416-4-23	0.1739 ± 0.0059	0.02098 ± 0.00029	133.8 ± 1.9	162.8 ± 5.5	82.2	0.60
100416-4-24	5.50 ± 0.15	0.3324 ± 0.0058	1850 ± 32	1901 ± 51	97.3	0.9
100416-4-25	0.483 ± 0.013	0.04213 ± 0.00072	266.0 ± 4.6	400 ± 11	66.5	0.38
100416-4-26	0.282 ± 0.011	0.0391 ± 0.0010	247.4 ± 6.4	253 ± 10	97.9	0.12
100416-4-27	0.1482 ± 0.0062	0.02134 ± 0.00056	136.1 ± 3.6	140.3 ± 5.9	97.0	0.87
100416-4-28	0.1909 ± 0.0082	0.02622 ± 0.00069	166.9 ± 4.4	177.4 ± 7.6	94.1	0.4
100416-4-29	1.215 ± 0.043	0.0920 ± 0.0024	568 ± 15	807 ± 29	70.3	0.40
100416-4-30	0.1967 ± 0.0069	0.02159 ± 0.00055	137.7 ± 3.5	182.4 ± 6.4	75.5	1.6
100416-4-31	0.1532 ± 0.0088	0.02033 ± 0.00056	130 ± 4	145 ± 8	89.6	2.0
100416-4-32	0.2705 ± 0.0087	0.0380 ± 0.0010	240.6 ± 6.1	243.0 ± 7.8	99.0	0.31
100416-4-33	0.376 ± 0.014	0.0498 ± 0.0015	313.1 ± 9.6	324 ± 12	96.5	0.28
100416-4-34	1.041 ± 0.038	0.0839 ± 0.0026	519 ± 16	724 ± 27	71.7	0.35
100416-4-35	5.05 ± 0.17	0.3191 ± 0.0098	1785 ± 55	1828 ± 62	97.6	0.18
100416-4-36	4.94 ± 0.17	0.3153 ± 0.0097	1767 ± 54	1810 ± 62	97.6	0.70
100416-4-37	0.294 ± 0.012	0.0409 ± 0.0013	258.5 ± 8.0	262 ± 10	98.6	0.4
100416-4-38	0.1479 ± 0.0076	0.02113 ± 0.00067	134.8 ± 4.3	140.1 ± 7.2	96.2	1.1
100416-4-39	0.256 ± 0.012	0.0365 ± 0.0011	231.1 ± 7.3	231 ± 11	99.9	0.4
100416-4-40	0.260 ± 0.011	0.0370 ± 0.0012	234.4 ± 7.3	234 ± 10	100.0	0.3
100416-4-41	0.389 ± 0.011	0.04383 ± 0.00090	276.5 ± 5.7	333.3 ± 9.8	83.0	0.19
100416-4-42	0.2892 ± 0.0085	0.03911 ± 0.00080	247.3 ± 5.1	257.9 ± 7.6	95.9	0.1
100416-4-43	0.191 ± 0.010	0.02588 ± 0.00058	164.7 ± 3.7	178 ± 9	92.8	1.1
100416-4-44	0.1432 ± 0.0061	0.02082 ± 0.00045	132.8 ± 2.8	136 ± 6	97.8	0.74
100416-4-45	0.3009 ± 0.0090	0.04151 ± 0.00085	262.2 ± 5.4	267 ± 8	98.2	1.0
100416-4-46	3.94 ± 0.11	0.2584 ± 0.0053	1482 ± 30	1622 ± 44	91.3	0.2
100416-4-47	7.49 ± 0.20	0.3984 ± 0.0081	2162 ± 44	2171 ± 57	99.6	0.67
100416-4-48	0.1483 ± 0.0047	0.02084 ± 0.00043	133.0 ± 2.7	140.4 ± 4.4	94.7	0.83
100416-4-49	0.252 ± 0.018	0.0359 ± 0.0016	227 ± 10	228 ± 16	99.7	0.60
100416-4-50	0.180 ± 0.011	0.0258 ± 0.0011	164.1 ± 7.3	168 ± 10	97.7	0.61
100416-4-51	0.161 ± 0.012	0.02029 ± 0.00093	129.5 ± 5.9	152 ± 12	85.5	0.71
100416-4-52	0.177 ± 0.011	0.0253 ± 0.0011	160.9 ± 7.2	165.4 ± 9.9	97.3	2.0
100416-4-53	4.17 ± 0.20	0.2711 ± 0.0119	1546 ± 68	1667 ± 80	92.8	0.3
100416-4-54	0.1389 ± 0.0096	0.02001 ± 0.00090	127.7 ± 5.8	132.1 ± 9.1	96.7	0.80
100416-4-55	0.143 ± 0.011	0.02071 ± 0.00095	132.1 ± 6.0	136 ± 11	97.0	0.8
100416-4-56	0.248 ± 0.014	0.0351 ± 0.0016	222.3 ± 9.9	225 ± 13	98.7	1.2
100416-4-57	0.263 ± 0.011	0.0365 ± 0.0012	231.0 ± 7.4	237 ± 10	97.6	0.12
100416-4-58	0.1504 ± 0.0082	0.02068 ± 0.00068	132 ± 4	142 ± 8	92.8	0.72
100416-4-59	3.54 ± 0.13	0.2244 ± 0.0071	1305 ± 41	1536 ± 55	85.0	0.4
100416-4-60	0.149 ± 0.011	0.02022 ± 0.00069	129 ± 4	141 ± 10	91.6	1.3
100416-4-61	0.1478 ± 0.0080	0.02076 ± 0.00068	132.4 ± 4.3	140.0 ± 7.6	94.6	0.6
100416-4-62	0.156 ± 0.010	0.02079 ± 0.00070	133 ± 4	147 ± 9	89.9	0.93
100416-4-63	0.203 ± 0.012	0.02674 ± 0.00089	170.1 ± 5.7	187 ± 11	90.8	0.7
100416-4-64	0.1430 ± 0.0085	0.02014 ± 0.00067	129 ± 4	136 ± 8	94.7	1.1
100416-4-65	4.71 ± 0.17	0.2990 ± 0.0087	1686 ± 49	1769 ± 62	95.3	0.2
100416-4-66	3.46 ± 0.12	0.2273 ± 0.0066	1320 ± 38	1517 ± 55	87.0	0.27
100416-4-67	2.94 ± 0.10	0.1960 ± 0.0057	1154 ± 33	1392 ± 49	82.9	0.20
100416-4-68	5.85 ± 0.20	0.2927 ± 0.0085	1655 ± 48	1953 ± 68	84.7	0.6
100416-4-69	0.1815 ± 0.0083	0.02133 ± 0.00063	136.0 ± 4.0	169.4 ± 7.7	80.3	1.2
100416-4-70	0.1666 ± 0.0098	0.02108 ± 0.00065	134.5 ± 4.1	156.5 ± 9.2	85.9	0.7
100416-4-71	0.1889 ± 0.0080	0.02672 ± 0.00078	170.0 ± 5.0	176 ± 7	96.8	0.28
100416-4-72	0.171 ± 0.015	0.02091 ± 0.00068	133 ± 4	161 ± 14	83.0	1.2
100416-4-73	0.2065 ± 0.0093	0.02914 ± 0.00068	185.2 ± 4.3	191 ± 9	97.1	0.69
100416-4-74	0.2492 ± 0.0099	0.03638 ± 0.00084	230.4 ± 5.3	226 ± 9	102.0	0.3
100416-4-75	0.284 ± 0.010	0.03270 ± 0.00075	207.4 ± 4.7	254 ± 9	81.6	0.75
100416-4-76	0.1594 ± 0.0081	0.01989 ± 0.00048	126.9 ± 3.0	150 ± 8	84.5	1.0
100416-4-77	0.1732 ± 0.0083	0.02154 ± 0.00051	137 ± 3	162 ± 8	84.7	0.80
100416-4-78	0.1386 ± 0.0058	0.02064 ± 0.00048	132 ± 3	132 ± 5	99.9	0.72
100416-4-79	4.43 ± 0.12	0.2821 ± 0.0063	1602 ± 36	1719 ± 47	93.2	0.28
100416-4-80	0.230 ± 0.011	0.02857 ± 0.00068	181.6 ± 4.3	210 ± 10	86.4	0.46
100416-4-81	0.1818 ± 0.0065	0.02546 ± 0.00058	162 ± 4	170 ± 6	95.5	0.33
100416-4-82	0.423 ± 0.022	0.0561 ± 0.0027	352 ± 17	358 ± 19	98.4	0.39
100416-4-83	0.142 ± 0.013	0.0197 ± 0.0010	125.9 ± 6.3	135 ± 12	93.4	0.84
100416-4-84	0.213 ± 0.011	0.0257 ± 0.0012	163.4 ± 7.7	196 ± 10	83.2	0.29
100416-4-85	0.1452 ± 0.0089	0.0211 ± 0.0010	134.6 ± 6.4	137.6 ± 8.4	97.8	1.10
100416-4-86	0.191 ± 0.010	0.0264 ± 0.0013	168 ± 8	177 ± 9	94.8	0.45
100416-4-87	0.144 ± 0.012	0.0214 ± 0.0011	136.3 ± 6.7	136 ± 12	100.0	1.2
100416-4-88	0.148 ± 0.012	0.0208 ± 0.0010	133.0 ± 6.5	140 ± 11	94.8	1.0
100416-4-89	0.148 ± 0.011	0.0212 ± 0.0010	135.3 ± 6.6	140 ± 11	96.6	0.64
100416-4-90	0.1461 ± 0.0085	0.02102 ± 0.00050	134.1 ± 3.2	138 ± 8	96.9	1.28
100416-4-91	0.427 ± 0.022	0.0560 ± 0.0013	351 ± 8	361 ± 18	97.4	0.40
100416-4-92	0.268 ± 0.014	0.03766 ± 0.00088	238 ± 6	241 ± 13	98.8	0.19
100416-4-93	0.159 ± 0.013	0.0219 ± 0.0011	140 ± 7	150 ± 12	93.3	0.76
100416-4-94	0.155 ± 0.012	0.0210 ± 0.0010	134.2 ± 6.5	146 ± 11	91.9	1.0
100416-4-95	0.263 ± 0.015	0.0396 ± 0.0019	250 ± 12	237 ± 13	105.7	0.3
100416-4-96	0.147 ± 0.011	0.0201 ± 0.0010	128.5 ± 6.2	139 ± 11	92.1	0.99
100416-4-97	0.290 ± 0.020	0.0403 ± 0.0019	254 ± 12	259 ± 18	98.4	0.54
100416-4-98	0.200 ± 0.014	0.0280 ± 0.0011	178.2 ± 6.8	185 ± 13	96.2	0.47
100416-4-99	0.261 ± 0.011	0.0369 ± 0.0014	233.5 ± 8.6	236 ± 10	99.1	0.12
100416-4-100	0.1713 ± 0.0079	0.02436 ± 0.00090	155.1 ± 5.7	160.5 ± 7.4	96.7	0.6
100416-4-101	0.1359 ± 0.0093	0.02072 ± 0.00078	132.2 ± 5.0	129.4 ± 8.9	102.1	1.2
100416-4-102	0.1676 ± 0.0078	0.02041 ± 0.00030	130.2 ± 1.9	157.3 ± 7.4	82.8	0.8
100416-4-103	0.158 ± 0.011	0.02095 ± 0.00034	134 ± 2	149 ± 10	89.8	1.5
100416-4-104	0.2001 ± 0.0089	0.02787 ± 0.00040	177 ± 3	185 ± 8	95.7	0.93
100416-4-105	0.1551 ± 0.0082	0.02103 ± 0.00031	134.2 ± 2.0	146.4 ± 7.7	91.7	0.99